1994

Contingency filtering scheme for on-line dynamic security assessment

Chadalavada Vamsi Krishna
Iowa State University

Order Number 9518363

Contingency filtering scheme for on-line dynamic security assessment

Krishna, Chadalavada Vamsi, Ph.D.

Iowa State University, 1994

U·M·I
300 N. Zeeb Rd.
Ann Arbor, MI 48106

Contingency filtering scheme for on-line dynamic security assessment

by

Chadalavada Vamsi Krishna

A Dissertation Submitted to the
Graduate Faculty in Partial Fulfillment of the
Requirements for the Degree of
DOCTOR OF PHILOSOPHY

Department: Electrical Engineering and Computer Engineering
Major: Electrical Engineering (Electric Power Systems)

Approved:

Signature was redacted for privacy.

In Charge of Major Work

Signature was redacted for privacy.

For the Major Department

Signature was redacted for privacy.

For the Graduate College

Members of the Committee:

Signature was redacted for privacy.

Signature was redacted for privacy.

Signature was redacted for privacy.

Signature was redacted for privacy.

Iowa State University
Ames, Iowa

1994

TABLE OF CONTENTS

LIST OF FIGURES

LIST OF TABLES

1 INTRODUCTION

1.1 Power System Security

The increasing dependence of modern society on a reliable supply of electricity has made it imperative for electric utilities to maintain the reliability and security of the power system. Economy energy transactions, reliance on external sources of capacity, and competition for transmission resources have all resulted in higher loading of the transmission system. Some transmission systems are being operated at, or near, limits. Operation of the power system has become very complex and difficult for the system operator. A variety of scenarios are being selected by operations planning engineers to test the strength of the network and to ascertain that the reliability criteria, which apply to dynamic system performance are met.

Electric power system reliability encompasses many aspects. Some of these aspects which have been prevalent for a long time [1] include

- Assurance of sufficient generation and transmission capacity to meet the load.
- Assurance of sufficient fuel supplies.
- Ability to withstand sudden loss of any major generator or transmission line.
- Ability to restore load service quickly and smoothly in case of a breakdown or service interruption.
- Ability to withstand specified line faults without losing generators.

- Reliable operation of the equipment like relays and breakers.

In addition, in recent years, factors such as delays in licensing of nuclear generation, electromagnetic fields, environmental constraints, regulatory uncertainty, deregulation, transmission access legislation, non-utility generation, load management programs and others, make it more difficult to plan for the future or to evaluate what the reliability of the system is. The North American Electric reliability council (NERC) [2] defines reliability as follows,

> *Reliability, in a bulk electric system, is the degree to which the performance of the elements of that system results in electricity being delivered to customers within accepted standards and in the amount desired. The degree of reliability may be measured by the frequency, duration, and magnitude of adverse effects on the electric supply (or service to customers).*

The concern with electric system reliability has brought to the forefront two basic aspects which are adequacy and security. Referring to the NERC [1] definitions again,

> *Adequacy is the ability of the bulk electric system to supply the aggregate electrical demand and energy requirements of the customers at all times, taking into account scheduled and unscheduled outages of system components.*
>
> *Security is the ability of the bulk electric system to withstand sudden disturbances such as electric short circuits or unanticipated loss of system components.*

To be able to achieve a reliable service, security must be maintained at all times. The uncertainties of future conditions-rate of growth of demand, demand-supply options, regulatory climate, and growing need to address environmental concerns can mean delays in the development of new generation facilities and in large transmission additions. These deferrals result in a greater need for security assessment to reliably operate the system.

Security is usually classified into either static or dynamic security. Static security concerns itself with ensuring that the inequality constraints on the system are not violated (line flows do not exceed the thermal rating, bus voltages remain within acceptable ranges etc.). Dynamic security assessment deals with the analysis of the system in the transition from the initial to the final operating condition following a disturbance. The dynamic behavior of the power system is of great importance in determining how secure the power system is. This results in a need for a proper methodology for dynamic security assessment [3]. It should be capable of

- Offering a clear definition of the operating states of a power system and of what constitutes an acceptable dynamic system performance.
- Recognizing the dynamic state of the system (in real time)
- Detecting contingent situations that may lead to emergencies
- Assessing the security of the system
- Identifying the weak links and suggesting preventive measures

An important aspect of security is the stability of the power system. For a system to be stable, it should be both steady-state and transiently stable. Transient stability [4] is defined as follows,

A power system is transiently stable for a particular steady-state operating condition and for a particular disturbance if, following that disturbance, it reaches an acceptable steady-state operating condition.

It is evident that transient stability is a very important aspect of power system behavior. A transient stability study is capable of assessing the system dynamic response to various stimuli. It characterizes the transition from pre-disturbance to post-disturbance operating conditions. A potential tool capable of transient stability study needs to be developed. This is discussed in Section 1.2.

1.2 Tools for Security Assessment

Time domain simulation is accepted as a standard practice of stability analysis. The conventional approach for transient stability assessment requires off-line analysis of many contingencies for various operating conditions. Operating limits are derived from these studies for a variety of system conditions. These limits are usually determined in terms of the critical system operating parameters. While this method is robust and reliable, it is computationally intensive and time consuming. There is a demand for skilled manpower to analyze the output and to properly interpret the voluminous amount of information. Also, the information provided by these off-line studies is not adequate to account for all operating conditions encountered. There is a need in the industry for improved dynamic analysis capability.

The ultimate objective of security assessment is to track, in real time, the current, changing level of system security vis-a-vis the system load and

environment. In an operations environment, the system operator is faced with ever changing conditions. The operator needs to know the stability limits in order to recognize the potential problems and to take appropriate action. Obtaining safe limits in a typical operations environment in real time would be invaluable to an operator in taking necessary preventive action to avoid a stability crisis.

There is a need for development of methods that could be used on-line. This brings us to the concept of direct methods. The importance of these methods would be in their ability to assess the security of the system in near real time. The direct methods determine the stability of the power system without explicitly solving the differential equations describing the dynamics of the system. These methods also provide a qualitative measure of the degree of stability. This can be analyzed as a function of important system parameters such as generation shifts, power flows in critical lines and changes in loads and has tremendous potential for use in an operating environment. These are discussed in detail in later sections.

1.3 Origin of the Direct Methods

Early work on development of criteria for transient stability of power systems involved energy methods. These are "direct methods" in the sense that transient stability was to be determined without a time solution. All direct methods of stability assessment are directly or indirectly related to Lyapunov's direct method and Hamiltonian mechanics.

The most familiar energy criterion is the equal area criterion [5, chapter 4]. This criteria states that the rotor of the perturbed machine moves till the

kinetic energy is totally converted to potential energy. The acceleration of the rotor then reverses direction. The neglected system damping is assumed to bring the machine to a new steady state operating point. This technique is easy to apply to a two-machine system. Difficulty arises when we apply direct methods to multi-machine power systems.

In the 1930's, Gorev [6] used the first integral of energy to obtain a criterion for power system stability. He considered the classical model with the assumption of zero transfer conductances.

The first major work on the subject in English was by Magnusson [7] in 1947. Magnusson's work was very similar to Gorev's. The significant difference was that Magnusson derived a potential energy function with respect to the post transient equilibrium point.

In 1958, Aylett [8] proposed an energy-integral criterion to obtain the transient stability limit. He explained the physical meaning of the unstable equilibrium point (UEP) by means of phase plane trajectories. The criterion was based on the comparison of the phase plane trajectories with a critical trajectory which passes through a saddle point.

Many researchers in earlier works have neglected the transfer conductances on the basis that these are small. This assumption is false, since constant impedance loads are reflected in the transfer conductance terms of the network.

After the early work on energy methods, greater emphasis was given to shaping Lyapunov's direct method into an effective tool for the assessment of power system stability. Pioneering work in this area was done by Gless [9]. In 1966, El-Abiad and Nagappan [10] proposed a procedure of assessing the

transient stability region of a multi-machine power system. Transfer conductances of the power system were included in formulating the Lyapunov function. They manipulated the energy terms corresponding to transfer conductances to be integrable analytically. Incorporation of transfer conductances requires computing path-dependent integrals that cannot be computed without knowing the trajectories.

Uyemura et. al. [11] suggested a linear trajectory approximation for the case where transfer conductances are non-zero. The authors concluded that if a multi-machine system swings like a two-machine system, then the energy function obtained by the linear trajectory approximation will yield an approximately good results. Their formulation of the systems equations is identical to that of Aylett [8].

In 1972, Tavora and Smith [12] developed the concept of the center of inertia. They analyzed the transient energy of a multi-machine system, and examined the equilibrium conditions. The mathematical model used here was the classical model with zero transfer conductances.

The following section deals with the more recent advances in direct methods.

1.4 Transient Energy Function Method and its Improvements

In the late 1970's considerable effort was focused towards developing a suitable Lyapunov function expressed in terms of tangible quantities.

In 1979, System Control Incorporated [13] published a report in which the overall objective was to develop the transient energy function method (TEF)

into a potential tool for the transient stability analysis of power systems. Their contributions include:

- A clear understanding of the fact that by appropriately accounting for the fault location, the stability of a multi-machine system can be accurately assessed.
- Development of the transient energy stability analysis that is based on Lyapunov theory.
- Development of techniques for direct determination of critical clearing times, an approximate method of incorporating the effects of transfer conductances, accurate fault-on trajectory approximation and calculation of unstable equilibrium points.
- Identification of the potential energy boundary surface (PEBS) which allows for significant improvements in direct stability assessments.

This work did not prove sufficiently reliable for practical application. In certain complex modes of instability, the correct UEP could not be accurately predicted. Predictions using the PEBS gave conservative estimates of critical clearing time.

The concept of the PEBS had been proposed by Kakimoto et. al. [14] in 1978 using a Lure' type Lyapunov function. Bergen and Hill [15] developed a technique of constructing a Lyapunov function using the sparse network formulation, thus overcoming the problem of transfer conductances.

Fouad and co-workers [16,17] used a series of simulations on a practical power system to provide a physical insight into the instability phenomenon. Their conclusions may be summarized as:

- The concept of the controlling UEP is valid.

- The critical trajectory of the critical generators is controlled by the relevant UEP.
- The mode of disturbance in the controlling UEP includes severely disturbed generators not losing synchronism.
- Not all the kinetic energy contributes directly to the separation of the critical machines from the rest of the system.
- If more than one generator tends to lose synchronism, instability is determined by the gross motion of these machines.
- For practical purposes, the critical energy is equal to the energy level at the controlling UEP.
- The tool for assessing the quality of the transient response of the power system is as defined in the following paragraph. The power system, at the end of the disturbed period, possesses excess energy that must be absorbed by the system for stability to be maintained. The maximum capacity of the system to absorb this excess energy is indicative of the critical amount of transient energy that the system can initially have. The transient energy margin, is the difference between this critical amount and the actual value of transient energy the system has at the beginning of the post disturbance period. This energy margin is an indicator of the robustness of the power system (explained in section 2.5).

Further investigations followed in order to identify the complex mode of disturbances, because simulations of the fault trajectory showed that not all the severely disturbed machines lose synchronism. Fouad, Vittal and Oh [18] developed a fast and reliable technique to determine the controlling UEP by

identifying the weakest link. This technique uses the concept of "mode of disturbance (MOD)" to identify the machines that are severely affected by the disturbance. These machines are called the critical machines and generally have UEP angles greater than 90 degrees. A new technique to determine the controlling UEP was developed [19] and this uses the concept of stable manifolds of the controlling UEP and the associated gradient system. This is dealt with in detail in section 2.7.

An exhaustive analysis of the TEF method and recent improvements in the method is presented in [20]. Amongst the more recent advances in the TEF method and its applications are:

- Determination of generation shedding requirement [21]
- Dynamic security assessment by determining critical interface power flow limits [22]
- Application of TEF method to large scale power systems [23]
- Incorporation of out-of-step impedance relay [24]
- Incorporation of exciters [25]
- Incorporation of two-terminal HVDC lines [26]
- Incorporation of non-linear load models [27]
- Sensitivity of energy margin to system variables [28,29]

As a result of these advances, the conservativeness of the TEF method has been significantly reduced and the TEF method has become a very powerful tool for use by system planners and operators.

1.5 Statement of the Problem

In system operation, static security assessment is usually carried out by on-line simulation of critical contingencies to ensure that bus voltage limits and thermal limits are not exceeded. On the other hand, overall dynamic security assessment is not presently computed on-line. Current industry practice is to perform off-line studies involving typical operating conditions. These off-line studies are used to provide operating guidelines and limits to dispatchers. However, during actual operations, conditions do not correspond exactly to the scenarios used in off-line studies. As a consequence, operators use conservative limits and guidelines that result in higher operating costs. Also, it is impossible to do enough off-line simulations to provide stability guides for all possible operating conditions. For a given system, dynamic security analysis should deal with both the level of the indicator(s) of dynamic security and their trend with changing system conditions. The need for performing dynamic security analysis much closer to real time is highly recognized. In stability limited networks, several hundred contingencies have to be analyzed in short periods of time (15-30 minute cycles) to determine secure limits of operation. For this to be made possible, a smaller number of possible critical contingencies must be identified and analyzed to determine safe regimes of operation. The time constraint calls for a simplification in the computation of security margins. Also, the information obtained from the dynamic analysis should be in a framework that is suited for swift decision-making in an operating environment. An effective approach is to conduct the analysis at near real time, using actual system conditions and analyzing only those contingencies likely to cause dynamic violations. In order to expedite the

process, a contingency selection method is required to determine in advance and with assurance the set of contingencies that are severe.

1.6 Scope of this Work

The initial framework for this project was developed by Siemens, EMPROS Power Systems Division and Iowa State University. In this work, a contingency filtering scheme for on-line dynamic security assessment is developed. Severity ranking and analysis of contingencies is thought of as a filtering process. A cascade of progressively restrictive filters are used to classify and rank contingencies for dynamic security assessment. Potentially severe cases are ranked high on the contingency list for detailed analysis while non-severe cases are filtered out of the list. It is envisaged that most of the non-severe cases are identified and eliminated in the early levels of filters. The analytical work and the methodology used in these filters was developed in this work. Also, different techniques were identified and implemented to enhance accuracy and efficiency. The ultimate objective is to develop an on-line dynamic analysis program that is fully integrated with an energy management system.

2 TRANSIENT ENERGY FUNCTION METHOD

This chapter briefly introduces the TEF method, which is dealt with exhaustively in [20]. Some of the main concepts behind the TEF method, pertinent to this research, are highlighted.

2.1 The Mathematical Model - The Classical Power System Model

The mathematical model used in this work is the classical power system model [30, chapter 2]. This is the simplest power system model used in transient stability studies. It is limited to analysis of first swing transients. The assumptions made for the classical model are:

- Mechanical power input is constant.
- Damping or asynchronous power is neglected.
- The generator is represented by a constant voltage behind the direct axis transient reactance.
- The mechanical rotor angle of a synchronous generator can be represented by the angle of the voltage behind the transient reactance.

The load is usually represented by passive admittances. These admittances, calculated from the predisturbance conditions, are held constant throughout the stability study. The load nodes and the terminal voltage nodes of the generators are eliminated. The resulting bus admittance matrix contains

only the internal generator nodes. The dynamic equations for an n-machine system are given by:

$$M_i \dot{\omega}_i = P_{mi} - P_{ei} \tag{2.1}$$

$$\dot{\delta}_i = \omega_i \qquad i = 1, 2, \ldots, n \tag{2.2}$$

where,

$$P_{ei} = E_i^2 G_{ii} + \sum_{\substack{j=1 \\ j \neq i}}^{n} \left[C_{ij} \sin(\delta_i - \delta_j) + D_{ij} \cos(\delta_i - \delta_j) \right] \tag{2.3}$$

$C_{ij} = E_i E_j B_{ij}$

$D_{ij} = E_i E_j G_{ij}$

P_{mi} : Mechanical power input to generator i

E_i : Internal voltage of machine i

M_i : Inertia constant of machine i

δ_i : Electrical angle of machine i with respect to a synchronous frame of reference

ω_i : Angular speed of machine i with respect to a synchronous frame of reference

G_{ij} : Real part of the ij^{th} element of the reduced admittance matrix

B_{ij} : Imaginary part of the ij^{th} element of the reduced admittance matrix

2.2 Center of Inertia Formulation

It is necessary to distinguish between the forces that accelerate the inertial center and those that are tending to separate certain machines from the rest of the system. This is accomplished by transforming the equations into

center of inertia (COI) frame of reference [20, chapter 2]. COI formulation helps account for the energy responsible for stability (or instability) more accurately. The position of the center of inertia is defined by:

$$\delta_o = \frac{1}{M_T} \sum_{i=1}^{n} M_i \, \delta_i \tag{2.4}$$

$$\dot{\delta}_o = \frac{1}{M_T} \sum_{i=1}^{n} M_i \, \dot{\delta}_i \tag{2.5}$$

where,

$$M_T = \sum_{i=1}^{n} M_i \tag{2.6}$$

The motion of the COI is defined by the equations

$$M_T \, \dot{\omega}_o = \sum_{i=1}^{n} (P_{mi} - P_{ei}) = P_{COI} \tag{2.7}$$

$$\dot{\delta}_o = \omega_o \qquad i = 1, 2, \ldots, n \tag{2.8}$$

Define the generator's angles and speeds relative to the COI by

$$\theta_i = \delta_i - \delta_o \tag{2.9}$$

$$\tilde{\omega}_i = \dot{\delta}_i - \dot{\delta}_o \tag{2.10}$$

The equations of motion of the generators in the COI frame of reference are now given by

$$M_i \, \dot{\tilde{\omega}}_i = P_{mi} - P_{ei} - \frac{M_i}{M_T} P_{COI} \tag{2.11}$$

$$\dot{\theta}_i = \tilde{\omega}_i \qquad i = 1, 2, \ldots, n \tag{2.12}$$

By definition of the COI coordinates, θ_i and $\tilde{\omega}_i$ are not linearly independent and satisfy the relationship

$$\sum_{i=1}^{n} M_i \, \theta_i = 0 \tag{2.13}$$

$$\sum_{i=1}^{n} M_i \, \tilde{\omega}_i = 0 \tag{2.14}$$

2.3 The Transient Energy Function

The energy function [20, chapter 5] for the post-disturbance system is obtained in the following manner. The i^{th} post-disturbance dynamic equation is multiplied by $\dot{\theta}_i$. The following sum is then formed

$$\sum_{i=1}^{n} \left(M_i \dot{\tilde{\omega}}_i - P_{mi} + P_{ei} + \frac{M_i}{M_T} P_{COI} \right) \dot{\theta}_i \tag{2.15}$$

The above expression is integrated with respect to time. Using as a lower limit $t = t^s$ (where $\tilde{\omega}(t^s) = 0$ and $\theta(t^s) = \theta^{s2}$, the post-disturbance equilibrium point), we obtain

$$V = \frac{1}{2} \sum_{i=1}^{n} M_i \tilde{\omega}_i^2 - \sum_{i=1}^{n} P_i (\theta_i - \theta_i^{s2})$$

$$- \sum_{i=1}^{n-1} \sum_{j=i+1}^{n} \left[C_{ij} (\cos\theta_{ij} - \cos\theta_{ij}^{s2}) - \int_{\theta_i^{s2} + \theta_j^{s2}}^{\theta_i + \theta_j} D_{ij} \cos\theta_{ij} d(\theta_i + \theta_j) \right] \tag{2.16}$$

The terms of the transient energy function can be interpreted in the following manner (all changes are calculated with respect to the post-disturbance stable equilibrium point)

- $\frac{1}{2} \sum_{i=1}^{n} M_i \tilde{\omega}_i^2$ (2.17)

  This represents the total change in kinetic energy of all generator rotors relative to the COI.

- $\sum_{i=1}^{n} P_i (\theta_i - \theta_i^{s2})$ (2.18)

This represents the change in position energy of all rotors relative to the COI.

- $C_{ij}\,(cos\theta_{ij} - cos\theta_{ij}^{s2})$ (2.19)

  This represents the change in the stored magnetic energy of branch ij.

- $\int_{\theta_i^{s2} + \theta_j^{s2}}^{\theta_i + \theta_j} D_{ij}\, cos\theta_{ij} d(\theta_i + \theta_j)$ (2.20)

  This represents the change in the dissipation energy of branch ij.

The term in the energy expression corresponding to the dissipation component consists of a path dependent integral. To evaluate this integral, the system trajectory must be known. Uyemura [11] developed an approximation to this term based on a linear angle trajectory approximation. Using this approximation, equation (2.16) can be rewritten as

$$V = \frac{1}{2} \sum_{i=1}^{n} M_i\, \tilde{\omega}_i^2 - \sum_{i=1}^{n} P_i\, (\theta_i - \theta_i^{s2}) - \sum_{i=1}^{n-1} \sum_{j=i+1}^{n} \left[C_{ij}\,(cos\theta_{ij} - cos\theta_{ij}^{s2}) - I_{ij} \right] \tag{2.21}$$

where,

$$I_{ij} = D_{ij}\, \frac{\theta_i + \theta_j - \theta_i^{s2} - \theta_j^{s2}}{\theta_{ij} - \theta_{ij}^{s2}} (sin\,\theta_{ij} - sin\,\theta_{ij}^{s2}) \tag{2.22}$$

2.4 Corrected Kinetic Energy

It was observed [3] that not all the transient kinetic energy, created by the disturbance, contributes to the instability of the system. Some of this kinetic

energy is responsible for the inter-machine motion between the generators and does not contribute to the separation of the severely disturbed generators from the rest of the system. For more accurate transient stability assessment, the component of kinetic energy not contributing to system separation should be subtracted from the energy that needs to be absorbed for stability to be maintained. The transient kinetic energy responsible for separation of the critical generators from the rest of the system was that associated with the gross motion of the critical generators.

The disturbance splits the generators into two groups: (1) the critical machines, and (2) the rest of the generators. Let their inertial centers have inertia constants and angular speeds M_{cr}, $\tilde{\omega}_{cr}$ and M_{sys}, $\tilde{\omega}_{sys}$ respectively. The kinetic energy causing the separation of the two groups is termed as the corrected kinetic energy and is given by

$$V_{KEcorr} = \frac{1}{2} M_{eq} \tilde{\omega}_{eq}^2 \tag{2.23}$$

where,

cr = index for set of critical generators

sys = index for set of non-critical generators (rest of the system)

$$M_{eq} = \frac{M_{cr} \cdot M_{sys}}{M_{cr} + M_{sys}}$$

$$\tilde{\omega}_{eq} = \tilde{\omega}_{cr} - \tilde{\omega}_{sys}$$

$$M_{cr} = \sum_{i \in cr} M_i$$

$$M_{sys} = \sum_{i \in sys} M_i$$

$$\tilde{\omega}_{cr} = \left(\sum_{i \in cr} M_i \tilde{\omega}_i \right) / M_{cr}$$

$$\tilde{\omega}_{sys} = \left(\sum_{i \in sys} M_i \tilde{\omega}_i \right) / M_{sys}$$

2.5 Transient Stability Assessment

Transient stability assessment is done by comparing two values of the transient energy V. The first value of V is computed at the end of the disturbance, i.e., at fault clearing (V_{cl}). The second value of V, which determines the accuracy of the stability assessment, is the critical value, V_{cr}. V_{cr} is the potential energy at the controlling unstable equilibrium point (UEP) for the fault under consideration. The concept of controlling UEP is dealt with in the next section. The assessment is made as

$$\Delta V = V_{cr} - V_{cl} \tag{2.24}$$

Using the linear angle path trajectory for the dissipation term between the conditions at clearing and the controlling UEP, ΔV can be rewritten as

$$\Delta V = -\frac{1}{2} M_{eq} \tilde{\omega}_{eq}^2 - \sum_{i=1}^{n} P_i \left(\theta_i^u - \theta_i^{cl}\right) - \sum_{i=1}^{n-1} \sum_{j=i+1}^{n} \left[C_{ij} \left(\cos\theta_{ij}^u - \cos\theta_{ij}^{cl}\right) - D_{ij} \frac{\theta_i^u + \theta_j^u - \theta_i^{cl} - \theta_j^{cl}}{\theta_{ij}^u - \theta_{ij}^{cl}} \left(\sin\theta_{ij}^u - \sin\theta_{ij}^{cl}\right) \right] \tag{2.25}$$

where $(\theta^{cl}, \tilde{\omega}^{cl})$ are the conditions at clearing and $(\theta^u, 0)$ represents the controlling UEP.

If $\Delta V > 0$, the system is stable. On the other hand, if $\Delta V < 0$, the system is unstable. The transient energy margin gives an indication of how much energy the system can absorb before instability occurs. A more severe disturbance, as indicated by the transient energy at the end of the disturbance,

can be tolerated if it does not exceed the margin. The component of transient energy at the end of the disturbance that needs to be converted to other forms of energy for stability to be maintained is the corrected kinetic energy. A qualitative measure of the degree of stability is obtained if ΔV is normalized with respect to the corrected kinetic energy at the end of the disturbance [3]. This normalized energy margin is given by

$$\Delta V_n = \Delta V \ / \ V_{KEcorr} \tag{2.26}$$

and is a true measure of the severity of the disturbance.

2.6 Concept of the Controlling Unstable Equilibrium Point

The UEP refers to a set of generator angles that satisfy the equation

$$f_i = P_{mi} - P_{ei} - \frac{M_i}{M_T} P_{COI} = 0 \quad i = 1, 2, \ldots, n \tag{2.27}$$

For a power system with n-generators, there are $(2^{n-1} - 1)$ solutions to the above equation. Each of these solutions give a different transient stability assessment. It is absolutely essential to identify the correct controlling UEP for accurate transient stability assessment.

Different theories [10,13,31,32] have been proposed to determine the correct controlling UEP. Analysis done in [3,16] showed that the controlling UEP could be among a group of UEP's located in the direction in which the severely disturbed generators following a disturbance move. In [18], it was determined that following the transient, the severely disturbed generators may not lose synchronism with the rest of the system. It was also proposed in [18] that

The post-disturbance trajectory approaches (if the disturbance is large enough) the controlling UEP. This is the UEP with the lowest normalized potential energy margin at the instant the disturbance is removed.

The normalized potential energy margin is given by

$$\Delta V_{PEn} = \Delta V_{PE} \; / \; V_{KEcorr} \tag{2.28}$$

where,

$$\Delta V_{PE} = - \sum_{i=1}^{n} P_i \, (\theta_i^u - \theta_i^{cl}) - \sum_{i=1}^{n-1} \sum_{j=i+1}^{n} \left[C_{ij} \, (\cos\theta_{ij}^u - \cos\theta_{ij}^{cl}) - D_{ij} \, \frac{\theta_i^u + \theta_j^u - \theta_i^{cl} - \theta_j^{cl}}{\theta_{ij}^u - \theta_{ij}^{cl}} \, (\sin\theta_{ij}^u - \sin\theta_{ij}^{cl}) \right] \tag{2.29}$$

and V_{KEcorr} is the corrected kinetic energy based on the mode of disturbance (MOD) [20, chapter 6] of the UEP chosen. The advanced generators for the controlling UEP constitute the MOD of that particular UEP.

The TEF procedure has the capability to determine the controlling UEP based on either the

- Mode of disturbance procedure [20, chapter 6]
- Exit point procedure [19, 20 (chapter 6)]

In this research, the exit point procedure is used to identify the controlling UEP.

2.7 Potential Energy Boundary Surface (PEBS)

Mathematically, the transient stability analysis is conducted to determine the stability of the post-fault system trajectory. The concept of PEBS was initially propounded by Kakimoto et. al. [14] and later extended by Athay et. al.

[33] and other researchers. This method, for a given disturbance trajectory, determines a local approximation of the stability boundary. It is basically defined by the following constructive procedure [34].

Starting from the post-fault stable equilibrium point (SEP), draw a ray in every direction in angle-space in the COI reference frame. Along each ray emanating from the SEP find the first point where the potential function achieves its relative maximum. The set of points found in this way characterize the boundary surface of interest.

For a n-machine power system, we have

$$f_i(\theta) = P_{mi} - P_{ei} - \frac{M_i}{M_T} P_{COI} \tag{2.30}$$

The potential energy is then given by

$$V_{PE}(\theta) = - \sum_{i=1}^{n} \int_{\theta_i^{s2}}^{\theta_i} f_i(\theta)\, d\theta_i \tag{2.31}$$

where, θ_i^{s2} is the post-disturbance SEP. Using a linear path assumption, we can approximate the potential energy function. Now, if the equation

$$\frac{dV_{PE\,approx}}{d\theta} = 0 \tag{2.32}$$

is satisfied for some θ^*, then it implies θ^* satisfies

$$\sum_{i=1}^{n} f_i(\theta)\,(\theta_i - \theta_i^{s2}) = 0 \tag{2.33}$$

The significance of this is that, along the straight path (in θ-space) emanating from the post fault SEP, the potential function is maximized for the first time at θ^*. This means that the PEBS can be characterized in θ-space by

setting the directional derivative of the potential energy function equal to zero along rays emanating from the post-fault SEP.

2.7.1 Characterization of the PEBS

Consider the differential equation

$$\dot{X} = f(X) \tag{2.34}$$

The derivative of f at a point X^a is called the Jacobian matrix at X^a. An equilibrium point is hyperbolic if the Jacobian has no eigenvalues with zero real parts. If X^a is a hyperbolic equilibrium point, then the stable and unstable manifolds of X^a are defined as

$$W^s(X^a) = \{X_0 : X(t,X_0) \to X^a \text{ as } t \to \infty\} \tag{2.35}$$

$$W^u(X^a) = \{X_0 : X(t,X_0) \to X^a \text{ as } t \to -\infty\} \tag{2.36}$$

Where W^s refers to the stable manifold and W^u to the unstable manifold.

Let X^i, i = 1,2,3, ... be the unstable equilibrium points on the stability boundary of a SEP X^s and E be the set of all equilibrium points, then

$$\partial A = \bigcup_{X^i = E \cup \partial A} W^s(X^i) \tag{2.37}$$

The stability boundary ∂A is the union of all the stable manifolds of those UEPs contained in the intersection of E and ∂A. This stability boundary helps us determine the PEBS [20, chapter 4].

2.7.2 The Exit Point

The exit point of the trajectory $x(t)$ determined by the point x^c is the point where the fault-on trajectory crosses the stability boundary $\partial A(X^s)$. If the exit point lies on the stable manifold of the point x^{co}, then we call x^{co} as the

controlling UEP. The concept of controlling UEP is justified by the PEBS [20, chapter 4].

The exit point is determined by the following procedure. For the faulted system trajectory, the first maximum of the potential energy is found, with respect to the post-disturbance network. The faulted trajectory is obtained by integrating the equations

$$M_i \dot{\tilde{\omega}}_i = P^f_{mi} - P^f_{ei} - \frac{M_i}{M_T} P^f_{COI} \tag{2.38}$$

$$\dot{\theta}_i = \tilde{\omega}_i \quad i = 1,2, \ldots, n \tag{2.39}$$

The values of θ obtained from solving for the above conditions are now substituted into the post-fault mismatch equations. The mismatch function is given by

$$f_i = P^{pf}_{mi} - P^{pf}_{ei} - \frac{M_i}{M_T} P^{pf}_{COI} \tag{2.40}$$

The exit point is determined when the condition $\sum_{i=1}^{n} - f_i \tilde{w}_i = 0$ is satisfied. The zero crossing along the faulted trajectory is detected by a change in the sign of the quantity $\sum_{i=1}^{n} - f_i \tilde{w}_i$. Once the change has been detected, the bisection method is used to determine the exit point accurately.

2.8 Steps to Determine the Controlling UEP using the Exit Point Method

The procedure to determine the controlling unstable equilibrium point consists of the following steps:

- Determine the exit point x^e on the stable manifold of the controlling UEP as explained in the above section.

- Use θ^{e} obtained in the previous step as the starting point. Integrate the associated gradient system equations that are given by

$$\dot{\theta}_i = P_{mi}^{pf} - P_{ei}^{pf} - \frac{M_i}{M_T} P_{COI}^{pf} \qquad i = 1, 2, \ldots, n-1 \tag{2.41}$$

$$\dot{\theta}_n = - \sum_{i=1}^{n-1} M_i \dot{\theta}_i \; / M_n \tag{2.42}$$

At each step of the integration the quantity $\sum_{i=1}^{n} |f_i| = F$ is evaluated. This is done to determine the first minimum of F along the gradient surface. This point is referred to as the *minimum gradient point* (MGP). θ^{*} denotes the vector of rotor angles at this point.

- θ^{*} is used as the starting point and the UEP solution is obtained. The equilibrium point (the unstable equilibrium point here) is found by determining the solution to the system of nonlinear algebraic equations given by

$$f_i = P_{mi} - P_{ei} - \frac{M_i}{M_T} P_{COI} = 0 \qquad i = 1, 2, \ldots, n \tag{2.43}$$

The two popular approaches to solving such a system of equations are the direct solution approach and the indirect solution approach. The modified Newton-Raphson procedure and the Newton method of nonlinear least squares minimization are used to determine the equilibrium point.

3 CONTINGENCY FILTERING SCHEME

This chapter details the contingency filtering scheme for the selection and ranking of contingencies for dynamic security analysis. The framework was developed by Siemens, EMPROS Power Systems Division and Iowa State University. The proposed scheme is based on the use of a cascade of progressively more restrictive filters to classify and rank contingencies. Severity ranking and analysis of contingencies is thought of as a filtering process where the most severe cases are identified and ranked high on the contingency list for more detailed analysis. The non-severe cases, on the other hand are filtered out of the list.

There are three different levels of filters used in this scheme. The model used in all the filters is the classical power system model. These filters differ in the approximations made in the transient stability assessment. Successive levels of contingency filters are computationally more intensive and more accurate. Once the final list of critical contingencies is obtained, they can be analyzed in detail using conventional time domain simulation.

3.1 Assumptions and Philosophy of Filters

It is assumed that the dynamic security being assessed is of a power system subjected to a large disturbance. A large disturbance is defined as a sudden change in a power system parameter or operating condition such that the equations describing the transient response cannot be linearized for the

purpose of analysis [4]. The phenomena of interest are whether the disturbance will cause loss of synchronism among generators, or unacceptable system performance like transient voltage dips, power swings etc. The analysis focuses only on the transient phenomena following a large disturbance. The transient analysis can be considered as being divided into two periods. Each of these periods is characterized by different forces determining the system behavior. These periods are

- The inertial transient period in which the dominant forces are the generator's synchronizing powers and their inertias. Continuous controls like high gain and fast exciters may influence this period. This transient is commonly thought of as being of 2 seconds duration. However, the current stressed network conditions could lead to longer transients. An inertial transient period of 0 - 5 seconds is adopted.
- The post-inertial transient period in which the dominant forces in addition to the network conditions, are the controls. The controls mainly include protective schemes and discrete supplementary controls. It is assumed that following the initial disturbance, no other external event takes place. All additional disturbances are introduced internally as a result of built in controls or protection schemes. The period considered is 5 - 20 seconds after the inception of the disturbance.

Following a large disturbance, the power system goes through two distinct phases. These are the disturbance phase and the restorative phase. The outcome, e.g., whether angle stability or instability may result, will

depend on the relative influence of both phases. There are two distinct aspects of the problem.

- the *disturbance severity*
- the post-disturbance *network robustness*

The significance of the above distinction is that it permits the grouping of diverse events and situations in a more concise framework for classification and screening. For example, the severity of the disturbance can be measured by the degree with which the severely disturbed generators are impacted by it. A certain 'class' of severity can be reached by a variety of factors like type of disturbance, different scenarios of the same disturbance and different fault locations. Similarly, the post-disturbance network robustness depends on its ability to arrive at a stable equilibrium condition for the disturbed generators. This on the other hand depends on a number of factors like network connectivity, distribution and pattern of power flow in the transmission network, voltage and MVAR distribution.

In dealing with the post-inertial transient, as mentioned earlier, it is assumed that no additional external events are introduced. There are two main factors which determine the outcome of the post-inertial transient. The first factor is the structure of the power network, i.e., network robustness. The other factor is the additional events which may occur as a result of the inertial disturbance sequence. The attributes associated with the effect of the transient on the network can be identified at an earlier time in the transient, since they represent indications of a stressed power network. "Signatures" of such structurally weakened power networks are analyzed at the end of the inertial

transient period to provide an indication of potential problems during the post-inertial period.

3.2 Filter Development

In this contingency filtering scheme, three levels of filters are considered. At each level, there are two sets of filters

- *inertial transient filter (ITF)*
- *post-inertial transient filter (PITF)*

Figure 3.1 shows the configuration of the contingency screening filters. Let us consider n to be the total number of contingencies. These n contingencies (defined in terms of fault type, location, duration and sequence of events making up the scenario) are passed to the first inertial transient filter *(ITF 1)*. This filter will classify the n contingencies into three groups:

- x non-severe cases with respect to the inertial transient
- u severe cases
- z potentially severe cases

The severe cases are those cases which are steady state unstable or have a negative energy margin ($\Delta V_{napprox1} < 0$). A case is said to be steady state unstable if does not have a stable post-disturbance equilibrium point. In other words, the post-disturbance equilibrium point and the controlling unstable equilibrium point are the same. The concept of $\Delta V_{napprox1}$ is explained in the next section. The u severe cases are directly sent to *ITF 3*. The x non-severe cases are passed to the *PITF 1* and the z potentially severe cases are sent to the next level of filter *ITF 2*. This filter further classifies these retained cases into two groups:

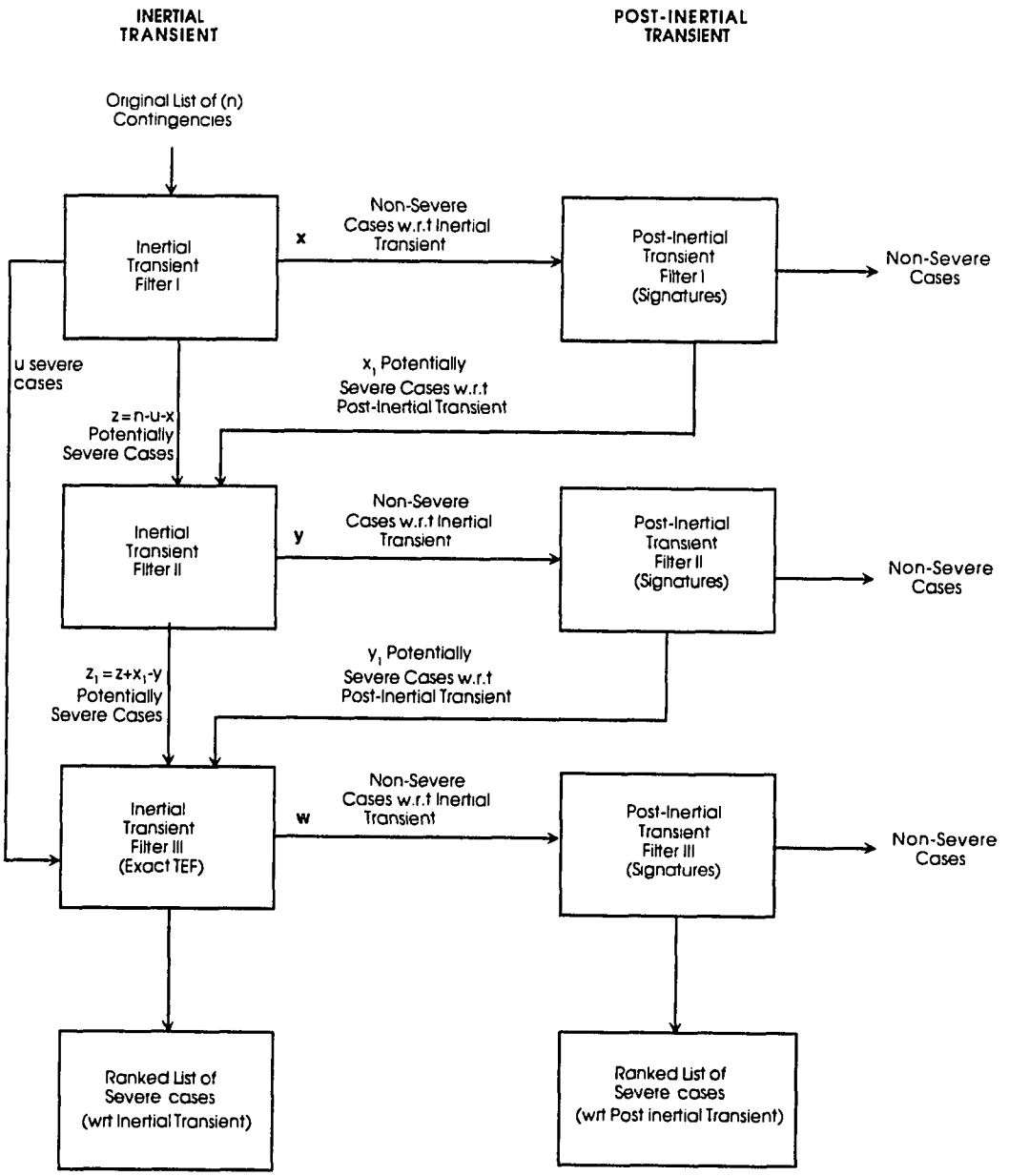

Fig. 3.1. Conceptual outline of the filtering scheme

- y non-severe cases with respect to the inertial transient
- z_1 potentially severe cases

The y non-severe cases with respect to the inertial transient are sent to the *PITF 2*. On the other hand, the z_1 potentially severe cases are passed to the last level of filters, *ITF 3*. *ITF 3* uses exact TEF calculations to classify the retained cases into two groups:

- w non-severe cases with respect to the inertial transient
- s_1 severe cases with respect to the inertial transient

The w non-severe cases with respect to the inertial transient are sent to *PITF 3* . This filter then creates a list

- s_2 severe cases with respect to the post-inertial transient

It can be noticed that for the different levels of inertial filters, all the cases deemed to be non-severe are passed on to the appropriate post-inertial transient filter. The motivation for this approach is to capture such peculiar cases which may indeed be harmless in the inertial transient period, but turn out to be problematic in the post-inertial transient period. Thus x non-severe cases from *ITF 1* are processed by *PITF 1*, resulting in x_1 potentially severe cases with respect to the post-inertial transient period. These are then fed to *ITF 2* for further analysis. Similarly, y non-severe cases are processed by *PITF 2*, resulting in y_1 potentially severe cases, which are fed to *ITF 3* for further analysis. Cases which are not deemed severe by the post-inertial transient filters are eliminated. It is envisaged that a large number of cases (from the original contingency list) get eliminated in the first and second level of filters. Table 3.1 lists the number of cases analyzed in each filter.

Table 3.1 Cases analyzed in each of the filters mentioned

Filter	*Number of Cases Analyzed*
ITF 1	n
ITF 2	z *(from ITF 1)* + x_1 *(from PITF 1)*
ITF 3	u *(from ITF 1)* + z_1 *(from ITF 2)* + y_1 *(from PITF 2)*
PITF 1	x *(from ITF 1)*
PITF 2	y *(from ITF 2)*
PITF 3	w *(from ITF 3)*

3.3 Inertial Transient Filters

There are three different levels of inertial transient filters *ITF 1*, *ITF 2* and *ITF 3*. The level of modeling in each of the filters is identical. The difference in the filters is characterized by the three distinct stages in the TEF method. These three stages are:

- Stage 1: Determination of the exit point
- Stage 2: Determination of the minimum gradient point
- Stage 3: Determination of the controlling UEP

Each of the above distinct stages are explained in chapter 2. It can be seen that the TEF procedure inherently refines the solution to the controlling unstable equilibrium point as it progresses through the various stages. In the design of the inertial transient filters, use is made of the progressive steps in the TEF method to construct progressively restrictive filters.

- Stage 1: Associated with *ITF 1* and *PITF 1*

- Stage 2: Associated with *ITF 2* and *PITF 2*
- Stage 3: Associated with *ITF 3* and *PITF 3*

A description of each of the filters is given below.

3.3.1 Inertial Transient Filter 1

This filter is intended to be a coarse filter and will perform fast approximate calculations using the TEF method. In this filter, the controlling UEP is not evaluated. The exit point is used as an approximation to the UEP. All the calculations are made at the exit point. As described earlier, the underlying philosophy hinges on dealing with the complete transient scenario as two distinct entities (the disturbance severity and the post-disturbance network robustness).

Disturbance Severity

In this filter, the disturbance is simulated and the conditions at the end of the disturbance are used to evaluate indices of disturbance severity. For disturbances with finite duration, this index is the total kinetic energy V_{KE} gained by the system during the disturbed period. This is a significant departure from the usual TEF analysis where the corrected kinetic energy ΔV_{KEcorr} [20, chapter 5] based on the mode of disturbance of the controlling UEP is used as a measure of disturbance severity. For disturbances which do not have a finite duration (like loss of generation, loss of a transmission line), where the system moves instantaneously from the pre-disturbance equilibrium to the post-disturbance state, this index will be characterized by the potential energy at the end of the disturbance.

Post-disturbance Network Robustness

Using the disturbance scenario, and knowing the equipment tripped following the disturbance, each post-disturbance configuration will be analyzed to obtain an approximation to the network robustness. The exit point is determined by integrating the faulted swing equations, and finding the first maximum of potential energy for the post-disturbance network along this trajectory. The potential energy difference between the exit point and the point at the end of the disturbance provides an index of the post-disturbance network robustness.

Categorizing the Scenarios

Based on the disturbance severity and the post-disturbance network robustness indices, an overall index is evaluated. This is the approximate normalized energy margin $\Delta V_{napprox1}$ given by

$$\Delta V_{napprox1} = (\Delta V_{PEapprox1} - V_{KE}) / V_{KE} \tag{3.1}$$

where $\Delta V_{PEapprox1}$ is the potential energy difference between the exit point and clearing. V_{KE} is the total kinetic energy. A threshold for $\Delta V_{napprox1}$ is selected. All contingencies with $\Delta V_{napprox1}$ below this threshold are passed on to the next level of filter *ITF 2*. All the other contingencies are passed on to *PITF 1*. As described in chapter 2, the exact expression for the normalized energy margin is given by

$$\Delta V_{n} = (\Delta V_{PE} - V_{KEcorr}) / V_{KEcorr} \tag{3.2}$$

where ΔV_{PE} is the potential energy difference between the exact controlling UEP and the conditions at the end of the disturbance. V_{KEcorr} is the corrected kinetic energy based on the mode of disturbance of the controlling UEP. V_{KE} is the total kinetic energy and is significantly greater than V_{KEcorr}. As a result, in using equation (3.2), a larger quantity is subtracted from $\Delta V_{PEapprox1}$. Also, the normalization is done by the same larger quantity.

3.3.2 Inertial Transient Filter 2

In this filter, the procedure described in *ITF 1* is repeated on the potentially severe cases retained by *ITF 1* and *PITF 1* respectively. The approximation to the controlling UEP is improved upon by using the minimum gradient point. The scenarios are categorized based on the approximate normalized energy margin

$$\Delta V_{napprox2} = (\Delta V_{PEapprox2} - V_{KE}) / V_{KE} \tag{3.3}$$

where $\Delta V_{PEapprox2}$ is the potential energy difference between the minimum gradient point and the conditions at the end of the disturbance. Similar to *ITF 1*, a threshold is chosen for $\Delta V_{napprox2}$. If $\Delta V_{napprox2}$ for a given contingency is below this threshold, it is sent to *ITF 2*. Otherwise it is sent to *PITF 2*.

3.3.3 Inertial Transient Filter 3

This filter derives its input from *ITF 1*, *ITF 2* and *PITF 2*. The disturbance severity and post-disturbance network robustness indices are evaluated using exact calculation of the controlling UEP. The exact

normalized energy margin is given in equation (3.2) and repeated here for convenience.

$$\Delta V_n = (\Delta V_{PE} - V_{KEcorr}) / V_{KEcorr} \quad (3.4)$$

It is possible now to compute the controlling UEP of all the cases that are in *ITF 3*. This is because of the fact that at the previous levels of filters, a large number of the original cases will have been eliminated. A final ranking is now provided of the cases retained in *ITF 3*. A description of the ranking scheme is given in section 3.5.

3.4 Post-Inertial Transient Filters

At each level of the filtering scheme, there is a post-inertial transient filter associated with the respective inertial transient filters. These post-inertial transient filters derive inputs from contingency cases deemed not severe by the inertial transient filters. These cases are analyzed to ascertain if they are potentially vulnerable to problems during the post-inertial transient period. The analysis is based on the argument that any power system which is vulnerable in the post-inertial period leaves a signature of its behavior during the inertial transient period. This signature is mainly characterized by a highly stressed post-disturbance network. As a result, these indicators of stress (discussed in section 3.4.1) are used to identify cases which could potentially cause problems in the post-inertial transient period.

3.4.1 Post-Inertial Transient Filter 1

This filter derives its inputs from contingency cases deemed not severe by *ITF 1*. The indicators of stress used in this filter are

- Threshold checks of the form $\Delta V_{napprox1} > Threshold\ a$ and $V_{KE} < Threshold\ b$.
- Large sensitivities of $\Delta V_{napprox1}$ to network topology changes and generation changes.
- Post-disturbance equilibrium θ^{s2} includes machines with large angles.
- Synchronizing power coefficients [30, chapter 3] P_{sij} with a very small positive value or negative value.

The significance of each of the candidate signatures mentioned above is explained here.

- Threshold checks of the form $\Delta V_{napprox1} > Threshold\ a$ and $V_{KE} < Threshold\ b$ are essential in terms of determining the post-disturbance network robustness and the disturbance severity. Cases which do not meet the check reflect a comparatively low post-disturbance network robustness or high disturbance severity or both.
- Sensitivities of the approximate energy margin $\Delta V_{napprox1}$ to changes in network topology and generation patterns help determine if the contingency is potentially severe with respect to these changes. If the sensitivities are large, there is a need to further analyze these cases. The concept of how these sensitivities are derived and used is described in detail in chapter 4.

- Large angles in the post-disturbance stable equilibrium points could imply the fact that the post-disturbance network is stressed. It could also happen that the system is steady state unstable. In this case θ^{s2} is the same as the controlling UEP.
- The synchronizing power coefficient is given by P_{sij} and can be defined as the"*change in the electrical power of a given machine due to the change in the angle between its internal voltage and any bus, with all other bus angles held constant*". A higher positive value of P_{sij} is indicative of a lower loading condition. It also implies a greater ability to transmit synchronizing power.

The following is a brief derivation of the synchronizing power coefficient. The electrical power output of a machine i is given by

$$P_{ei} = E_i^2 G_{ii} + \sum_{\substack{j=1 \\ j \neq i}}^{n} \left[C_{ij} \sin(\delta_i - \delta_j) + D_{ij} \cos(\delta_i - \delta_j) \right] \tag{3.5}$$

Making use of the incremental model where $\delta_{ij} = \delta_{ij0} + \delta_{ij\Delta}$ and the fact that

$$\sin\delta_{ij} \cong \sin\delta_{ij0} + \delta_{ij\Delta} \cos\delta_{ij0} \tag{3.6}$$

$$\cos\delta_{ij} \cong \cos\delta_{ij0} - \delta_{ij\Delta} \sin\delta_{ij0} \tag{3.7}$$

$P_{ei\Delta}$ can be computed as

$$P_{ei\,\Delta} = \sum_{\substack{j=1 \\ j \neq i}}^{n} \left[C_{ij} \sin(\delta_{ij0}) - D_{ij} \cos(\delta_{ij0}) \right] \delta_{ij\Delta} \tag{3.8}$$

In the above equation, if the initial conditions are given, the term $C_{ij} \sin(\delta_{ij0}) - D_{ij} \cos(\delta_{ij0})$ can be calculated. This implies that the equation (3.8) can be rewritten as

$$P_{ei\,\Delta} = \sum_{\substack{j=1 \\ j \neq i}}^{n} P_{sij}\,\delta_{ij\Delta} \tag{3.9}$$

where,

$$P_{sij} = \frac{\partial P_{ij}}{\partial \delta_{ij}} = C_{ij}\,sin\,(\delta_{ij0}) - D_{ij}\,cos\,(\delta_{ij0}) \tag{3.10}$$

The signatures are used in a logical fashion in the post-inertial transient filters. This is explained in the following sequential order for each case that enters the *PITF 1*. Also, the same is illustrated in figure 3.2.

step1: The case is checked against the threshold of the form $\Delta V_{napprox1} > Threshold\ a$ and $V_{KE} < Threshold\ b$.

step2: If the threshold conditions are met, go to step 4. Otherwise, go to step 3.

step3: Check the case for sensitivity of $\Delta V_{napprox1}$, P_{sij} and large angles in θ^{s2}. If the case does not meet the threshold for any of the above signatures, it is eliminated. Otherwise, it is sent to the next level of inertial transient filters.

step4: Check the case for P_{sij} and large angles in θ^{s2}. If the case does not meet the threshold for any of the signatures, it is eliminated. Otherwise, it is sent to the next level of inertial transient filters.

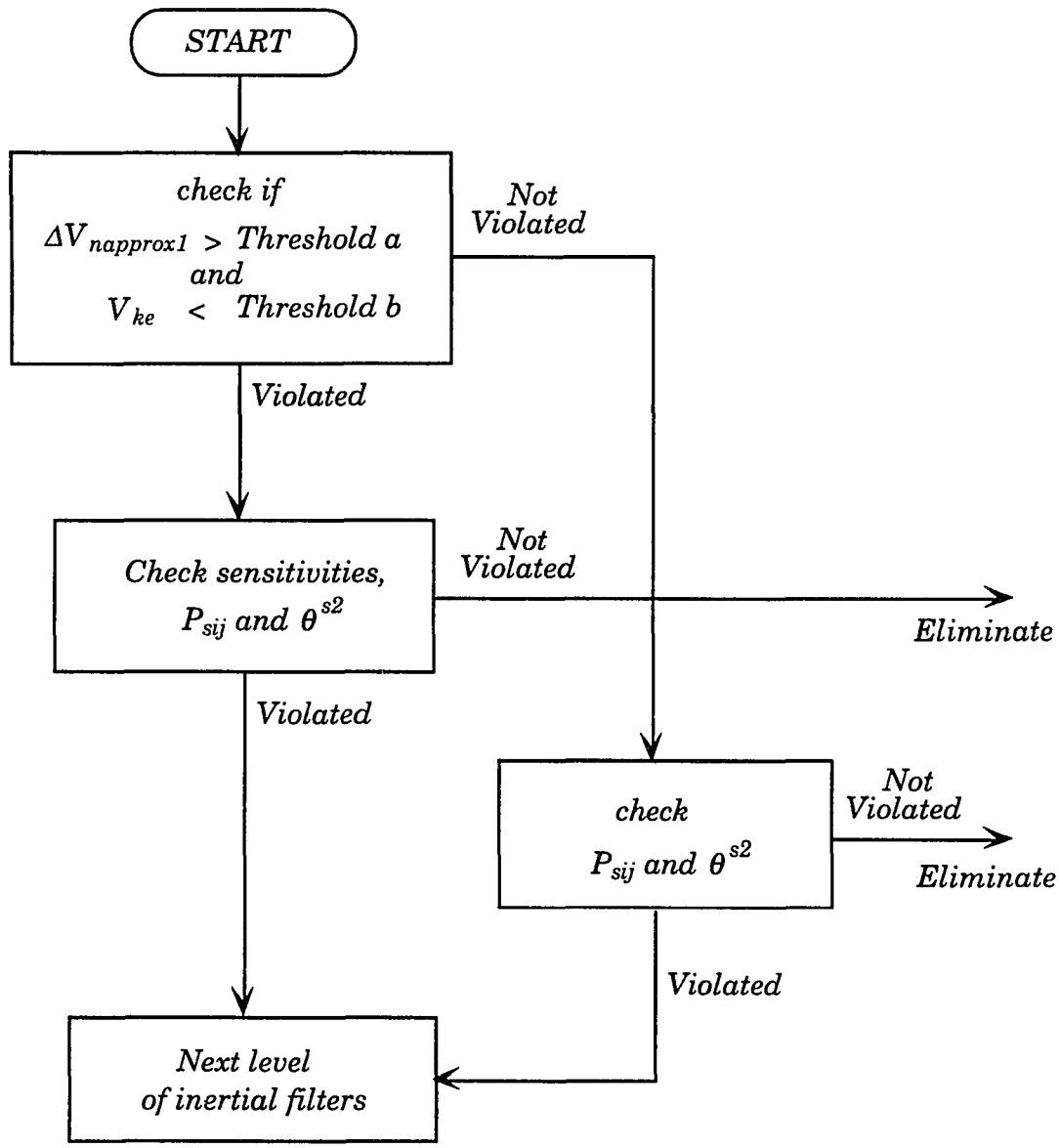

Fig. 3.2. Flow chart to illustrate the procedure followed in the post-inertial transient filters

3.4.2 Post-Inertial Transient Filter 2

This filter derives its inputs from contingency cases deemed non-severe by *ITF 2*. The philosophy and operation of this filter are identical to that of *PITF 1* described above. The improvement in this filter is derived from the use of more accurate calculations (at the minimum gradient point) in the TEF method. $\Delta V_{napprox2}$ replaces $\Delta V_{napprox1}$ in this filter. Cases which seem to have potential problems are sent to *ITF 3*.

3.4.3 Post-Inertial Transient Filter 3

This filter derives its input from *ITF 3* which uses the exact TEF analysis. The logic followed in this filter is identical to that in the previous *PITF* filters. The difference is that the analysis is carried out based on results obtained using the exact TEF analysis where the controlling UEP is explicitly determined. Also, a final ranking is provided in this filter of cases which are deemed to have potential problems with respect to the post-inertial transient period. A description of the ranking scheme is given in section 3.5.

3.5 Ranking

This section describes the methodology for the final ranking in *ITF 3* and *PITF 3* respectively. In both filters, two different ordered lists are formed. ΔV_n is not the only index based on which contingency ranking is done. ΔV_n provides only an overall ranking of the stability of the system for the existing conditions. However, in analyzing dynamic security, an important aspect of the analysis from an operator's perspective deals with the determination of the change of this index due to changes in system operating conditions and critical

system parameters [22]. These changes (like shifts in generation pattern, load or network structure) are pre-specified along with the original list of contingencies. Based on this information, sensitivity calculations are carried out. The concept of how sensitivity information is pertinent is illustrated in figure 3.3. Figure 3.3 shows two contingencies which have the same energy margin in the base case. However, on changing the operating parameter, contingency 2 can be seen to be more critical. This is because of the fact that contingency 2 as opposed to contingency 1 has a large sensitivity to the operating parameter which is likely to change.

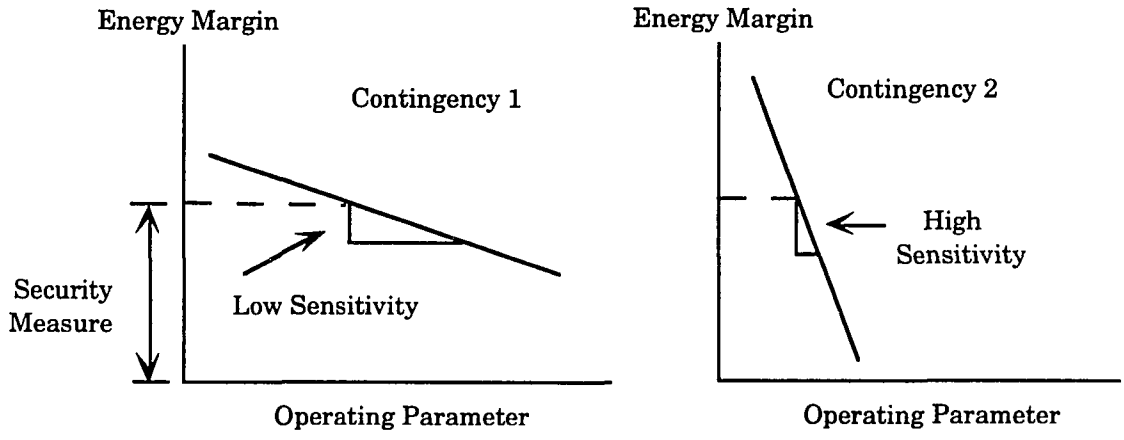

Figure 3.3 Illustration of the importance of sensitivity analysis

In *ITF 3*, the sensitivity of ΔV_n to plant generation changes provides the other ranked list. The initial ranked list is based on the magnitude of ΔV_n. In *PITF 3*, the sensitivity of ΔV_n to plant generation changes and network topology changes is considered. Here, ranked lists are provided for both susceptibility to plant generation changes and network topology changes. This is in addition to the ranked list based on the magnitude of ΔV_n. These lists give the operator the critical contingencies for the current operating conditions and

also for different scenarios (corresponding to new generation patterns and post-disturbance networks).

3.6 Determination of the different thresholds

Thresholds are used to distinguish between cases in both the inertial and post-inertial transient filters. The selection of these thresholds is important to ensure that all the critical contingencies are captured. In this research, a heuristic approach is used to determine these thresholds. These thresholds are system dependent. For a given system, a certain number of TEF calculations are made off-line over a range of operating conditions. These conditions include cases where the system is heavily stressed. Based on these studies, a conservative estimate is made for the thresholds. Further discussion of the determination of these thresholds is continued in chapter 7.

4 SENSITIVITY FORMULATION

4.1 Introduction

In transient stability analysis, given the stability results for a set of initial system conditions and a disturbance scenario, one would like to know how these results are affected by a change in a key system parameter. The change could be in plant generation, network configuration or the load. Analytic sensitivity formulation is one way of addressing this issue.

An inherent advantage of the TEF method is the availability of a qualitative measure of the degree of stability in terms of the transient energy margin. For the TEF method to be an effective tool, it is essential to relate the energy margin to system variables like plant generation, load and network changes. This would assist the system operator in determining how the system responds to a change in any one of the above parameters.

This chapter details the analytical sensitivity of the energy margin (coupled with the exit point based TEF method) to assess system stability when there is a change in system parameters: plant generation or network configuration.

In a power system operating under stability limited condition, the preventive action usually consists of generation shifts among generators or load shedding. It is useful to know how the energy margin varies when there is a shift in generation. This helps the system operator in his decision making process. Changes in load can easily be related to generation shifts.

Following a disturbance, a line is normally tripped to clear the fault. It is then quite probable that additional lines get tripped by relay action. In highly stressed networks, this could even cause system instability. The method proposed gives a fast assessment of how the system stability is affected. This would assist the operator in determining how stable the post disturbance network is with respect to different lines and identifying critical lines.

4.2 Review of Sensitivity Analysis Techniques

An inherent advantage of the TEF method is the availability of a qualitative measure of the degree of stability in terms of the transient energy margin. This is of importance in reducing the number of transient stability runs needed to obtain the transient stability loading limits. Also, in the case of large disturbances, it is possible to incorporate the necessary changes to improve the system transient behavior. However, there is a lack of an accurate procedure to obtain quantitative answers for these limits. The need for such a method has been the effort of many researchers.

In most of the earlier work, linearized sensitivity techniques have been proposed in order to facilitate fast transient stability analysis so that preventive action could be taken.

In [35], an analytical approach to determine the maximum load capability of the system is given. This approach neglected transfer conductances and only self clearing faults were considered.

Sauer et al. [36] used the sensitivities of the energy margin with respect to the total system load to derive a stability limited load supply capability, which was incorporated as a constraint in the optimal power flow problem.

In [22], a procedure was developed to evaluate the energy margin sensitivity using repetitive TEF analysis and linearized margin assumptions, combined with power flow distribution factors for computation of interface flow limits.

Vittal et al. [37] used the linearized sensitivity of the energy margin with respect to the loading of a single critical generator to obtain the stability-constrained plant generation limits, when increased loading is desired for economy or decreased loading may be necessary to maintain stability.

Moore [38] used linearized sensitivity methods to determine how line flows affect the robustness of the system.

Vittal et al. [39] obtained the sensitivities of the energy margin with respect to generation change at the critical machines and also the sensitivity of the energy margin with respect to network changes. These network changes were however, limited to changes in line impedances. It was also assumed in this work that the mode of disturbance (MOD) of the controlling unstable equilibrium point (UEP) does not change. This was an analytic technique for a first order approximation to the variation in the energy margin. The derivation of these sensitivities was obtained using the dynamic sensitivity equation formulation. Using such sensitivities, it is possible to obtain first order approximations to stability limited generator loading corresponding to zero energy margin.

D'souza [40] determined the second order sensitivities of the energy margin with respect to the generation shift at the critical generators. The dynamic sensitivity equation served as the key for the second order analytical formulation.

In [41], the first order sensitivity of the transient potential energy was derived. This was then used to predict a margin for voltage dip stability.

In [42], a sensitivity based BCU method was presented. This technique is free from the assumption that the MOD of the controlling UEP remains the same. The procedure is however, very time consuming. It necessitates integration of the sensitivity dynamic equations till the exit point followed by integration of the post-fault reduced system to find the first local minimum. The next step involves solving for the new controlling UEP and in the strict sense, is not a sensitivity technique. The distribution of computation time for reduced formulation is dependent on the system being used. While the time involved in integrating to the exit point and then to the first local minimum might exceed that required to solve for the controlling UEP in the 50-generator IEEE test system, it is not so for the 161 generator NSP system. Here it takes roughly three times as much time to solve for the controlling UEP. The method described in [42] would then take as much time as a new run. This would defeat the purpose of sensitivity analysis which is used for fast derivation of stability limits.

4.3 The Key Features of the proposed Sensitivity Formulation

The key features of the proposed sensitivity formulation include:

- Formulation of analytical sensitivity techniques for the exit point based technique to determine the controlling UEP.
- Introduction of sensitivities at the exit point and the minimum gradient point.

- Introduction of a very fast sensitivity technique to account for network configuration changes.
- Elimination of the assumption that the MOD of the controlling UEP does not change (for both network and plant generation changes).
- No prior knowledge required of the critical generators at which generation is shifted.

4.4 Energy Margin Sensitivity and Dynamic Sensitivity Equations

The mathematical model used in this analysis is the classical model [30, chapter 2]. In the TEF method the energy margin ΔV [20, chapter 5] is given by:

$$\Delta V = -\frac{1}{2} M_{eq} (\tilde{\omega}_{eq}^{cl})^2 - \sum_{i=1}^{n} P_i (\theta_i^u - \theta_i^{cl}) - \sum_{i=1}^{n-1} \sum_{j=i+1}^{n} C_{ij} (\cos \theta_{ij}^u - \cos \theta_{ij}^{cl})$$

$$+ \sum_{i=1}^{n-1} \sum_{j=i+1}^{n} \beta_{ij} D_{ij} (\sin \theta_{ij}^u - \sin \theta_{ij}^{cl}) \qquad (4.1)$$

where,

$$\beta_{ij} = \frac{\theta_i^u + \theta_j^u - \theta_i^{cl} - \theta_j^{cl}}{\theta_{ij}^u - \theta_{ij}^{cl}} \qquad (4.2)$$

The energy margin ΔV can be expressed as a function of several variables in the following fashion:

$$\Delta V = \Delta V \left[\theta^{cl}, \tilde{\omega}^{cl}, \theta^u, E_i, P_{mi}, G_{ij}^{pf}, B_{ij}^{pf} \right] \qquad (4.3)$$

If ΔV_{pe} denotes the potential energy margin and ΔV_{kecorr} represents the corrected kinetic energy margin based on the MOD, ΔV can also be expressed as

$$\Delta V = \Delta V_{pe} + \Delta V_{kecorr} \tag{4.4}$$

There are two important aspects to the analytical sensitivity formulation. These are the concepts of energy margin sensitivity and dynamic sensitivity equations. The derivation for these two concepts is presented in a general form below. These are then adapted to the specific requirement of the problem (plant generation change or network topology change). In the following equations, $\partial\alpha_k$ denotes the change in the system parameter α_k. $\partial\alpha_k$ could be a change in plant generation, load or network structure. Taking the partial of ΔV with respect to a change in a power system parameter denoted by α_k, we have,

$$\begin{aligned}
\frac{\partial \Delta V}{\partial \alpha_k} = & - M_{eq}\, \tilde{\omega}_{eq}^{cl} \frac{\partial \tilde{\omega}_{eq}^{cl}}{\partial \alpha_k} - \sum_{i=1}^{n} \Bigg\{ P_i^{pf} \left(\frac{\partial \theta_i^u}{\partial \alpha_k} - \frac{\partial \theta_i^{cl}}{\partial \alpha_k} \right) + \left(\theta_i^u - \theta_i^{cl} \right) \frac{\partial P_{mi}}{\partial \alpha_k} \\
& - \left(\theta_i^u - \theta_i^{cl} \right) \left(E_i^2 \frac{\partial G_{ii}^{pf}}{\partial \alpha_k} + 2 E_i G_{ii}^{pf} \frac{\partial E_i}{\partial \alpha_k} \right) \Bigg\} \\
& + \sum_{i=1}^{n-1} \sum_{j=i+1}^{n} \Bigg\{ \left(\cos \theta_{ij}^u - \cos \theta_{ij}^{cl} \right) \frac{\partial C_{ij}^{pf}}{\partial \alpha_k} - \beta_{ij} \left(\sin \theta_{ij}^u - \sin \theta_{ij}^{cl} \right) \frac{\partial D_{ij}^{pf}}{\partial \alpha_k} \Bigg\} \\
& + \sum_{i=1}^{n-1} \sum_{j=i+1}^{n} \Bigg\{ \left(\beta_{ij} D_{ij}^{pf} \cos \theta_{ij}^u + C_{ij}^{pf} \sin \theta_{ij}^u \right) \left(\frac{\partial \theta_i^u}{\partial \alpha_k} - \frac{\partial \theta_j^u}{\partial \alpha_k} \right) \\
& - \left(\beta_{ij} D_{ij}^{pf} \cos \theta_{ij}^{cl} + C_{ij}^{pf} \sin \theta_{ij}^{cl} \right) \left(\frac{\partial \theta_i^{cl}}{\partial \alpha_k} - \frac{\partial \theta_j^{cl}}{\partial \alpha_k} \right) \Bigg\} \\
& + \sum_{i=1}^{n-1} \sum_{j=i+1}^{n} D_{ij}^{pf} \left(\sin \theta_{ij}^u - \sin \theta_{ij}^{cl} \right) \Bigg\{ \lambda_{ij} \left(\frac{\partial \theta_i^u}{\partial \alpha_k} - \frac{\partial \theta_i^{cl}}{\partial \alpha_k} \right) \\
& + \eta_{ij} \left(\frac{\partial \theta_j^u}{\partial \alpha_k} - \frac{\partial \theta_j^{cl}}{\partial \alpha_k} \right) \Bigg\}
\end{aligned} \tag{4.5}$$

where,

$$\lambda_{ij} = \frac{-2\left(\theta_j^u - \theta_j^{cl}\right)}{\left(\theta_{ij}^u - \theta_{ij}^{cl}\right)^2} \tag{4.6}$$

$$\eta_{ij} = \frac{2\left(\theta_i^u - \theta_i^{cl}\right)}{\left(\theta_{ij}^u - \theta_{ij}^{cl}\right)^2} \tag{4.7}$$

The dynamic sensitivity equations are integral to the analytical formulation of sensitivity. These are obtained by taking the partial derivatives of the system dynamic equations as:

$$M_i \frac{\partial \dot{\tilde{\omega}}_i}{\partial \alpha_k} = \frac{\partial P_{mi}}{\partial \alpha_k} - 2E_i \frac{\partial E_i}{\partial \alpha_k} G_{ii} - E_i^2 \frac{\partial G_{ii}}{\partial \alpha_k}$$

$$- \sum_{\substack{j=1 \\ j \neq i}}^{n} \left\{ C_{ij} \cos\theta_{ij} \left[\frac{\partial \theta_i}{\partial \alpha_k} - \frac{\partial \theta_j}{\partial \alpha_k} \right] - D_{ij} \sin\theta_{ij} \left[\frac{\partial \theta_i}{\partial \alpha_k} - \frac{\partial \theta_j}{\partial \alpha_k} \right] \right\}$$

$$- \sum_{\substack{j=1 \\ j \neq i}}^{n} \left\{ \left[B_{ij} \sin\theta_{ij} + G_{ij} \cos\theta_{ij} \right] \left[\frac{\partial E_i}{\partial \alpha_k} E_j + \frac{\partial E_j}{\partial \alpha_k} E_i \right] \right\}$$

$$- \sum_{\substack{j=1 \\ j \neq i}}^{n} \left\{ E_i E_j \sin\theta_{ij} \frac{\partial B_{ij}}{\partial \alpha_k} + E_i E_j \cos\theta_{ij} \frac{\partial G_{ij}}{\partial \alpha_k} \right\}$$

$$- \frac{M_i}{M_T} \left\{ \sum_{j=1}^{n} \left[\frac{\partial P_{mj}}{\partial \alpha_k} - 2E_j \frac{\partial E_j}{\partial \alpha_k} G_{jj} - E_j^2 \frac{\partial G_{jj}}{\partial \alpha_k} \right] \right.$$

$$+ \sum_{i=1}^{n} \sum_{\substack{j=1 \\ j \neq i}}^{n} \left[D_{ij} \sin\theta_{ij} \left(\frac{\partial \theta_i}{\partial \alpha_k} - \frac{\partial \theta_j}{\partial \alpha_k} \right) \right.$$

$$- G_{ij} cos\,\theta_{ij} \left(\frac{\partial E_i}{\partial \alpha_k} E_j + \frac{\partial E_j}{\partial \alpha_k} E_i \right) - E_i E_j c\,os\,\theta_{ij} \frac{\partial G_{ij}}{\partial \alpha_k}] \} \tag{4.8}$$

$$\frac{\partial \dot{\theta}_i}{\partial \alpha_k} = \frac{\partial \tilde{\omega}_i}{\partial \alpha_k} \tag{4.9}$$

These dynamic sensitivity equations are a set of time-varying linear differential equations which can be solved numerically if the initial conditions are known. However, at the equilibrium points, the dynamic term in equation (4.8) $M_i \frac{\partial \tilde{\omega}_i}{\partial \alpha_k}$ is zero. The dynamic sensitivity equations, at these equilibrium points, become a set of algebraic equations which can be easily solved.

4.5 Analytical Sensitivity Formulation for Network Topology Changes

Existing literature does not provide sensitivity formulation for network topology changes. This section attempts to address this issue. A system which is stable with respect to a certain post-fault configuration might be unstable when a certain line(s) is removed. An assessment of the stability of the post-fault network with respect to certain key lines is possible by using the proposed formulation. It is assumed in this analysis that the change in network structure occurs at the end of the disturbance. This would then give a conservative assessment of stability compared to actual clearing following relay action.

4.5.1 Determination of Sensitivity Variables

The analytical formulation for network topology changes is different from that for plant generation changes. This is partly due to the assumption made that the change in network topology occurs at the end of the disturbance.

Mainly, this formulation was chosen to avoid the need for having to quantify $\Delta\alpha_k$. The parametric change introduced by trying to quantify $\Delta\alpha_k$ for network changes can be very large. This problem is overcome by the use of Householder's technique [3] to update the admittance matrix and is explained below. In this method, the *Y-bus* of the postfault network is modified directly instead of being reconstructed from scratch.

The full *Y-bus* can be written as

$$Y\text{-}bus = \begin{array}{c|cc} & IN & TN \quad LN \\ \hline IN & Y_A & Y_B \\ TN & Y_C & Y_D \\ LN & & \end{array}$$

where *IN* are the internal nodes, *TN* are the terminal buses of the machines, *LN* are the load buses in the system and Y_A , Y_B , Y_C , and Y_D are given by the following matrices. In the following matrices y_{m1} , y_{m2} , ... are the reactances of the respective machines.

$$Y_A = \begin{array}{c|c} & IN \\ \hline IN & \begin{matrix} y_{m1} & & & \\ & y_{m2} & & \\ & & y_{m3} & \\ & & & \ddots \\ & & & \ddots \end{matrix} \end{array}$$

$$Y_B = Y_C{}^T = \quad IN \quad \begin{array}{c|c} TN & LN \\ \hline -y_{m1} \\ \quad -y_{m2} \\ \quad\quad \cdot \\ \quad\quad\quad \cdot \\ \quad\quad\quad\quad \cdot & 0 \end{array}$$

$$Y_D = \quad \begin{array}{c} \\ TN \\ \\ LN \end{array} \quad \begin{array}{c|c} TN & LN \\ \hline & \\ Y_D & \\ & \end{array}$$

The *Y-bus* matrix reduced to the internal nodes is given by

$$Y\text{-}bus\ (reduced) = Y_A - Y_B\, Y_D{}^{-1}\, Y_C \qquad (4.10)$$

Any changes in the system configuration can be reflected by changes in the matrix Y_D . Let a line i-j be considered for outage. Then the change in the Y_D matrix is given by

$$\Delta Y_D = \quad \begin{array}{c} \\ i \\ \\ j \end{array} \quad \begin{array}{c|c} i & j \\ \hline & \\ a & b \\ & \\ b & a \end{array}$$

where

$a = -y_{ij} - (c_{ij} / 2)$

$b = y_{ij}$

y_{ij} is the line admittance

c_{ij} is the total line charging (susceptance)

ΔY_D can now be rewritten as $\Delta Y_D = KDL$.

K, D, and L are shown in the following expression.

$$\Delta Y_D = \begin{array}{c} \\ i \\ \\ \\ j \\ \\ \end{array} \begin{bmatrix} 0 & 0 \\ \cdot & \cdot \\ 1 & 1 \\ 0 & 0 \\ -1 & 1 \\ 0 & 0 \\ \cdot & \cdot \end{bmatrix} \quad K \qquad \begin{bmatrix} \frac{a-b}{2} & \\ & \frac{a+b}{2} \end{bmatrix} \quad D$$

$$\begin{array}{c} \\ i \\ \\ \\ j \\ \\ \end{array} \begin{array}{c} \\ \\ \\ \\ \\ \\ \end{array} \begin{array}{c} \\ \\ \\ \\ \\ \\ \end{array} \begin{array}{c} \\ \\ \\ \\ \\ \\ \end{array} \begin{array}{c} \\ \\ \\ \\ \\ \\ \end{array} \begin{array}{c} \\ \\ \\ \\ \\ \\ \end{array} \begin{array}{c} \\ \\ \\ \\ \\ \\ \end{array}$$

$$\begin{bmatrix} 0 & \cdot & 1 & 0 & -1 & 0 & \cdot \\ 0 & \cdot & 1 & 0 & 1 & 0 & \cdot \end{bmatrix} \quad L$$

Now, the reduced *Y-bus* matrix equation with the change in the system configuration incorporated is given by

$$Y\text{-}bus\ (reduced,\ new) = Y_A - Y_B\,(Y_D + KDL)^{-1}\,Y_C \qquad (4.11)$$

By Householder's theorem,

$$(Y_D + KDL)^{-1} = Y_D^{-1} - Y_D^{-1}\,K\,(D^{-1} + L\,Y_D^{-1}\,K)^{-1}\,L\,Y_D^{-1} \qquad (4.12)$$

Substituting in equation (4.11)

$$Y\text{-}bus\ (reduced,\ new) = Y_A - Y_B\, Y_D^{-1}\, Y_C + Y_B Y_D^{-1} K\,(D^{-1} + L\, Y_D^{-1} K)^{-1}\, L\, Y_D^{-1}\, Y_C \tag{4.13}$$

By comparing equations (4.10) and (4.13), the modifications to the reduced Y-bus matrix due to the outage of line *i-j* is given by

$$\Delta Y\text{-}bus\ (reduced) = Y_B Y_D^{-1} K\,(D^{-1} + L\, Y_D^{-1} K)^{-1}\, L\, Y_D^{-1}\, Y_C \tag{4.14}$$

This matrix ($\Delta Y\text{-}bus\ (reduced)$) contains as its terms ΔB_{ij} and ΔG_{ij}. ΔB_{ij} corresponds to the difference between the susceptance terms of the original *Y-bus* and the new *Y-bus*. Similarly ΔG_{ij} corresponds to the difference between the conductance terms of the original *Y-bus* and the new *Y-bus*.

In section 4.4, the concepts of energy margin sensitivity and dynamic sensitivity equations were presented in a general form. A lot of variables need to be determined before actual assessment can be made for the new case.

For network topology changes, the variables $\frac{\partial \theta_i^{cl}}{\partial \alpha_k}$, $\frac{\partial \tilde{\omega}_i^{cl}}{\partial \alpha_k}$, $\frac{\partial P_{mi}}{\partial \alpha_k}$, and $\frac{\partial E_i}{\partial \alpha_k}$ are equal to zero. The change is introduced at the end of the disturbance and hence, the conditions at clearing remain unchanged. For the classical machine, the internal voltage is assumed to remain constant in a transient stability study. Also, the internal voltage is computed using the predisturbance terminal voltage, complex power generation at the generator bus and the transient reactance. These, in turn, are assumed to be unaffected by a change in the network topology. This implies that the variables which need to be evaluated are $\frac{\partial \theta_i^{u}}{\partial \alpha_k}$, $\frac{\partial B_{ij}}{\partial \alpha_k}$ and $\frac{\partial G_{ij}}{\partial \alpha_k}$. Using Householder's method to update the admittance matrix gives us ΔB_{ij} and ΔG_{ij}. This implies that we do not have to calculate

$\frac{\partial B_{ij}}{\partial \alpha_k}$ and $\frac{\partial G_{ij}}{\partial \alpha_k}$. The advantage of this formulation is that it allows us to directly compute $\Delta\,\theta_i$ rather than $\frac{\partial \theta_i^{\,u}}{\partial \alpha_k}$.

As mentioned earlier, the dynamic sensitivity equations become a set of algebraic equations at an equilibrium point. These algebraic equations can be easily solved for the unknown variable (which in this case is $\Delta\,\theta_i$). For an assessment to be made of how the change affects system stability, the sensitivity of the controlling UEP needs to be determined. At the controlling UEP, the dynamic sensitivity equation is of the form:

$$(\widehat{A})(\Delta\,\theta_i^{\,u}) = R_i \tag{4.15}$$

where,

$$A_{ii} = \left(1 - 2\frac{M_i}{M_T}\right) \sum_{\substack{j=1 \\ j\neq i}}^{n} D_{ij}\sin\theta_{ij}^{u} - \sum_{\substack{j=1 \\ j\neq i}}^{n} C_{ij}\cos\theta_{ij}^{u} \tag{4.16}$$

$$A_{ij} = \left(2\frac{M_i}{M_T}\right) \sum_{\substack{l=1 \\ l\neq j}}^{n} D_{lj}\sin\theta_{lj}^{u} + C_{ij}\cos\theta_{ij}^{u} - D_{ij}\sin\theta_{ij}^{u} \tag{4.17}$$

$$R_i = E_i^2\,\Delta G_{ii} - \frac{M_i}{M_T}\sum_{j=1}^{n} E_j^2\,\Delta G_{jj} - \frac{M_i}{M_T}\sum_{l=1}^{n}\sum_{\substack{j=1 \\ j\neq l}}^{n} E_l\,E_j\cos\theta_{lj}\,\Delta G_{lj}$$

$$+ \sum_{\substack{j=1 \\ j\neq i}}^{n}\left[E_i\,E_j\sin\theta_{ij}^{u}\,\Delta B_{ij} + E_i\,E_j\cos\theta_{ij}^{u}\,\Delta G_{ij}\right] \tag{4.18}$$

Solving the equation (4.15) gives us $\Delta\theta_i^{\,u}$. Once, the sensitivity of the controlling UEP has been determined, the threshold for stability assessment can be made. This is discussed in the next section.

4.5.2 New Controlling UEP and Stability Assessment

There is a significant departure in the evaluation of the energy margin ΔV, corresponding to the new case, from previous work on sensitivity. Earlier work assumed that there was no change in the MOD of the controlling UEP. This implies that in the calculation of the corrected kinetic energy margin for the new case, the MOD corresponding to the base controlling UEP is used. This assumption is not true in general, because certain changes in system parameters might alter the MOD. For a more accurate stability assessment, it is essential that the change in the MOD of the controlling UEP be appropriately identified.

Let $\theta_i^{u}{}_{(base)}$ and $\theta_i^{u}{}_{(new)}$ denote the controlling UEP corresponding to the base case and new case respectively. These are related by the equation,

$$\theta_i^{u}{}_{(new)} = \theta_i^{u}{}_{(base)} + \Delta\theta_i^{u} \tag{4.19}$$

Note that in the above equation, $\Delta\theta_i^{u}$ represents the actual change (in degrees) from the base controlling UEP. Once the new controlling UEP $\theta_i^{u}{}_{(new)}$ has been determined, it can be checked for any change in the MOD (as compared to the base case). By looking at the angles in the new controlling UEP, the advanced machines can be picked up. These advanced machines constitute the MOD of the new controlling UEP.

The energy margin ΔV, corresponding to the new case needs to be determined now. This is computed as,

$$\Delta V_{new} = \Delta V \left[\theta^{cl}, \tilde{\omega}^{cl}, \theta_{new}^{u}, E_i, G_{ij}^{pf\text{-}new}, B_{ij}^{pf\text{-}new}\right] \tag{4.20}$$

In the above expression, each of the variables are known. θ_{new}^{u} is computed as illustrated in equation (4.19). $G_{ij}^{pf\text{-}new}$ and $B_{ij}^{pf\text{-}new}$ are computed by using the

householder technique as explained in section 4.5.1. It should be noted that ΔV_{new} is directly evaluated. This avoids the need to quantify $\Delta\alpha_k$ while evaluating ΔV_{new}. ΔV_{new} gives an indication of how the system is affected when there is a change in the network structure.

4.6 Analytical Sensitivity Formulation for Plant Generation Changes

This section addresses the issue of sensitivity formulation for changes in plant generation. The change could be at any of the machines that are modeled. This analysis helps determine critical plant loading. For a given fault scenario, a certain generation pattern might not affect the system stability. However, alterations in this generation pattern (by increasing generation at certain machines) could have an adverse affect on system stability. Also of significance is the fact that the number of transient stability needed to obtain the transient stability loading limits are reduced. This work was initially investigated in [28,39]. However, the formulation presented here is devoid of some of the assumptions made earlier. Also, the concept of sensitivity was extended to include the exit point and the minimum gradient point.

4.6.1 Determination of Sensitivity Variables

When there is a shift in plant generation at one or more machines, the stable equilibrium point (θ_i^s), clearing angles (θ_i^{cl}), clearing speeds ($\tilde{\omega}_i^{cl}$), unstable equilibrium point (θ_i^u), the constant voltage behind transient reactance (E_i) and mechanical power input (P_{mi}) change. This implies that the sensitivity parameters which need to be determined are $\frac{\partial\theta_i^{cl}}{\partial P_{mk}}$, $\frac{\partial\tilde{\omega}_i^{cl}}{\partial P_{mk}}$, $\frac{\partial P_{mi}}{\partial P_{mk}}$, $\frac{\partial E_i}{\partial P_{mk}}$ and $\frac{\partial\theta_i^u}{\partial P_{mk}}$.

The variables $\frac{\partial B_{ij}}{\partial P_{mk}}$ and $\frac{\partial G_{ij}}{\partial P_{mk}}$ are assumed to be zero. Actually, the reduced admittance matrix terms B_{ij} and G_{ij} also change. This is because, if there is a shift in the generation, the pre-disturbance power flow solution changes. As a result, the load bus voltages change and the admittance corresponding to the load changes. However, these changes are minuscule and can be neglected. The determination of $\frac{\partial P_{mi}}{\partial P_{mk}}$ and $\frac{\partial E_i}{\partial P_{mk}}$ is given in appendix 1. For convenience, let the sensitivity variables be denoted by the following notation.

At the SEP: $x_{ik}^{s} = \frac{\partial \theta_i^{s}}{\partial P_{mk}}$

At clearing: $x_{ik}^{cl} = \frac{\partial \theta_i^{cl}}{\partial P_{mk}}$ and $y_{ik}^{cl} = \frac{\partial \tilde{\omega}_i^{cl}}{\partial P_{mk}}$

At the UEP: $x_{ik}^{u} = \frac{\partial \theta_i^{u}}{\partial P_{mk}}$

4.6.2 Determining the Sensitivities at the SEP

The SEP sensitivity coefficients x_{ik}^{s}, have to be determined before the sensitivity variables at clearing (x_{ik}^{cl} and y_{ik}^{cl}) can be calculated. As mentioned earlier, the sensitivity dynamic equations are a set of second order linear differential equations which can be solved for numerically if the appropriate initial conditions are known. x_{ik}^{s} serves as part of the initial condition required to integrate the dynamic equations. At the SEP, which is static in nature, the dynamic terms can be set to zero. This implies that in equation (4.8), the term $M_i \frac{d}{dt^2}(x_{ik})$ is zero. The sensitivity dynamic equations now reduce to a set of simultaneous linear equations. These equations can be represented by

$$\sum_{j=1}^{n} A_{ij}^{pr} x_{ik}^{s} = T_{ik}^{pr} \tag{4.21}$$

where,

$$A_{ii}^{pr} = \left(1 - 2\frac{M_i}{M_T}\right) \sum_{\substack{j=1 \\ j \neq i}}^{n} D_{ij} \sin\theta_{ij}^{s} - \sum_{\substack{j=1 \\ j \neq i}}^{n} C_{ij} \cos\theta_{ij}^{s} \tag{4.22}$$

$$A_{ij}^{pr} = \left(2\frac{M_i}{M_T}\right) \sum_{\substack{l=1 \\ l \neq j}}^{n} D_{lj} \sin\theta_{lj}^{s} + C_{ij} \cos\theta_{ij}^{s} - D_{ij} \sin\theta_{ij}^{s} \tag{4.23}$$

$$T_{ik}^{pr} = \frac{M_i}{M_T} - \Delta_{ik} + \sum_{\substack{j=1 \\ j \neq i}}^{n} \left(\frac{\partial E_i}{\partial P_{mk}} E_j + \frac{\partial E_j}{\partial P_{mk}} E_i\right) \left(B_{ij}^{pr} \sin\theta_{ij}^{s} + G_{ij}^{pr} \cos\theta_{ij}^{s}\right)$$

$$- \frac{M_i}{M_T} \sum_{\substack{j=1 \\ j \neq i}}^{n} \sum_{l=1}^{n} \left(\frac{\partial E_l}{\partial P_{mk}} E_j + \frac{\partial E_j}{\partial P_{mk}} E_l\right) \left(G_{ij}^{pr} \cos\theta_{ij}^{u}\right) \tag{4.24}$$

In the above formulation, there are only (n-1) independent equations. The nth variable can be determined by making use of the COI constraint. From equation (2.12), we can formulate

$$\sum_{i=1}^{n} M_i x_{ik}^{s} = 0 \tag{4.25}$$

which gives us x_{nk}^{s} . The next step is to determine the sensitivity variables at clearing.

4.6.3 Determining the Sensitivities at Clearing

In order to determine the sensitivities at clearing (x_{ik}^{cl} and y_{ik}^{cl}), the set of (n-1) ordinary differential equations with time varying coefficients need to be solved. These equations are given by

$$M_i \frac{d}{dt^2}(x_{ik}) = -T_{ik}^f + \sum_{j=1}^{n} A_{ij}^f x_{ik} \tag{4.26}$$

The initial conditions for the above set of equations are provided by

$$x_{ik}(0) = x_{ik}^s$$

$$\dot{x}_{ik}(0) = 0$$

Dynamic sensitivity equations (4.26) with the above initial conditions are integrated until fault clearing. This gives us the conditions at clearing as

$$x_{ik}(t^{cl}) = x_{ik}^{cl}$$

$$\dot{x}_{ik}(t^{cl}) = \dot{x}_{ik}^{cl} = y_{ik}^{cl}$$

4.6.4 Determining the Sensitivities at the UEP

The sensitivities at the UEP (x_{ik}^{μ}) can be determined in the same fashion as the SEP. Again at the UEP, which is static in nature, the dynamic term in equation (4.26) can be set to zero. The resulting set of linear equations are

$$\sum_{j=1}^{n} A_{ij}^{pf} x_{ik}^{\mu} = T_{ik}^{pf} \tag{4.27}$$

A_{ij}^{pf} is the same as given in equation (4.22) and (4.23) but for the fact that the post fault admittance matrix is used instead of the prefault admittance matrix and θ_{ij}^{u} is replaced by θ_{ij}^{u}. The same holds true for T_{ik}^{pf} also.

4.6.5 Determining Change in MOD and Stability Assessment

As mentioned earlier in section (4.5.2), it is quite probable that there is a change in the MOD of the controlling UEP. It is essential that this new MOD be

captured before the stability assessment can be made. While the procedure for this is the same as that followed for network structure changes, there is one difference. For sensitivities with respect to plant generation, rather than evaluating the change in the UEP angles directly (via sensitivity dynamic equations), $\frac{\partial \theta_i^u}{\partial P_{mk}}$ is evaluated. Now the new controlling UEP is evaluated as

$$\theta_{i\,(new)}^{u} = \theta_{i\,(base)}^{u} + \sum_{k=1}^{NG} \frac{\partial \theta_i^u}{\partial P_{mk}} \Delta P_{mk} \tag{4.28}$$

where, ΔP_{mk} denotes the actual change in generation made at plant k. NG represents the total number of generators at which generation chage is made.

The stability assessment can be made now that the new MOD has been determined. It should be noted that there is also a probability of the MOD for the new case being the same as that for the base case. In this case, the stability assessment can be made in one of two ways. One of these methods is similar to that followed for network configuration changes. In this method, rather than calculating the sensitivity of the energy margin with respect to the change, the new energy margin is directly evaluated. In other words,

$$\Delta V_{new} = \Delta V \left[\theta_{new}^{cl},\ \tilde{\omega}_{new}^{cl},\ \theta_{new}^{u},\ E_{new},\ P_{m\,(new)},\ G_{ij}^{pf},\ B_{ij}^{pf}\right] \tag{4.29}$$

In the second method, ΔV_{new} is calculated as

$$\Delta V_{new} = \Delta V_{base} + \sum_{k=1}^{NG} \frac{\partial \Delta V}{\partial P_{mk}} \Delta P_{mk} \tag{4.30}$$

where, $\frac{\partial \Delta V}{\partial P_{mk}}$ can be calculated using equation (4.5).

4.7 Steps to Evaluate sensitivities for Network Changes

- Step 1: Calculate the reduced admittance matrix for the new post-fault network using the method described in section (4.5.1). Obtain the changes in $Y\text{-}bus$ parameters, namely, ΔB_{ij} and ΔG_{ij} respectively.

- Step 2: The sensitivity of the controlling UEP to the network change ($\Delta \theta_i^{\,u}$) needs to be determined. These can be obtained by using equation (4.15).

- Step 3: Once $\Delta \theta_i^{\,u}$ has been evaluated, the new controlling UEP ($\theta_{i\,(new)}^{\,u}$) can be determined by using equation (4.19). From this, obtain the MOD corresponding to the new case.

- Step 4: Calculate ΔV corresponding to the new case (ΔV_{new}) by using equation (4.20).

4.8 Steps to Evaluate sensitivities for Plant Generation Changes

- Step 1: Evaluate $\frac{\partial E_i}{\partial P_{mk}}$ and $\frac{\partial P_{mi}}{\partial P_{mk}}$ as explained in section (4.6.1)

- Step 2: Obtain the SEP sensitivities, $x_{ik}^{s} = \frac{\partial \theta_i^{s}}{\partial P_{mk}}$. These serve as the initial conditions in the integration of the dynamic sensitivity equations.

- Step 3: Once the SEP sensitivities have been determined, the dynamic sensitivity equations are integrated till fault clearing. This gives us the sensitivities at clearing as $x_{ik}^{cl} = \frac{\partial \theta_i^{cl}}{\partial P_{mk}}$ and $y_{ik}^{cl} = \frac{\partial \tilde{\omega}_i^{cl}}{\partial P_{mk}}$.

- Step 4: The UEP sensitivities need to be determined now. The procedure followed here is the same as in step 2 and is explained in section (4.6.4). This gives us $x_{ik}^{u} = \frac{\partial \theta_i^{u}}{\partial P_{mk}}$.

- Step 5: Calculate the new controlling UEP ($\theta_{i\,(new)}^{u}$) and identify the change in the MOD.

- Step 6: Calculate ΔV corresponding to the new case (ΔV_{new}) using (4.29) or (4.30).

4.9 Comments on the Sensitivity Procedure for Network Changes

For changes in plant generation, the parametric change (ΔP_{mk}) is not large and can easily be quantified. This allows us to formulate the analytical sensitivity equations in a straightforward fashion. On the other hand, for network topological changes, it is not possible to quantify $\Delta \alpha_k$. Attempts to quantify $\Delta \alpha_k$ (e.g., as the magnitude of the admittance value) result in extremely large parametric changes. It is very difficult to come up with a exact measure of what should be used to quantify $\Delta \alpha_k$. This, in turn, leads to inaccuracies in the analytical sensitivity formulation. This motivated the approach where the quantification of $\Delta \alpha_k$ is avoided. The use of the householder's technique to update the post-fault admittance matrix is instrumental in this new formulation. This technique enables us to determine directly the change in the post-fault

admittance matrix of the base case. In other words, it helps determine ΔB_{ij} and ΔG_{ij} rather than $\frac{\partial B_{ij}}{\partial \alpha_k}$ and $\frac{\partial G_{ij}}{\partial \alpha_k}$. Also, in the analytical sensitivity formulation for plant generation changes, the change in energy margin is evaluated as

$$\Delta(\Delta V) = \sum_{k=1}^{NG} \frac{\partial \Delta V}{\partial P_{mk}} \Delta P_{mk} \tag{4.31}$$

However, for network topological changes, the new energy margin is directly computed as

$$\Delta V_{new} = \Delta V \left[\theta^{cl}, \tilde{\omega}^{cl}, \theta^{u}_{new}, E_i, P_{mi}, G_{ij}^{pf\text{-}new}, B_{ij}^{pf\text{-}new}\right] \tag{4.32}$$

It was also observed that the potential energy margin decreased when an additional line was tripped. This was true in all the cases tried. The cases tried included both stressed and unstressed cases. It appears from this that the stability boundary (PEBS) shows a decrease in the region of interest. Though network topology change is discrete, discontinuity in the energy margin, if any, is introduced by a change in the MOD. The change in MOD is however identified by this technique. This helps us predict ΔV_{new} with accuracy

Another important aspect of this procedure is its speed. The computation involved in terms of updating the *Y-bus* corresponding to the base case and solving a linear system of equations is minimal. There are a large number of commercial software packages which could be used for this purpose. By comparison, repetitive TEF methods and conventional time domain methods are time consuming procedures. As the system size increases, the advantage of the proposed technique is very pronounced.

4.10 Sensitivities at the Exit Point and the Minimum Gradient Point

As mentioned earlier in Chapter 3, the contingency filtering scheme hinges on the three main procedures in the TEF method. These procedures determine the exit point, minimum gradient point and the controlling UEP in that order. Associated with each of these points is an inertial transient filter (*ITF*) and a post-inertial transient filter (*PITF*). The exit point is associated with *ITF1* and *PITF1*, the minimum gradient point with *ITF2* and *PITF2* and the controlling UEP with *ITF3* and *PITF3*. In the first level of filters, all calculations are performed assuming the exit point as an approximation to the controlling UEP. Similarly, in the second level of filters, calculations are performed assuming the minimum gradient point as an approximation to the controlling UEP. In the third and final level of filters, the exact calculations are carried out based on the controlling UEP. In accordance with this scheme, it should be possible to perform sensitivity calculations in each of these filters. This implies that sensitivities at the exit point and the minimum gradient point need to be implemented. This section deals with this aspect of analytical sensitivity formulation for both plant generation and network structure changes.

4.10.1 Network Topological Changes

The formulation of the sensitivities at the exit point is essentially the same as that at the controlling UEP. The only difference is that the controlling UEP is replaced by the exit point. The analytical expression in equation 4.15 is valid only for equilibrium points. Essentially, this implies that the exit point is being treated as an equilibrium point. The validity of this assumption was

verified by comparing the results against those obtained from re-running TEF. Let θ^e represent the angle vector at the exit point.

- Step 1: Calculate the reduced admittance matrix for the new post-fault network using the method described in section (4.5.1). Obtain the changes in $Y\text{-}bus$ parameters, namely, ΔB_{ij} and ΔG_{ij} respectively.

- Step 2: The sensitivity of the exit point to the network change ($\Delta\theta_i{}^e$) needs to be determined. These can be obtained by using equation (4.15) where θ^e replaces θ^u.

- Step 3: Once $\Delta\theta_i{}^e$ has been evaluated, the new exit point ($\theta_i{}^e{}_{(new)}$) can be determined by using equation (4.19). Here again, all angles correspond to the exit point. From this, obtain the MOD corresponding to the new case.

- Step 4: Calculate ΔV corresponding to the new case (ΔV_{new}) by using equation (4.20).

Sensitivities at the minimum gradient point are evaluated in the same fashion as above with the exception being that θ^{mgp} replaces θ^e. θ^{mgp} refers to the angle vector at the minimum gradient point.

4.10.2 Plant Generation Changes

For plant generation changes, the formulation of the sensitivities at the exit point was tried out using two different methods. The first method is essentially the same as that used for calculating the sensitivities at the

controlling UEP. The main difference is in substituting the conditions at the UEP by that at the exit point. Briefly, the steps involved in this method are

- Step 1: Evaluate $\frac{\partial E_i}{\partial P_{mk}}$ and $\frac{\partial P_{mi}}{\partial P_{mk}}$ as explained in section (4.6.1)

- Step 2: Obtain the SEP sensitivities, $x_{ik}^{s} = \frac{\partial \theta_i^{s}}{\partial P_{mk}}$. These serve as the initial conditions in the integration of the dynamic sensitivity equations.

- Step 3: Once the SEP sensitivities have been determined, the dynamic sensitivity equations are integrated till fault clearing. This gives us the sensitivities at clearing as $x_{ik}^{cl} = \frac{\partial \theta_i^{cl}}{\partial P_{mk}}$ and $y_{ik}^{cl} = \frac{\partial \tilde{\omega}_i^{cl}}{\partial P_{mk}}$.

- Step 4: The exit point sensitivities need to be determined now. The procedure followed here is the same as in section (4.6.4). The difference is that θ^{e} replaces θ^{u}. This gives us $x_{ik}^{e} = \frac{\partial \theta_i^{e}}{\partial P_{mk}}$.

- Step 5: Calculate the new exit point ($\theta_{i\,(new)}^{e}$) and identify the change in the MOD.

- Step 6: Calculate ΔV corresponding to the new case.

The second method differs slightly in terms of the formulation of the problem. In this method, step 1 through step 3 remain the same. The exit point sensitivities are calculated in a different fashion. Here, the integration of the dynamic sensitivity equations is carried out all the way till the instant t_e where, t_e denotes the instant in time at which the exit point is determined. At this

instant, the sensitivities at the exit point $x_{ik}^{e} = \frac{\partial \theta_i^e}{\partial P_{mk}}$ are obtained. Steps 5 and 6 are again identical as above. The sensitivities at the the minimum gradient point are determined in the same fashion as that for the exit point using the first method. The only difference being in the fact that θ^{mgp} replaces θ^{e} in the equations used.

4.11 Sample results

The sensitivity technique for plant generation and network topology changes was tried on two different systems. These are the 50 generator IEEE test system and the 161 generator NSP system. Table 4.1 illustrates the results obtained with regard to network topology changes. Listed in the table are details of the fault (faulted bus, line cleared and clearing time), additional line tripped, normalized energy margin ΔV_n for the base case, ΔV_n for the new case (from sensitivity and rerun TEF) and results obtained from comventional time domain simulation. The base case refers to the system under consideration without any changes introduced. The additional line tripped refers to the change introduced in the system. The new case pertains to the system under consideration, but with the change introduced. The network sensitivity procedure was tested over a wide range of loading conditions for the 50 generator IEEE system. Also, different faults were considered at different clearing times. The base case consists of 700 MW each at bus #93 and bus #110. The results shown in table 4.1 indicate the efficacy of the network change procedure. Included in the table is a case (#5) where the system goes unstable following an additional line being tripped. This underlines the possible significance of this technique. In addition, the stability assessment is verified by time simulation.

Figures 4.1 and 4.2 obtained from time simulation provide additional verification of the results. In figure 4.1, the relative rotor angle plot of one of the most critical generators (machine #20) for case 5 is shown. In the base case, the machine is stable. However, for the new case, the machine #20 loses synchronism. Figure 4.2 is an illustration of the accuracy of the technique. In cases 11 and 12, for the same base case, two different lines were tripped. These are lines 1695 - 1707 and 1853 - 4010. Sensitivity analysis predicted that the system is more vulnerable with respect to the line 1853 - 4010 being tripped. This in turn can be observed from the fact that the plot for machine #42 (close to the fault) swings higher with 1853 - 4010 being tripped. Table 4.2 displays the results for plant generation changes. Two different scenarios were considered.

- The amount of increase in generation that can be handled by a stable system ($\Delta V_n > 0$) before it becomes critically stable ($\Delta V_n = 0$).
- The amount of generation that needs to be backed off for an unstable system ($\Delta V_n < 0$) to become critically stable ($\Delta V_n = 0$).

Figures 4.3 and 4.4 provide verification of the sensitivity technique (for plant generation changes) for cases 13 and 15. In case 13, the base system is unstable. The generation is then backed off at the critical generators to regain stability. In case 15, the base case is stable and the generation is increased till the system is close to being critically unstable.

Table 4.3 lists the MOD of the controlling uep for the base case and the new case (from sensitivity analysis and repetitive TEF analysis). Changes in the MOD were appropriately identified.

Table 4.1. Stability assessment for network topology changes

Case#	Flt. Bus	Line Cleared	Clr. time (sec)	Addl. Line Tripped	ΔV_n for BC[1] (TEF)	ΔV_n for NC[2] (Sens.)	ΔV_n for NC[2] (TEF)	Result from etmspv3
Generation at bus #93 and bus #110: 450 MW each								
1	100	100-72	0.200	72-101	1.559	1.534	1.534	Stable
2	105	105-73 1 105-73 2	0.088	73-74	0.268	0.149	0.151	Stable
3	33	33-39	0.260	33-110	3.588	3.452	3.437	Stable
4	91	91-74	0.140	91-108	2.092	1.507	1.507	Stable
Generation at bus #93 and bus #110: 700 MW each								
5	6	6-7	0.090	7-104	0.263	-1.566	-1.273	Unst.
Generation at bus #93 and bus #110: 1000 MW each								
6	100	100-72	0.200	72-101	1.543	1.521	1.522	Stable
7	105	105-73 1 105-73 2	0.088	73-74	1.132	0.820	0.836	Stable
8	33	33-39	0.260	33-110	0.545	0.366	0.361	Stable
9	91	91-74	0.140	91-108	2.124	1.565	1.565	Stable
161 generator system								
10	1757	1757 - 1709	0.100	1709-1727	2.165	1.235	1.256	Stable
11	1695	1695 - 1853	0.100	1695 - 1707	1.266	1.198	1.149	Stable
12	1695	1695-1853	0.100	1853-4010	1.266	0.985	0.948	Stable

1: BC refers to the base case

2: NC refers to the new case (with the change introduced)

Table 4.2. Generation change limits for stable and unstable cases

Case #	Fault Bus	Line cleared	Clr. Time (sec)	ΔV_n for BC (TEF)	Gen. Limits (MW)	ΔV_n for NC (Sens.)	ΔV_n for NC (TEF)	Result from etmspv3
50 generator system								
13	66	66 - 111 1, 2, & 3	0.125	-0.472	26: -185	0.051	0.064	Stable
14	112	112 - 69	0.272	-0.676	9: -25; 27: -45	0.019	0.056	Stable
15	106	106 - 74	0.125	1.283	22:170	0.071	0.073	Stable
16	33	33 - 39	0.362	0.289	9:40; 20:35 25:40; 26:30	0.069	0.071	Stable
161 generator system								
17	1662	1662-1667	0.108	0.380	1683:50	0.077	0.091	Stable

Table 4.3. Prediction of change in the MOD of the controlling UEP

Case #	MOD of the Controlling UEP	MOD of the Controlling UEP (NC, From Sen.)	MOD of the Controlling UEP (NC, From TEF)
7	6, 14, 20, 21	14, 20, 21	14, 20, 21
10	8-13, 15-17, 19-21, 23-27 29-41, 65-80	8-17, 19-21, 23-42, 44-49 65-80	8-17, 19-21, 23-42, 44-49, 65-80
12	8-50, 57, 65-80	8-50, 56, 57, 65-80	8-50, 56, 57, 65-80
17	8-13, 15-17, 19-21, 23-27, 29-35, 38-41, 65-80	8-13, 15-17, 19-21, 23-27, 29-42,65-80	8-13, 15-17, 19-21, 23-27, 29-42, 65-80

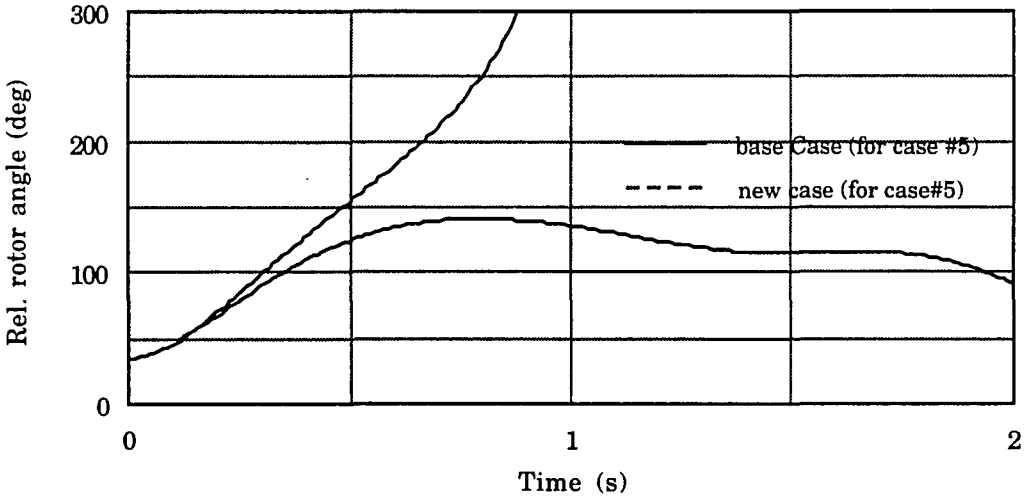

Fig 4.1. Relative rotor angle plot of machine #20 for case 5

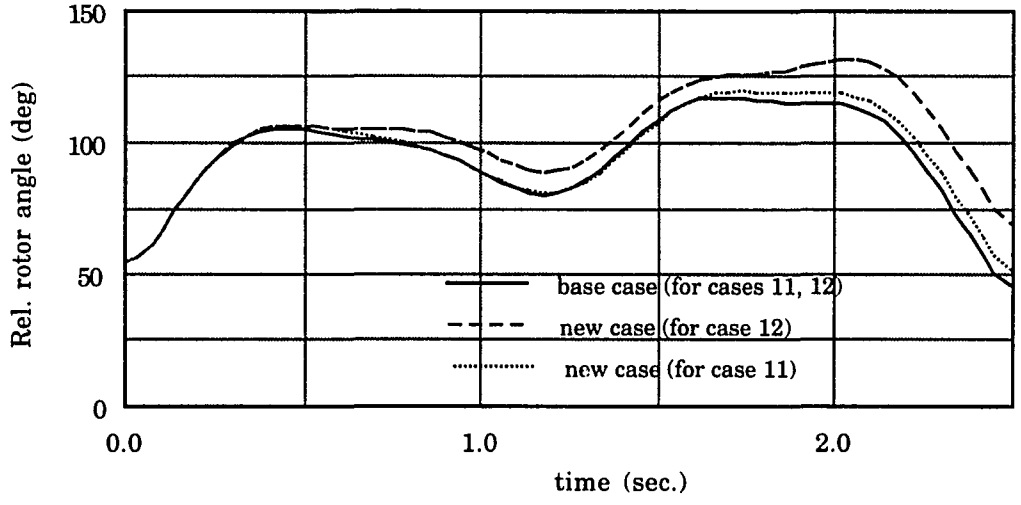

Fig 4.2. Relative rotor angle plot of machine #42 for cases 11 and 12

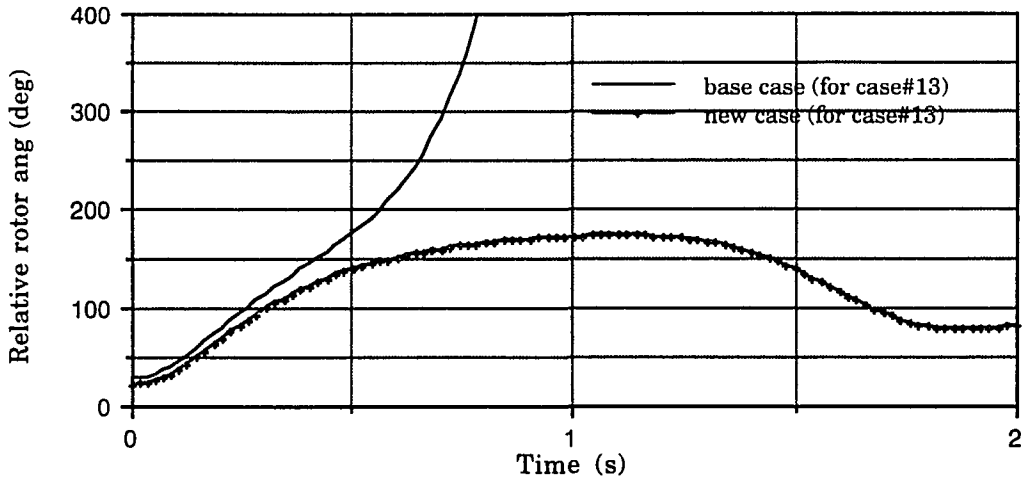

Fig 4.3. Relative rotor angle plot of machine #26 for case 13

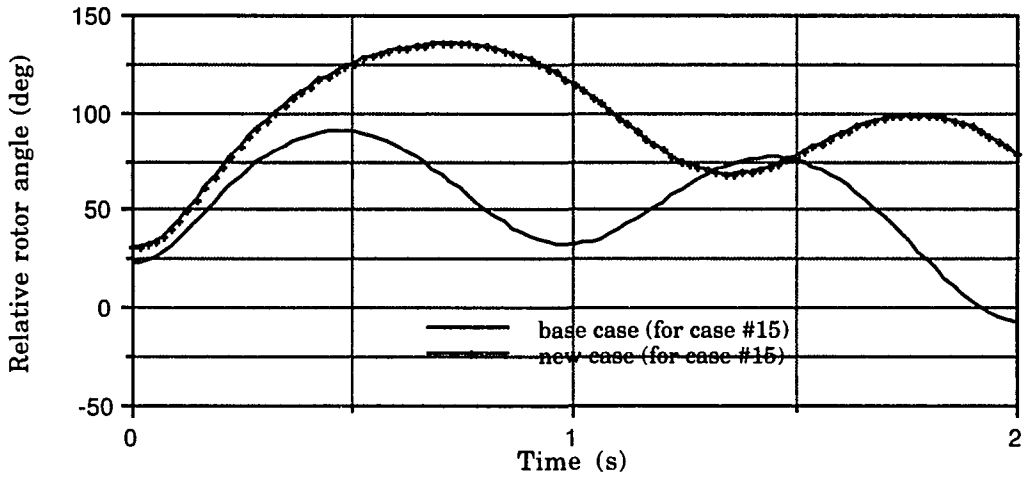

Fig 4.4. Relative rotor angle plot of machine #22 for case 15

5 SPARSE TRANSIENT ENERGY FUNCTION FORMULATION

The reduced formulation was used in the TEF method explained in chapter 2. The initial feasibility of the project was tested using the above method. For sufficiently large number of generators, the reduced formulation results in a computationally demanding *Y-bus*. In other words, the *Y-bus* is a full matrix. The method which is based on reduced formulation has a computational complexity of $O(n^3)$. The reduced admittance matrix mentioned above is used in all the major steps of the TEF method. These major steps are the determination of the exit point, minimum gradient point, UEP and the computation of the energy margin.

One of the main requirements for the on-line implementation of this contingency filtering scheme is speed. Some power system models used in the Energy Management System (EMS) consist of about 200 generators and 1200 buses. Analysis of a number of contingencies (in the hundreds) for such a large system in real time would be impossible with the reduced formulation. The best alternative to the reduced formulation is the use of sparse formulation. In the sparse formulation, all the steps involved in the TEF method are carried out using sparse matrices. The computational complexity of an algorithm using sparse formulation is $O(n)$. This is in contrast to the complexity of order $O(n^3)$ mentioned earlier. Also, the full network topology is retained. This makes the implementation of special controls like HVDC and SVC easier. This chapter very briefly highlights the main features of the

sparse TEF (STEF) method. Earlier work in the implementation of sparse techniques in the TEF method was done in [13, 45]. The STEF method described below is the result of work done in [46].

5.1 Mathematical Model

A multimachine power system is represented by a set of differential and algebraic equations which are of the general form

$$\dot{y} = f(y,x) \tag{5.1}$$

$$0 = g(y,x) \tag{5.2}$$

Equation (5.1) represents the set of differential equations for all the generators. These generators could be modeled in detail or classically. Equation (5.2) represents the algebraic equations. These are the stator algebraic equations coupled with the equations of the transmission network and loads.

The differential equations for the generator are given by

$$M_i \dot{\omega}_i = P_{mi} - P_{ei} \tag{5.3}$$

$$\dot{\delta}_i = \omega_i \tag{5.4}$$

$$\tau'_{doi} \dot{E}'_{qi} = E_{FDi} - E'_{qi} + (x_{di} - x'_{di}) I_{di} \tag{5.5}$$

$$\tau'_{qoi} \dot{E}'_{di} = - E_{di} - (x_{qi} - x'_{qi}) I_{qi} \tag{5.6}$$

$$\tau_{Ei} \dot{E}'_{FDi} = - E'_{FDi} + K_{Ai} (V_{REFi} - V_{ti}) \tag{5.7}$$

where

τ'_{do} = Open circuit direct axis time constant

τ'_{qo} = Open circuit quadrature axis time onstant

E_{FD} = Stator EMF corresponding to the field voltage after limiter

τ_{Ei} = Exciter Time Constant

$x_d^{'}$ = Direct axis transient reactance

$x_q^{'}$ = Quadrature axis transient reactance

$E_q^{'}$ = Direct axis stator EMF corresponding to rotor flux components

$E_d^{'}$ = Quadrature axis stator EMF corresponding to rotor flux components

I_d = Direct axis stator current

I_q = Quadrature axis stator current

x_d = Direct axis synchronous reactance

x_q = Quadrature axis synchronous reactance

$E_{FD}^{'}$ = Stator EMF corresponding to the field voltage before limiter

V_{REF} = Exciter reference voltage

V_t = Terminal voltage

The whole set of equations given above is required for detailed machine modeling. In this, the generator is represented by the two axis model [30, chapter 4]. The exciter equation represents a one gain, one time constant exciter model [20, chapter 8]. If the generator is represented classically, equations (5.3) and (5.4) are sufficient.

The stator algebraic equations are given by

$$E_{qi}^{'} - V_{qi} = I_{di}X_{di}^{'} + I_{qi}r_s \tag{5.9}$$

$$E_{di}^{'} - V_{di} = -I_{qi}X_{qi}^{'} + I_{di}r_s \tag{5.10}$$

where

V_q = q axis component of the terminal voltage

V_d = d axis component of the terminal voltage

r_s = resistance of the stator winding

The network equations are of the form

$$\sum_m (G_{km} + jB_{km})(e_m + jf_m) = \frac{P_k - jQ_k}{e_k - jf_k} \tag{5.11}$$

where,

m = All the buses in the network

k = Ranges from *1* to m

P_k = Net real power at bus k

Q_k = Net reactive power a bus k

e_k = Real part of the terminal voltage

f_k = Imaginary part of the terminal voltage

The above equation is in the form of current injection at each load bus. If the load is modeled as a constant shunt admittance, the right hand side of equation (5.11) is zero. The stator algebraic equations are included in the network solution.

5.2 Determination of the Exit Point and the Minimum Gradient Point

The determination of the fault-on trajectory requires solutions of the sets of differential and algebraic solutions with the fault applied. The machine differential equations are solved separately using a variable order, variable step integration algorithm followed by the network solution. The integration is done by using a modified *ODEPACK* [47]. The modification was essential to make use of the sparse structure in the solution of the differential equations. The network solution is obtained using the factorized bus admittance matrix.

The formulation in [48] is followed to solve the linear system of equations given by

$$Y V = I \tag{5.12}$$

The above equation is solved for the bus voltages V.

The fault on trajectory is integrated till fault clearing. This gives us the conditions at clearing. The computation of the fault-on trajectory is continued till the exit point is reached. The exit point (like in the reduced formulation) is characterized by the first maximum of the potential energy with respect to the post-disturbance network. The exit point is determined when the condition $\sum_{i=1}^{n} - f_i \tilde{\omega}_i = 0$ is satisfied. $\tilde{\omega}_i$ is the fault on speed of generator i. f_i is the power mismatch vector with respect to the post-fault network for generator i. The equation corresponding to f_i is given below.

$$f_i = P_{mi} - P_{ei} - \frac{M_i}{M_T} P_{COI} \tag{5.13}$$

$$P_{COI} = \sum_{i=1}^{n} (P_{mi} - P_{ei}) \tag{5.14}$$

The zero crossing along the faulted trajectory is detected by a change in the sign of the quantity $\sum_{i=1}^{n} - f_i \tilde{\omega}_i = 0$. Once the change in sign is detected, the previous step is taken as the exit point. This is possible because of the accuracy of the integration scheme.

To determine the minimum gradient point, the gradient system equations in the COI formulation ($\dot{\theta}_i = f_i$) need to be integrated with the post-fault network solution. The gradient system of differential equations is integrated starting from the initial conditions provided by the exit point. At each step of the integration the quantity $\sum_{i=1}^{n} |f_i| = F$ is evaluated. f_i is given by

equation (5.13). This is done to determine the first minimum of F along the gradient surface. This point is the minimum gradient point. The numerical integration of the gradient system equations needs to be very accurate. The minimum gradient point acts as the starting point for the UEP solution. Inaccurate starting points could sometimes lead to the wrong controlling UEP. Also, this system of differential equations is stiff. A robust and accurate integration method is needed to solve these equations. A variable step, variable order integration method based on the backward difference formulas [45] is used. One of the main differences in the computation of the minimum gradient point as compared to reduced formulation is the fact that the COI constraint is not implemented. In the reduced formulation, the COI constraint is implemented by eliminating the dynamic equation of the generator chosen as the slack generator. The angle for this generator was derived from the COI constraint equation

$$\sum_{i=1}^{n} M_i \, \theta_i = 0 \tag{5.15}$$

However, in the sparse formulation, the dynamic equations of all the generators are integrated.

5.3 Identifying the Controlling UEP

At the equilibrium points (both the SEP and UEP), the generator accelerations are zero. In a general form, at these equilibrium points, the differential equations can be written as $f(y,x) = 0$. This set of equations is solved along with the network power flow equations given by $g(y,x) = 0$. In the sparse formulation, the equilibrium point is solved for as an ordinary power

flow. The unknowns in this power flow problem are the terminal bus voltage magnitudes and angles, angles at the internal generator buses, the generator electrical power P_{ei} and P_{COI}. The P_{COI} is treated as the primary unknown. The P_{COI} power is allocated to the generators in proportion to their inertias.

5.4 Computation of the Energy Margin

The energy margin computation involves the calculation of the kinetic energy and the potential energy. The kinetic energy is evaluated using the conditions at clearing. As mentioned earlier in chapter 2, in the reduced formulation, the potential energy term is divided into three components. These are the position energy, magnetic energy and the dissipation energy terms. In the sparse formulation, the potential energy is divided into two terms. The position energy constitutes one term and the magnetic and dissipation energies together account for the second term. This is because the contributions from the magnetic energy and dissipation energy terms cannot be separated. The whole potential energy, is in fact, computed by numerically integrating equation (5.16).

$$PE = \sum_i \int_{\theta_i^{cl}}^{\theta_i^{u}} (P_{mi} - P_{ei})\, d\theta_i \qquad (5.16)$$

The linear angle trajectory approximation used in the integration of equation (5.16) is of the form

$$\theta_i = \theta_i^{cl} + (\theta_i^{u} - \theta_i^{cl})\, t, \quad 0 \le t \le 1 \qquad (5.17)$$

However, one of the advantages of this scheme is that any trajectory can be used for the angles between clearing and the UEP. In terms of problem definition, the computation of the potential energy margin is formulated as an ordinary differential equation of the form

$$\dot{y}_i = (P_{mi} - P_{ei}) (\theta_i^u - \theta_i^{cl}) \tag{5.18}$$

$$\dot{\theta}_i = (\theta_i^u - \theta_i^{cl}) \tag{5.19}$$

This set of equations is integrated in the time interval of 0.0 to 1.0. At the end of the integration, the potential energy margin is computed as

$$PE = \sum_i y_i \tag{5.20}$$

5.5 Implementation of the filtering scheme with sparse formulation

The concept behind the filtering scheme which was explained in chapter 3 remains the same. There are three stages of filtering and each stage is associated with an inertial transient filter and a post inertial transient filter. The tool used for analysis in each of these filters is the STEF. A description of the filtering scheme which is in full implementation is given below.

5.5.1 Inertial Transient Filters

Inertial transient filters 1 and 2 (*ITF 1* and *ITF 2*) are identical to those mentioned in chapter 3. In *ITF 1*, $\Delta V_{napprox1}$ categorizes the contingency. $\Delta V_{napprox1}$ is derived from the disturbance severity and post-disturbance network robustness.

$$\Delta V_{napprox1} = (\Delta V_{PEapprox1} - V_{KE}) / V_{KE} \tag{5.21}$$

$\Delta V_{PEapprox1}$, the potential energy difference between exit point and clearing provides a measure of the post-disturbance network robustness. V_{KE} , the total kinetic energy is a measure of the disturbance severity. Similarly in *ITF 2*, $\Delta V_{napprox2}$, given below, categorizes the contingency.

$$\Delta V_{napprox2} = (\Delta V_{PEapprox2} - V_{KE}) / V_{KE} \qquad (5..22)$$

In *ITF 3*, the index used is the exact normalized energy margin which is calculated as

$$\Delta V_n = (\Delta V_{PE} - V_{KEcorr}) / V_{KEcorr} \qquad (5.23)$$

Earlier, for the overall ranking of contingencies severe in the inertial transient period, both ΔV_n and its sensitivity to plant generation change were used as indices. Here, final ranking and screening for the inertial transient is provided based only on the magnitude ofΔV_n.

5.5.2 Post Inertial Transient filters

The post inertial transient filters (*PITF 1, PITF 2, PITF 3*) derive inputs from contingency cases deemed not severe by the respective inertial transient filters (*ITF 1, ITF 2, ITF 3*). In the sparse formulation, synchronizing power coefficients are used as an indicator of stress. The synchronizing power coefficients computed in the sparse formulation provide a lot of insight into the actual robustness of the network. This concept is explained later in this section. In *PITF 1, PITF 2* and *PITF 3* two sequential checks are made to ascertain if the system is potentially severe with respect to the post inertial transient period. If either of these checks is violated, the case is sent to the next level of filters (as depicted in figure 3.1). The first check is of the form

- $\Delta V_{napprox1} > Threshold\ 1$ and $V_{KE} < Threshold\ 2$

If the above check is violated (either $\Delta V_{napprox1} < Threshold\ \ 1$ or $V_{KE} > Threshold\ 2$ or both), the case is sent to the next level of inertial transient filter. This is because of the fact that this case exhibits a low post-disturbance network robustness and high disturbance severity (as compared to other contingencies in the same system). It should be noted that $\Delta V_{napprox2}$ and V_{KE} are used for the check in *PITF 2* . and ΔV_n and V_{KEcorr} in *PITF 3*. For cases which do not violate the above check, the analysis in each level of *PITF* consists of evaluating the synchronizing power coefficient and the terminal voltage of the advanced generators. This evaluation is done at either the exit point, the minimum gradient point or the UEP (each of which correspond to one level of filters). The calculation of the synchronizing power coefficient is done briefly explained below. In the sparse TEF method, the electrical power output at each machine i is given by

$$P_{ei} = \frac{1}{x'_{di}} \left[E_i V_i \sin \delta_i \cos\phi_i - E_i V_i \cos\delta_i \sin\phi_i \right] \tag{5.24}$$

where,

E_i : Internal voltage magnitude

δ_i : Internal voltage angle

V_i : Terminal voltage magnitude

ϕ_i : Terminal voltage angle

The synchronizing power coefficient S_i is then given by

$$S_i = \frac{\partial P_{ei}}{\partial d_i} = \frac{1}{x'_{di}} \left[E_i V_i \cos (\delta_i - \phi_i) \right] \tag{5.25}$$

The above expression describes the ability of the system to put out synchronizing power with respect to a change in the internal angle of the machine. It captures two essential features of the machine-network interaction. δ_i represents the reaction of the synchronous machines to the transient. V_i and ϕ_i which are obtained by a post-disturbance network solution represent the reaction of the network to the injections due to δ_i at the generator buses. Hence, S_i captures the effect of the interaction between the synchronous machines and the network due to the transient. A low or negative value of S_i indicates a potential inability to put out enough synchronizing power in response to the transient. In addition, the terminal voltage magnitude is also used as an indicator of potential problems in the post-inertial transient period. The filters compare the values of S_i andV_i for the advanced generators of the form

- S_i < *Threshold 3* andV_i < *Threshold 4*

Cases which meet the above check are deemed to have potential problems in the post-inertial transient period and as a result are sent to the next level of inertial transient filters. Similar to *ITF 3*, the final ranking in *PITF 3* is provided based only on the magnitude of ΔV_n.

5.6 Sample results on the post inertial filter signatures

The concept of using both the synchronizing power coefficient and the terminal voltage as a signature is very important. This is for the reason that it helps identify cases which could be multi swing unstable. Extensive testing of this signature was done on different systems. These system include

- 50 generator IEEE test system [43]

- 161 generator NSP system [44]
- 223 generator test system

Tables 5.1, 5.2, 5.3 and 5.4 give the details of the four cases which do not meet the check on the synchronizing power coefficients and terminal voltage. Also mentioned in the table is the system to which that particular case belongs. The values of the synchronizing power coefficients and the terminal voltages of those machines which do not meet the check are provided. These four cases were then run using time simulation. The machines picked up as being critical with respect to the post inertial period (by the signature) were monitored. Figures 5.1, 5.2, 5.3, 5.4, 5.5 and 5.6 illustrate the fact that the cases are indeed severe with repect to the post inertial period. Cases 1 and 2 are not nearly as severe as cases 3 and 4. Cases 3 and 4 are multi swing unstable cases. On the other hand, cases 1 and 2 are characterized by a voltage dip at about 8.5 seconds and a higher angular peak in the subsequent swings. The voltage was monitored at buses close to the disturbance.

Table 5.1. Synchronizing power coefficients and terminal voltages for case 1

Case 1 161 generator system Fault at : 605 Line removed : 605 - 506 Clearing Time : 0.1 sec		
Machine #	Synchronizing Power Coeff. (pu)	Terminal Voltage (pu)
At the Exit Point		
11	1.79459	0.71551
At the Minimum Gradient Point		
11	1.68261	0.73070

Table 5.2. Synchronizing power coefficients and terminal voltages for case 2

Case 4 161 generator system Fault at : 605 Line removed : 605 - 660 Clearing Time : 0.1 sec		
Machine #	Synchronizing Power Coeff. (pu)	Terminal Voltage (pu)
At the Exit Point		
11	1.79766	0.71754
At the Minimum Gradient Point		
11	1.68306	0.73314

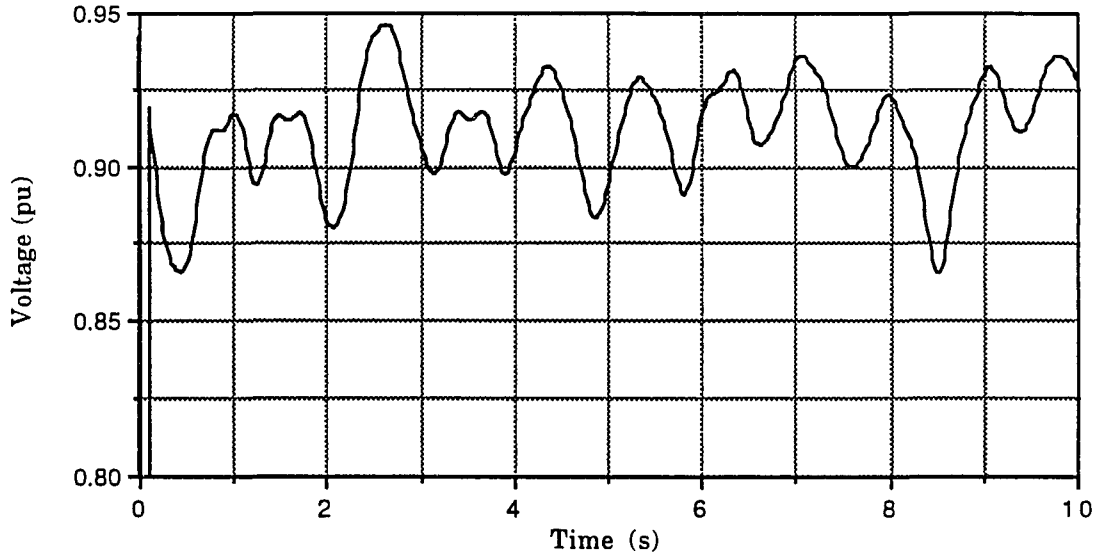

Fig 5.1 Voltage plot of bus #611 for case 1

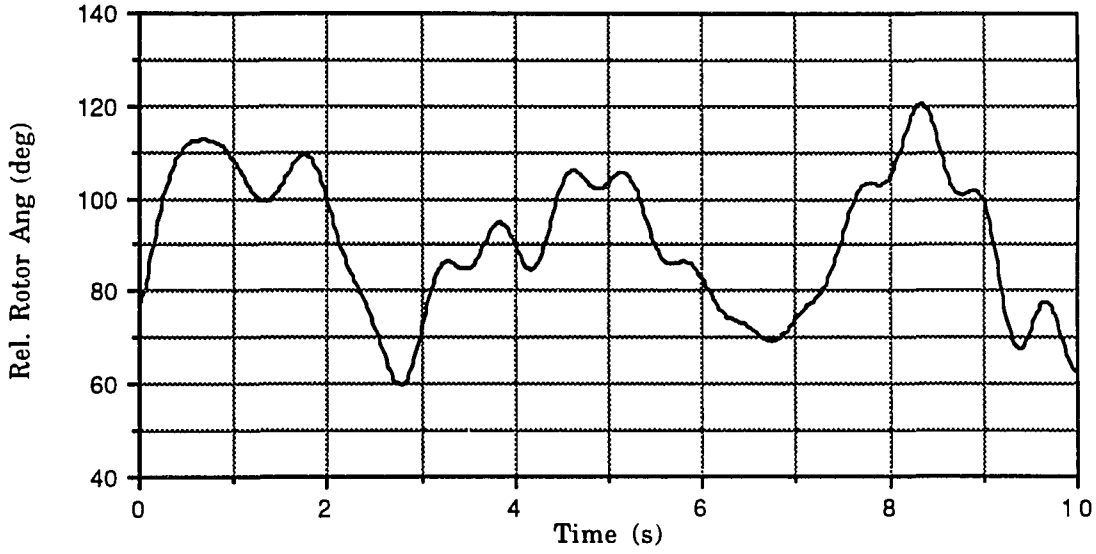

Fig 5.2 Relative rotor angle plot of machine #11 for case 1

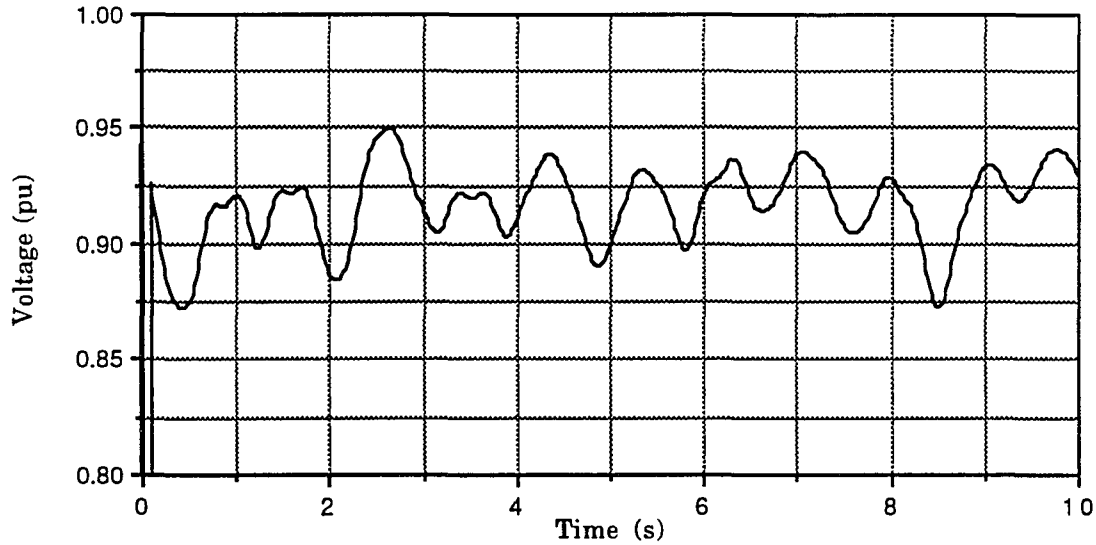

Fig 5.3 Voltage plot of bus #611 for case 2

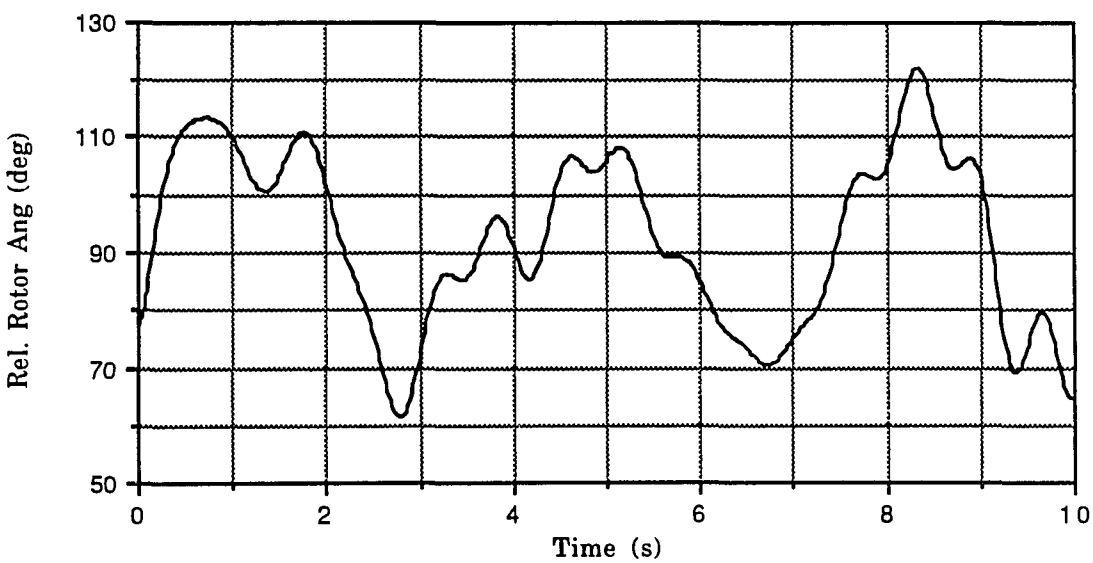

Fig 5.4 Relative rotor angle plot of machine #11 for case 2

Table 5.3. Synchronizing power coefficients and terminal voltages for case 3

Case 3 223 generator system Fault at Bus #311 Line cleared:310-311 Clearing Time:0.22 sec		
Machine #	Synchronizing Power Coeff (pu)	Terminal Voltage (pu)
At the Exit Point		
86	0.02466	0.748
31	0.1539	0.657
75	0.2588	0.703
143	0.7396	0.577
At the Minimum Gradient Point		
86	0.0458	0.760
31	0.3304	0.673
15	0.4371	0.689
75	0.6403	0.719
143	1.7491	0.588

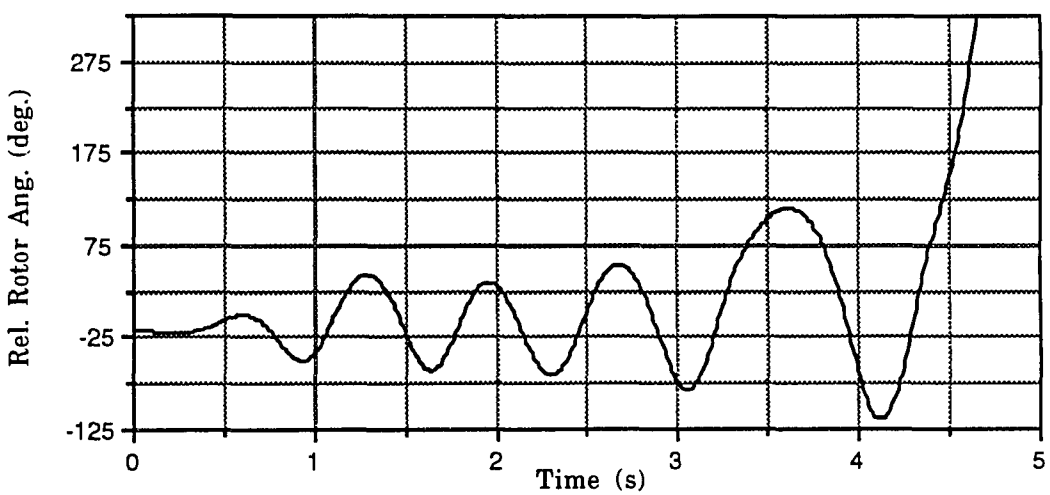

Fig 5.5. Relative rotor angle plot of machine #86 for case 3

Table 5.4. Synchronizing power coefficients and terminal voltages for case 4

Case 4 50 generator IEEE test system Fault at Bus #33 Line Cleared: 33-39 Clearing time: 0.2856 sec		
Machine #	Synchronizing Power Coeff (pu)	Terminal Voltage (pu)
At the Exit Point		
15	1.3863	0.432
At the Minimum Gradient Point		
15	1.1708	0.469

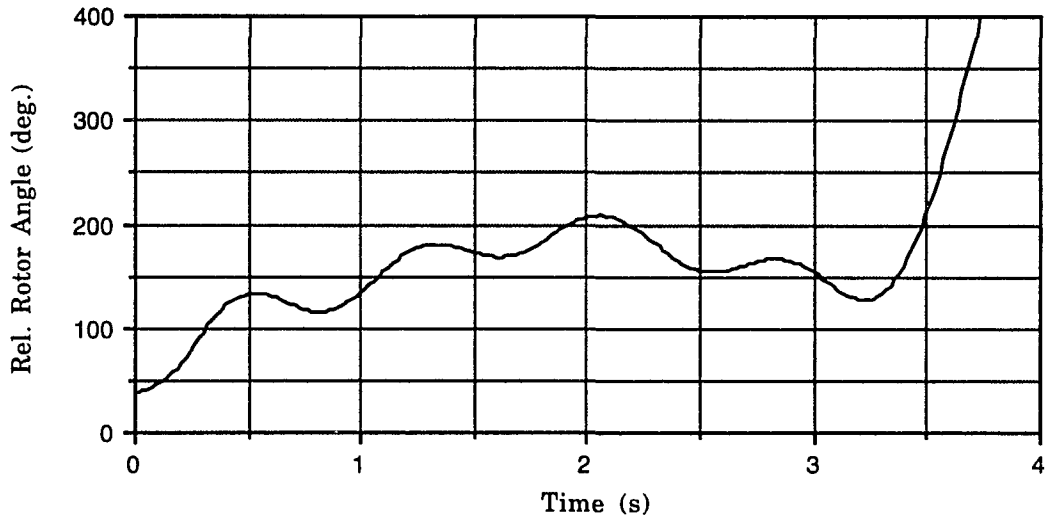

Fig 5.6. Relative rotor angle plot of machine #15 for case 4

6 ENHANCEMENTS TO THE SPARSE TEF METHOD

6.1 Exciter Reduction

In today's power system, increased interconnections with greater system inertias and relatively weaker ties result in longer transient periods of interest. Modern excitation systems are much faster than earlier ones. As mentioned earlier, the TEF method has emerged as a potential tool for dynamic security assessment. Its primary use is in determining the first swing transient stability. Any improvements which would increase the accuracy of results during the first swing transient would be of importance. Representation of certain power system components in the TEF method is essential for increased accuracy. These modeling improvements give a better estimate of the relevant system transient energy during the first swing transient. At present, the TEF method is capable of modeling the synchronous generator by the two axis model [30, chapter 4]. The excitation system is another component which needs to be modeled. However, the standard exciter models which are used need as many as 5-7 differential equations each. This would result in severely slowing down the transient stability assessment. The modeling complexity of these excitation systems needs to be simplified. At the same time, these reduced order models should be capable of accurately representing the effect on the dynamic performance of the system. A reduced

order model is developed for five of the standard exciter types used in today's power system. The approach used for this is that developed in [49]. In the approach suggested in [49], the concept of noise equivalent bandwidth [50] in is used to develop a procedure to obtain reduced order models over a specified frequency range. The excitation system is reduced to a simple one gain, one time constant, one limiter model [20, chapter 8]. In this study, five different exciter types were chosen based on actual field data supplied by Northern States Power Co. These were

- DC Generator Commutator Exciter Type 1
- Self Excited DC Generator Exciter Type 2
- Discontinuous Exciter Type 9
- Simplified Rotating Rectifier Excitation Exciter Type 10
- Static Exciter Type 30

A brief description of the method used [49] is given below.

6.1.1 Procedure to Obtain Reduced Order Excitation System Model

The procedure used is based on the concept of noise equivalent bandwidth. Figure 6.1 denotes the response of both an idealized filter (whose frequency response is unity over a prescribed bandwidth and zero outside this band) and an actual filter. In this figure, the gain has been normalized to yield a peak response of unity. The mean square responses of the actual filter and the idealized filter (as depicted above) to white noise of amplitude A are equated. The equality relation can be used to solve for the bandwidth B. This bandwidth B, where the mean square responses of the ideal and actual filter are the same is known as the noise equivalent bandwidth.

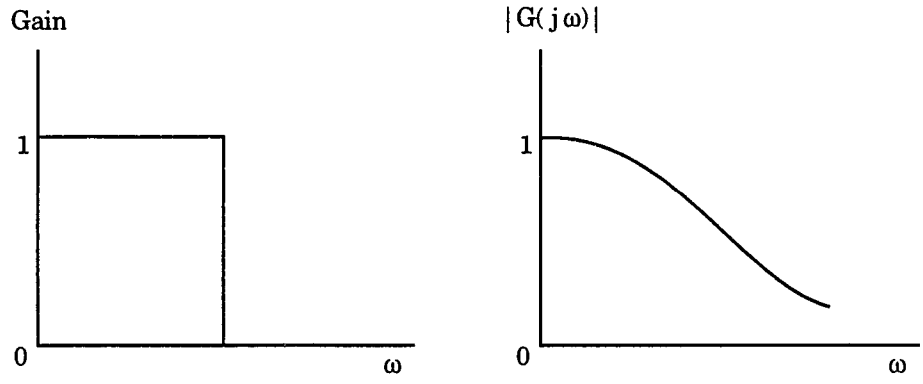

Fig 6.1. Idealized and actual filter response

Let $G_{exact}(s)$ denote the transfer function of the exact model and $G_{approx}(s)$ be the transfer function of the simplified model. The transfer function of the simplified model is given by

$$G_{approx}(s) = \frac{K}{1+TS} \tag{6.1}$$

The mean square response of the simplified system over a desired frequency range when driven by white noise with unity amplitude is made equal to the mean square response of the exact model to white noise with unit amplitude over the same frequency range. This equality is used to solve for the unknowns in the simplified exciter model.

The following steps are involved in the process of deriving the simplified model.

- The transfer function of the exact model $G_{exact}(s)$ is derived.
- The frequency range of interest is chosen. In this case, a frequency range of 0.1 - 1 hz was chosen. This is split into two intervals. The first interval is from 0.1 to 0.2 hz (0.62831 rad/s - 1.25662 rad/s) and the second interval from 0.2 to 1 hz (1.25662 rad/s - 6.2831 rad/s). In

today's power systems, the interarea modes occur at low frequencies (0.2 - 0.3 hz) and plant modes at around 0.7 to 1 hz. This was used as an approximate guideline in choosing the intervals.

- Let the mean square response of the exact model over the two intervals be denoted by E_{exact1} and E_{exact2} where

$$E_{exact1} = \frac{1}{2\pi}\int_{0.62831}^{1.25662} |G_{exact}(\omega)|^2 \, d\omega \tag{6.2}$$

$$E_{exact2} = \frac{1}{2\pi}\int_{1.25662}^{6.2831} |G_{exact}(\omega)|^2 \, d\omega \tag{6.3}$$

- The simplified first order exciter model has two unknowns and is given by

$$G_{approx}(s) = \frac{K}{1+TS} \tag{6.4}$$

From this, the approximate mean square response over the same two intervals can be calculated as

$$E_{approx1} = \frac{1}{2\pi}\int_{0.62831}^{1.25662} |G_{approx}(\omega)|^2 \, d\omega \tag{6.5}$$

$$E_{approx2} = \frac{1}{2\pi}\int_{1.25662}^{6.2831} |G_{approx}(\omega)|^2 \, d\omega \tag{6.6}$$

- The two unknowns which need to be solved for are K and T. For this we require two equations which are given by,

$$E_{approx1} = E_{exact1} \tag{6.7}$$

$$E_{approx2} = E_{exact2} \tag{6.8}$$

These are two nonlinear equations which can be solved easily. The method used to solve these equations is the bisection method.

It should be noted that in the above procedure, the nonlinearities are linearized around the operating point [30, chapter 7]. The nonlinearity is introduced by the presence of a saturation function. This saturation function, denoted by $S_e(E_{FD})$ is a nonlinear function of the exciter terminal voltage E_{FD}. This function is given by the equation

$$S_e = \frac{A_{ex}}{E_{FD}} exp(B_{ex} E_{FD}) \tag{6.9}$$

where

$$A_{ex} = \frac{(S_{emax})\,(E_{FDmax})}{exp(B_{ex}\,E_{FDmax})} \tag{6.10}$$

$$B_{ex} = \left(\frac{4}{E_{FDmax}}\right) ln \left(\frac{4}{3}\left(\frac{S_{emax}}{S_{e\,(0.75)}}\right)\right) \tag{6.11}$$

In the above equations, E_{FDmax} corresponds to the exciter ceiling voltage. S_{emax} and $S_{e\,(0.75)}$ are obtained by substituting E_{FDmax} and $0.75*E_{FDmax}$ in equation (6.10) respectively. The saturation function is now linearized as

$$S_{e\Delta} = \frac{\partial S_e}{\partial E_{FD}} E_{FD\Delta} = S_e^{'} E_{FD\Delta} \tag{6.12}$$

$$S_e^{'} = A_{ex} \{ E_{FD}^{-1} B_{ex} exp(B_{ex} E_{FD}) - \frac{exp(B_{ex} E_{FD})}{E_{FD}^{2}} \} \tag{6.13}$$

$S_e^{'}$ denotes the saturation in the vicinity of the initial operating point and is used in place of the nonlinear function $S_e(E_{FD})$. The operating point around which the linearization is done is dependent on the exciter type. Appendix B tabulates the operating points chosen for the different exciters used in this research. Also provided in appendix B is the original block diagram and the

analytical form of the approximate transfer function ($G_{approx}(s)$) of the different exciters.

6.1.1 Sample results with exciter reduction

The exciter reduction technique explained in the above section was tried on the 243 generator NSP system. This system has 170 generators modeled classically and 73 generators modeled with exiters. These exciters are among the 5 types mentioned earlier in section 6.1. Each of these exciters was reduced to an equivalent one gain one time constant exciter model. The original models were then replaced by these approximate exciter models. Time simulation was performed on three different cases. Each case was run with both actual and approximate models. The critical generators and buses in the system were monitored in each case. The three cases consideed are

- Case 1: Fault at 1695
  Line Removed: 1695 - 1742
  Clearing time: 0.100 sec.
- Case 2: Fault at 1604
  Line Removed: 1604 - 1702
  Clearing time: 0.100 sec.
- Case 3: Fault at 1662
  Line Removed: 1662 - 1655
  Clearing time: 0.100 sec.

Figures 6.2 through 6.13 depict the two most critical generators and buses in the system. The reponse of the system with the approximate exciter models is very similar to that with the actual models.

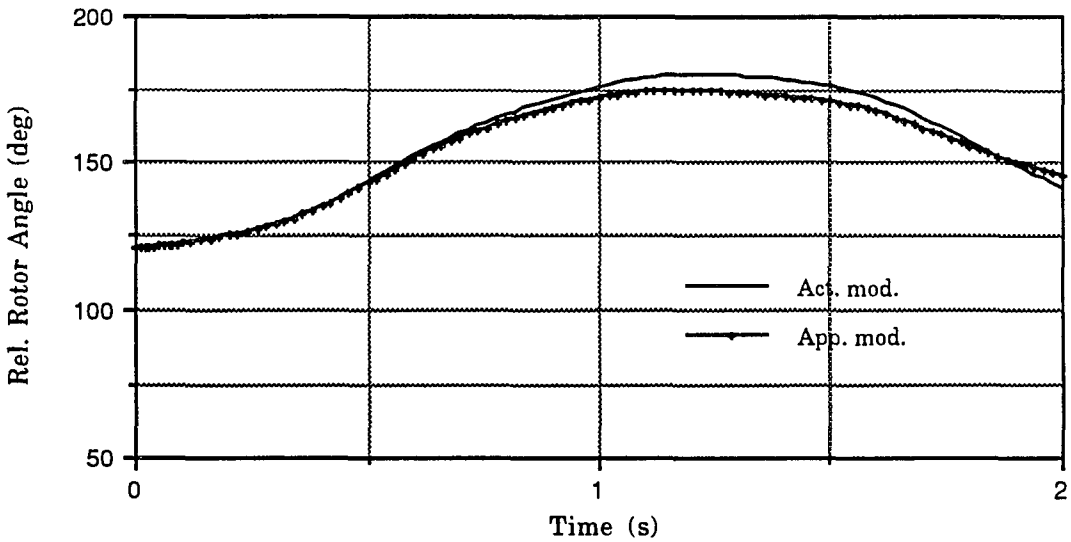

Fig 6.2. Relative rotor angle plot of machine #74 for case 1

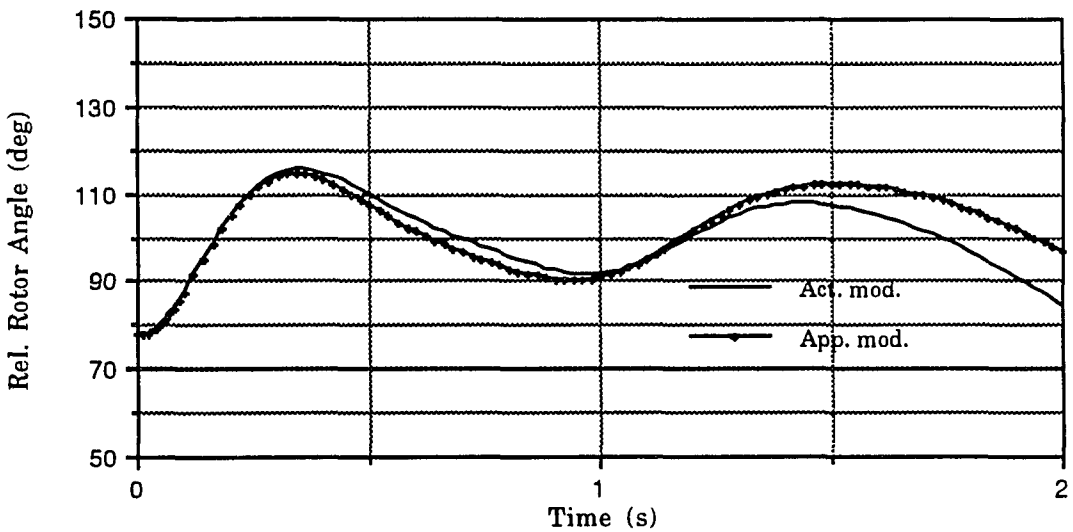

Fig 6.3. Relative rotor angle plot of machine #40 for case 1

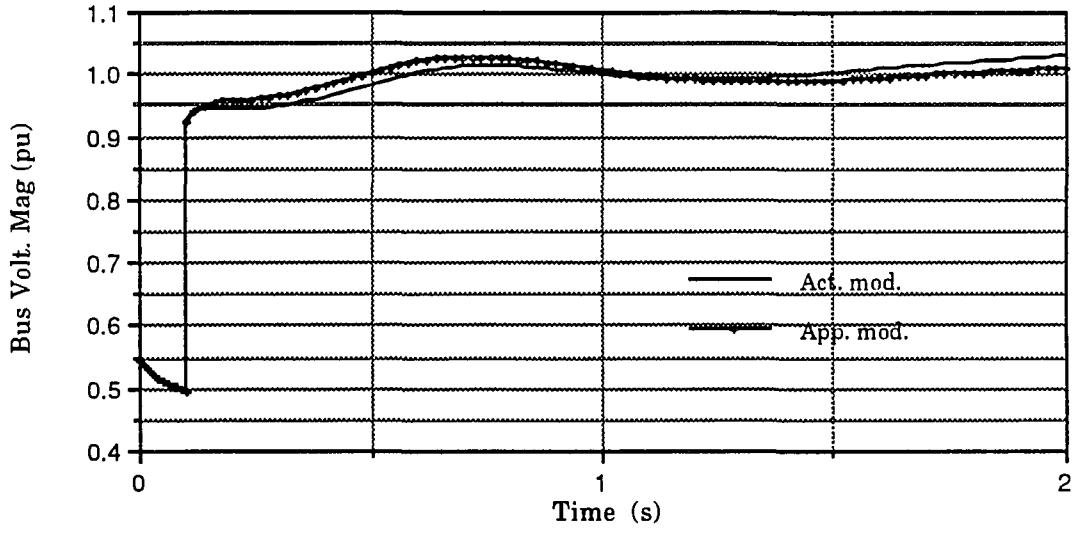

Fig 6.4. Voltage plot of bus #1604 for case 1

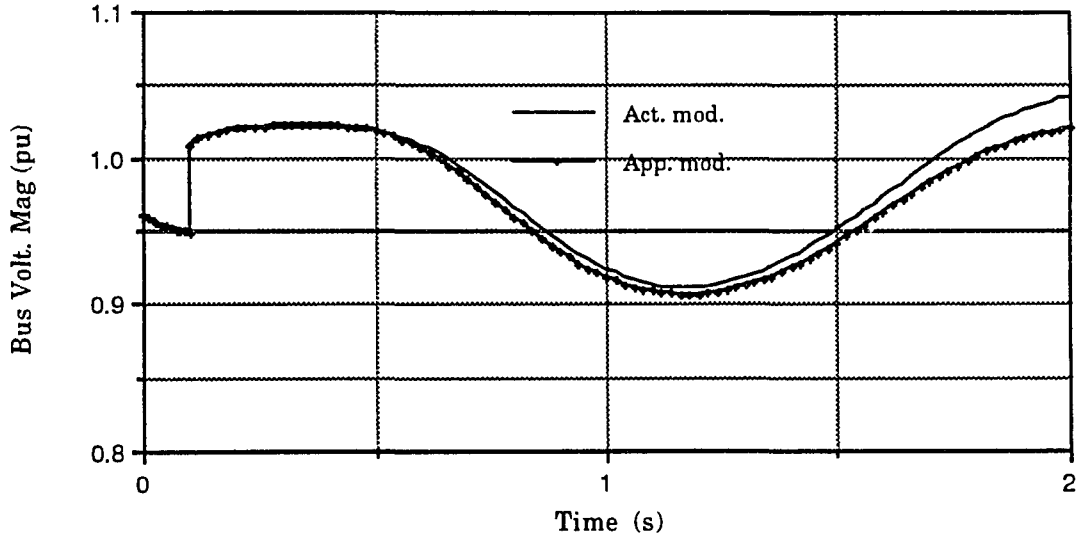

Fig 6.5. Voltage plot of bus #529 for case 1

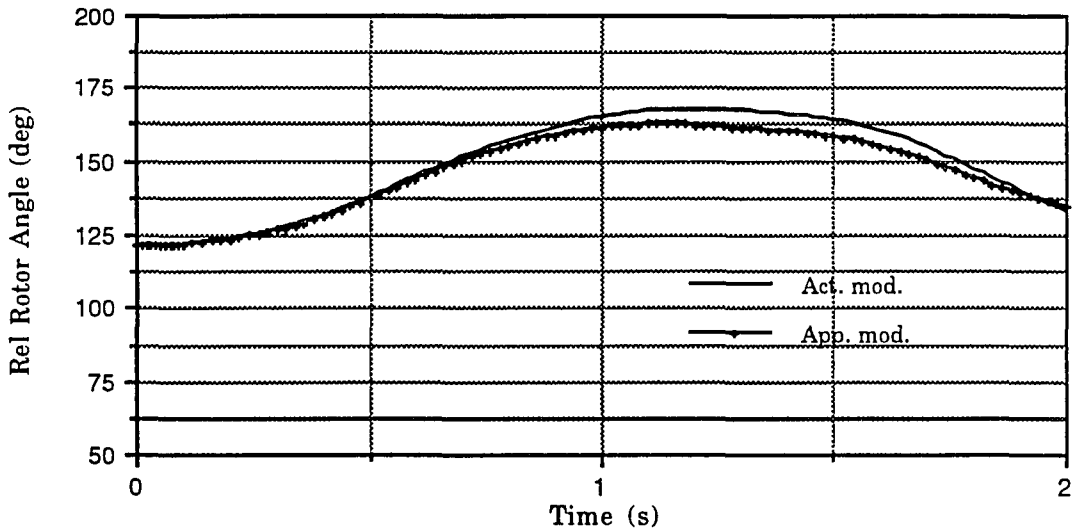

Fig 6.6. Relative rotor angle plot of machine #74 for case 2

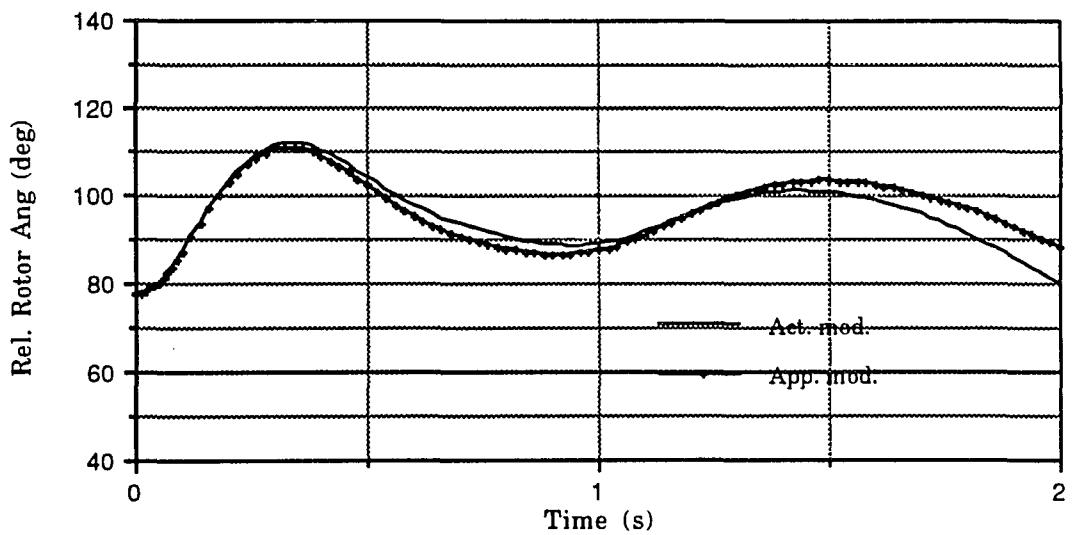

Fig 6.7. Relative rotor angle plot of machine #40 for case 2

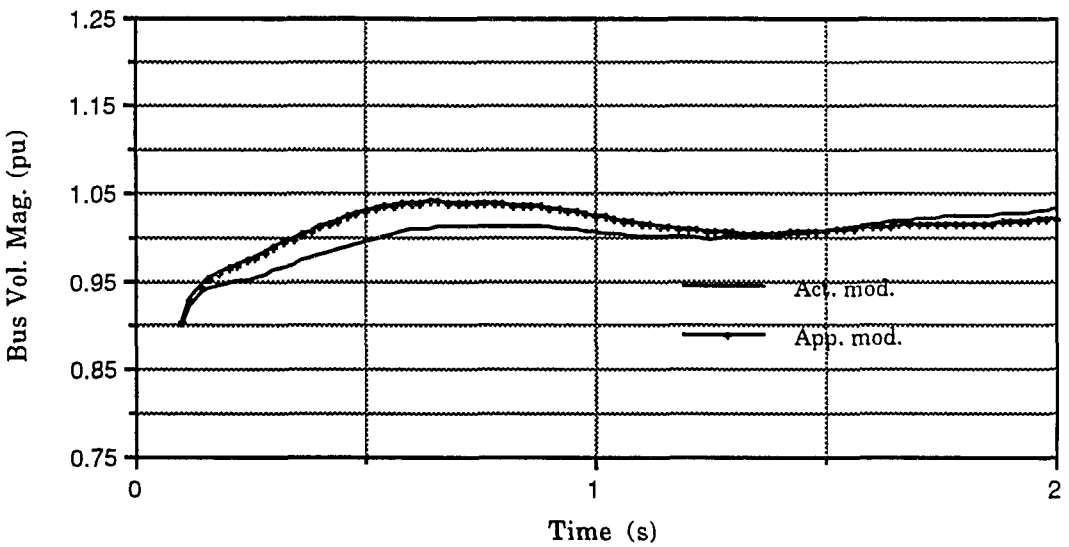

Fig 6.8. Voltage plot of bus #1604 for case 2

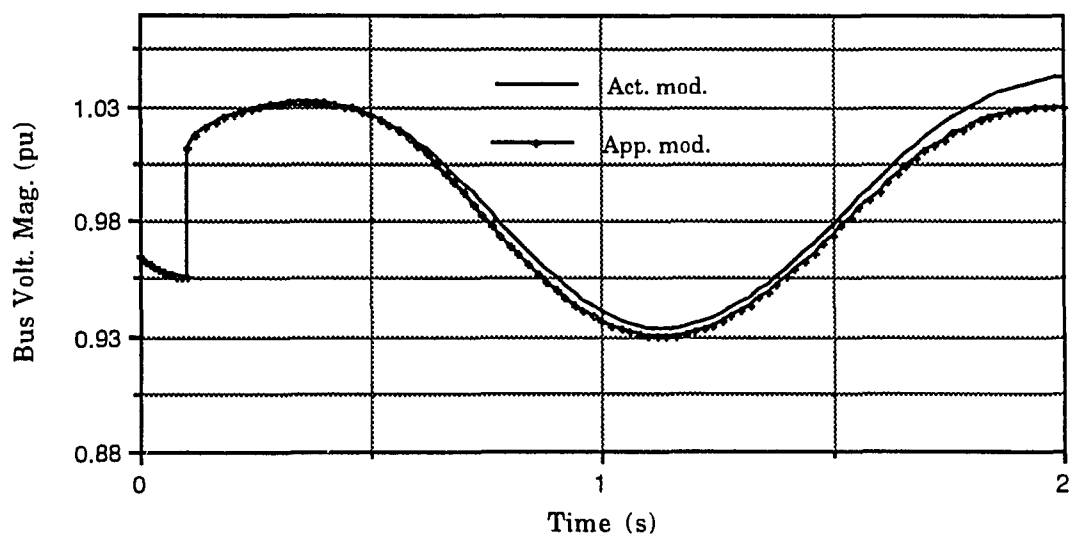

Fig 6.9. Voltage plot of bus #529 for case 2

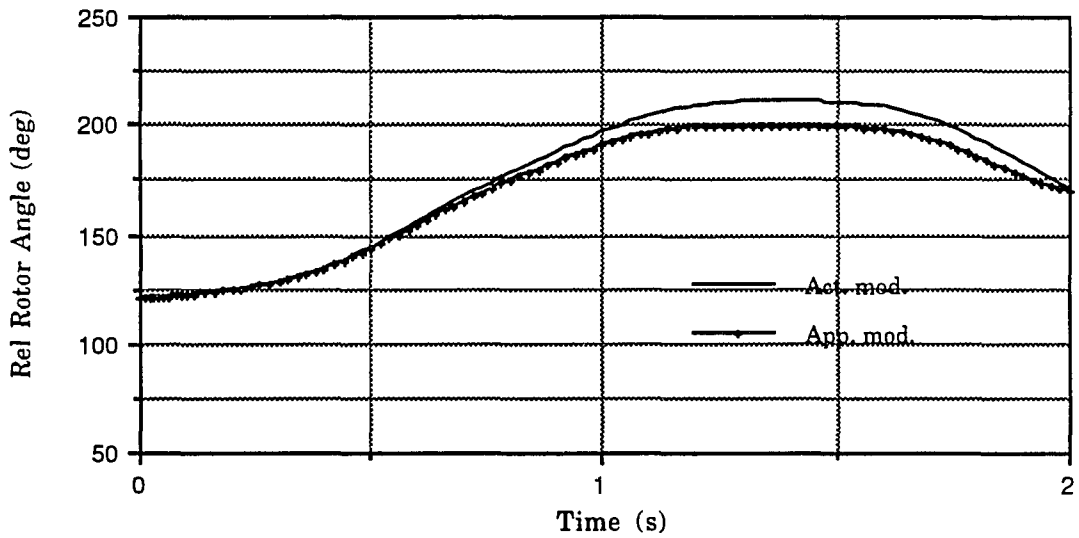

Fig 6.10. Relative rotor angle plot of machine #74 for case 3

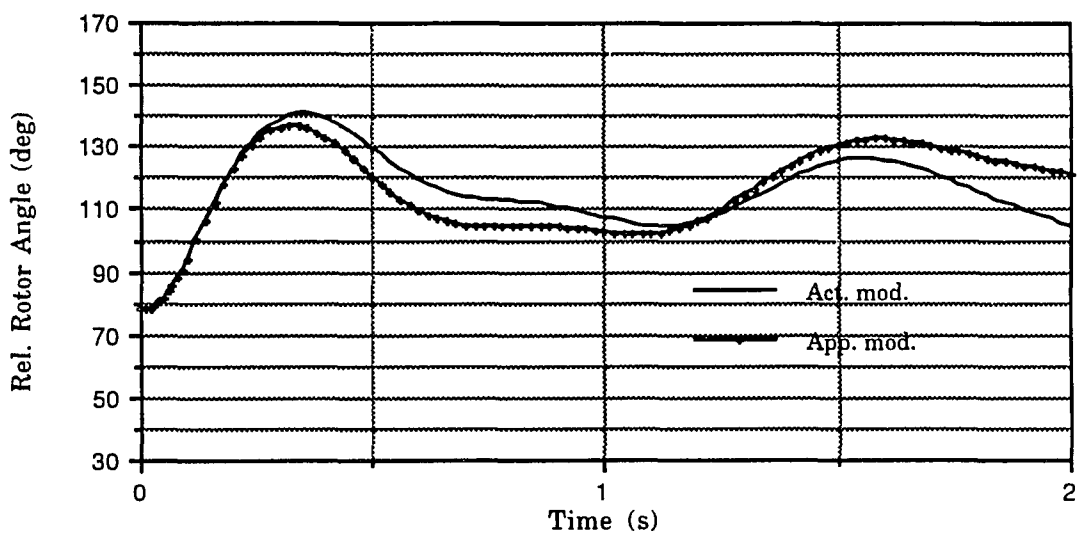

Fig 6.11. Relative rotor angle plot of machine #40 for case 3

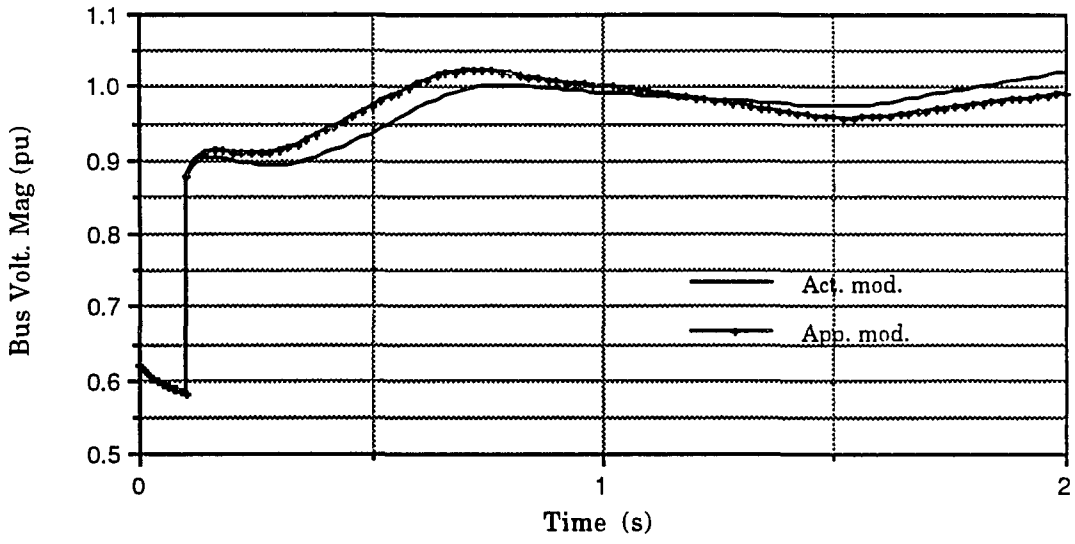

Fig 6.12. Voltage plot of bus #1604 for case 3

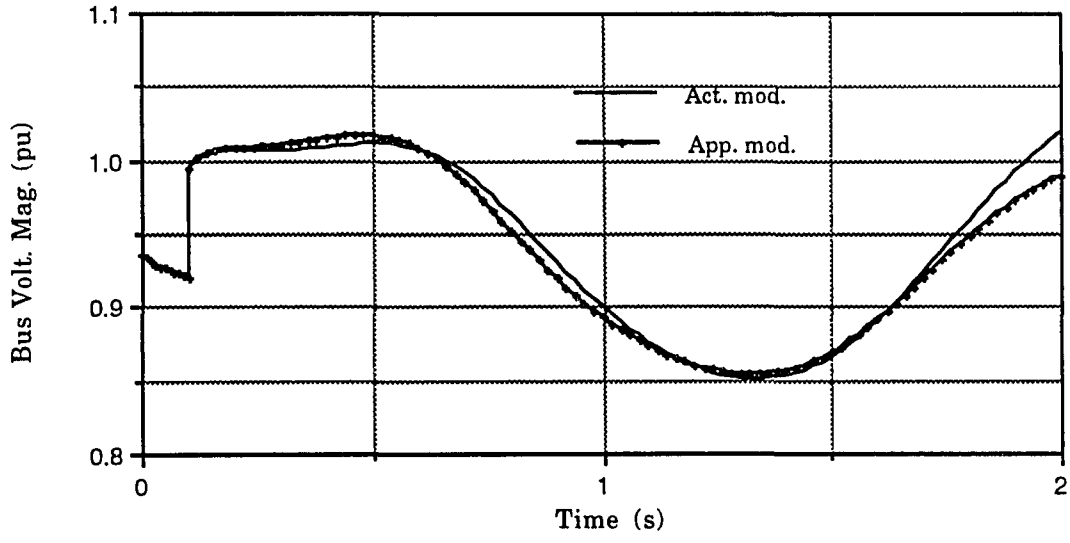

Fig 6.13. Voltage plot of bus #529 for case 3

6.2 Spline Function

Most of the discussion in the preceding chapters was for the classical power system model. Modeling developments which have been incorporated in the TEF method include the two axis representation [30, chapter 4] for generators and the one-gain one time constant model [20, chapter 8] for the exciters. The transient energy margin in the reduced formulation with the models described above is given by

$$\Delta V = \frac{1}{2} M_{eq}\, \tilde{\omega}_{eq}^2 + \sum_{i=1}^{n} - (P_{mi} - \alpha_{ii}\, G_{ii})\, (\theta_i^p - \theta_i^{cl}) +$$

$$\sum_{i=1}^{n-1} \sum_{j=i+1}^{n} \{ B_{ij}\alpha_{ij} [-\cos \theta_{ij}^p + \cos \theta_{ij}^{cl}] + \beta_{ij}\, B_{ij} [\sin \theta_{ij}^p - \sin \theta_{ij}^{cl}] \} +$$

$$\sum_{i=1}^{n-1} \sum_{j=i+1}^{n} \{ G_{ij}\, \alpha_{ij} \frac{\theta_i^p + \theta_j^p - \theta_i^{cl} - \theta_j^{cl}}{\theta_{ij}^p - \theta_{ij}^{cl}} [\sin \theta_{ij}^p - \sin \theta_{ij}^{cl}] +$$

$$G_{ij}\, \beta_{ij} \frac{\theta_i^p - \theta_j^p - \theta_i^{cl} - \theta_j^{cl}}{\theta_{ij}^p - \theta_{ij}^{cl}} [\cos \theta_{ij}^p - \cos \theta_{ij}^{cl}] \} \qquad (6.14)$$

where

α_{ij} = $E'_{dav,\,i}\, E'_{dav,\,j} + E'_{qav,\,i}\, E'_{qav,\,j}$

β_{ij} = $E'_{dav,\,i}\, E'_{qav,\,j} + E'_{qav,\,i}\, E'_{dav,\,j}$

E'_{di} = direct-axis stator EMF corresponding to rotor flux components

E'_{qi} = quadrature-axis stator EMF corresponding to rotor flux components

θ_i^p = the peak point angle of the i^{th} machine rotor in the COI reference frame

$$\theta_{ij}^{p} = \theta_{i}^{p} - \theta_{j}^{p}$$

The two main questions involved in calculating the transient energy margin when the machines are modeled in detail are

- How is the peak point [20, chapter 8, 51, 52] found?
- What values are used for $E_{dav}^{'}$ and $E_{qav}^{'}$ in equation (6.14)?

The first question of determining the peak point is addressed below. In the detailed modeling, the state variables include $E_q^{'}$, $E_d^{'}$, E_{FD}, θ, and ω [53]. This is different from the classical model where the state variables are given by θ and ω. The energy expression given by equation (6.14) assumes a two-axis generator model but with constant values of $E_q^{'}$ and $E_d^{'}$. Therefore, the gradient system for this energy function will be dependent only on the angle, (i. e., the values of $E_d^{'}$ and $E_q^{'}$ are held constant). The values of $E_q^{'}$ and $E_d^{'}$ to be used in the gradient system equations are determined by a procedure similar to that suggested in [50], in which the effect of post-disturbance network is to be accounted for in computing the values of $E_q^{'}$ and $E_d^{'}$ at the exit point.

The equations given by 5.3 - 5.7 are integrated with the appropriate initial conditions and representation of the fault to obtain the faulted trajectory. In addition, between the time instant corresponding to fault clearing, and the exit point, the equations corresponding to $E_q^{'}$, $E_d^{'}$ and E_{FD} given below are also integrated in parallel with the fault-on trajectory

$$\tau_{doi}^{'}\dot{E}_{qi}^{'} = E_{FDi} - E_{qi}^{'} + (x_{di} - x_{di}^{'})I_{di} \tag{6.15}$$

$$\tau_{qoi}^{'}\dot{E}_{di}^{'} = - E_{di} - (x_{qi} - x_{qi}^{'})I_{qi} \tag{6.16}$$

$$\tau_{Ei}\dot{E}_{FDi}^{'} = - E_{FDi}^{'} + K_{Ai}(V_{REF} - V_{ti}^{'}) \tag{6.17}$$

At each instant of integration, in the equations above, the currents I_d and I_q for the generators represented in detail are obtained using the angles from the faulted trajectory solution and the post-disturbance network admittance matrix. The values of $E_q^{'}$ and $E_d^{'}$ obtained with this procedure, at the exit point are used in the gradient system solution. This procedure then captures the effect of the post-disturbance network on the generator voltages [50].

The gradient system equation used for the post-fault network is given by

$$\dot{\theta}_i = P_i^{pf} - P_{ei}^{pf} - \frac{M_i}{M_T} P_{COI}^{pf} \tag{6.18}$$

where P_{ei} is used accordingly with the generator model (i.e), classical or detailed. For the generators modeled in detail, P_{ei} is given by

$$P_{ei} = E_{di}^{'} I_{di} + E_{qi}^{'} I_{qi} \tag{6.19}$$

with the values of $E_q^{'}$ and $E_d^{'}$ held constant at their exit point values as explained above. In equation (6.19), the term $(x_{qi}^{'} - x_{di}^{'}) I_{di} I_{qi}$ is neglected because of its extremely small magnitude. This gradient system equation is then integrated from the projection of the exit point to the point where $\sum_{i=1}^{n} f_i$ reaches its first minimum. This provides a set of angles θ^{mgp}. Here again, the assumption is made that the potential energy varies only with the generator angle.

The determination of the peak point is made by considering all the generators to be modeled classically. This implies that those generators equipped with exciters have to be converted to classical machines. With the

values of E'_{dav} and E'_{qav} having been calculated the conversion to equivalent classical machines is

$$E_i = (E'^{2}_{dav,\,i} + E'^{2}_{qav,\,i})^{1/2} \tag{6.20}$$

where E_i denotes the internal voltage magnitude of the classical machine.

The next step is to solve for the peak point [20, chapter 8] using θ^{mgp} as the starting point.

It is very essential that we get a good approximation of E'_{qav} and E'_{dav} for an accurate transient stability assessment. The method of evaluating E'_{qav} and E'_{dav} is described in this section. This method uses the fact that the equations corresponding to E'_q, E'_d and E_{FD} (6.15 - 6.17) are also integrated in parallel with the fault-on trajectory between the time instant corresponding to fault clearing, and the exit point. The procedure is outlined below.

The values of E'_{dav} and E'_{qav} are initialized to that of the values at clearing. Let E'^{cl}_q and E'^{cl}_d denote the values of E'_q and E'_d at clearing. This implies that at clearing

$$E'_{qav} = E'^{cl}_q \tag{6.21}$$

$$E'_{dav} = E'^{cl}_d \tag{6.22}$$

At each time step, the generator equations are solved for values of E'_q and E'_d. The new values of E'_{qav} and E'_{dav} are determined by taking the average of the previous value and the calculated value. This can be computed as follows:

$$E'_{qav}\,(new) = \frac{E'_{qav}\,(old) + E'_q(t)}{2} \tag{6.23}$$

$$E'_{dav}\,(new) = \frac{E'_{dav}\,(old) + E'_d(t)}{2} \tag{6.24}$$

where

- E'_{dav} *(old)* and E'_{qav} *(old)* are the values at the previous time step.
- $E'_q(t)$ and $E'_d(t)$ are the values of E'_q and E'_d calculated at the time step under consideration from the integration of the generator equations.
- E'_{dav} *(new)* and E'_{qav} *(new)* are the final calculated values at the time step under consideration.

Once the values of E'_{dav} and E'_{qav} have been evaluated the transient energy margin given by equation (6.14) can be determined.

In the sparse formulation of the TEF method, the procedure to determine the exit point and minimum gradient point is essentially the same as that in the reduced formulation. The main difference obviously is the use of sparsity throughout the integration process. Similar to the reduced formulation, the equations (6.15 - 6.17) are integrated in parallel. The energy margin is also computed taking advantage of sparse methods. The formulation for this part of the TEF method as explained in section 5.4 differs significantly from that followed in the reduced formulation. As mentioned earlier in chapter 2, in the reduced formulation, the potential energy term is divided into three components. These are the position energy, magnetic energy and the dissipation energy terms. In the sparse formulation, the potential energy is divided into two terms. The position energy constitutes one term and the magnetic and dissipation energies together account for the second term.

$$PE = \sum_i \int_{\theta_i^{cl}}^{\theta_i^{p}} (P_{mi} - P_{ei})\, d\theta_i \qquad (6.25)$$

The computation of the potential energy margin is formulated as an ordinary differential equation of the form

$$\dot{y}_i = (P_{mi} - P_{ei}) (\theta_i^p - \theta_i^{cl}) \tag{6.26}$$

$$\dot{\theta}_i = (\theta_i^p - \theta_i^{cl}) \tag{6.27}$$

This set of equations is integrated in the time interval of 0.0 to 1.0. At the end of the integration, the potential energy margin is computed as

$$PE = \sum_i y_i \tag{6.28}$$

It is essential that a good estimate of E_q' and E_d' be made for accurate transient stability assessment. The values used obtained using equations 6.23 and 6.24, while providing a good estimate are not the best approximations. This investigation focuses on if a polynomial interpolation can be performed on the two state variables E_q' and E_d' respectively. Of the varioius curve fits that were tried, the cubic polynomial and the cubic spline seemed to give a good approximation to the trajectory. The cubic spline, in fact, seemed to trace the trajectory exceedingly well.

The following gives a description of the cubic polynomial fit that was tried. The cubic polynomial fit is of the form

$$y = a_0 + a_1 t + a_2 t^2 + a_3 t^3 \tag{6.29}$$

Let

t_e : Instant when the exit point is reached

t_{cl} : Instant when the fault is cleared

y_e : Value of the state variable at the exit point

y_{cl} : Value of the state variable at clearing

dy_e : Value of the derivative of the state variable at the exit point

dy_{cl} : Value of the derivative of the state variable at clearing

Also, let

$$t_x = t_e - t_{cl}$$

$$t_y = t_e^2 - t_{cl}^2$$

$$t_x = t_e^3 - t_{cl}^3$$

$$y_y = y_e - y_{cl}$$

The coefficients a_0, a_1, a_2, and a_3 are then given by

$$a_{3n} = (y_y - dy_{cl}\, t_x) - \left[\frac{dy_e - dy_{cl}}{2\, t_x}\right](t_y - 2\, t_{cl}\, t_x) \tag{6.30}$$

$$a_{3d} = (t_z - 3\, t_{cl}^2\, t_x) - \left[\frac{3\, t_y}{2\, t_x}\right](t_y - 2\, t_{cl}\, t_x) \tag{6.31}$$

$$a_3 = \frac{a_{3n}}{a_{3d}} \tag{6.32}$$

$$a_2 = \frac{(dy_e - dy_{cl}) - 3\, a_3\, t_y}{2\, t_x} \tag{6.33}$$

$$a_1 = (dy_{cl} - 2\, a_2\, t_{cl}) - 3\, a_3\, t_{cl}^2 \tag{6.34}$$

$$a_0 = y_{cl} - a_1\, t_{cl} - a_2\, t_{cl}^2 - a_3\, t_{cl}^3 \tag{6.35}$$

Once the coefficients are determined, the polynomial can easily be scaled to reflect the values of the state variables in the time frame of 0.0 to 1.0. The cubic polynomial is then given by

$$y = a_0 + a_1\,(t_1\, d_t + t_{cl}) + a_2\,(t_1\, d_t + t_{cl})^2 + a_3\,(t_1\, d_t + t_{cl})^3 \tag{6.36}$$

where

$$d_t = t_e - t_{cl}$$

$$t_1 = \frac{(t - t_{cl})}{d_t}$$

A spline function, on the other hand, is a function consisting of polynomial pieces joined together with smoothness conditions. First and second-degree splines indicate a lack of continuity and smoothness. For the first degree spline, the slope of the spline changes abruptly from one point to another. In the case of quadratic splines, the discontinuity is in the second derivative. Higher degree splines are used when more smoothness is required in the approximating function. The choice of degree most frequently used while interpolating values with a spline function is 3. These are termed as cubic splines. The general definition of spline function of degree k is given as:

A function S is a spline function of degree k if

- The domain of S is an interval $[a, b]$
- $S, S', S'', ..., S^{(k-1)}$ are all continuous functions on $[a, b]$
- There are points t_i such that $a = t_1 < t_2 < ... < t_n = b$ and S is a polynomial of degree$\leq$ k on each subinterval $[t_i, t_{i+1}]$.

Let $t_1, t_2, t_3, ..., t_n$ represent the instants in time. Also, let the function value at these instants of time be represented by $y_1, y_2, y_3, ..., y_n$. The t_i's are defined as knots and are assumed to be in ascending order. The cubic spline function S consists of (n-1) cubic polynomials such that

$$S(x) = \begin{cases} S_1(x) & t_1 \leq x \leq t_2 \\ S_2(x) & t_2 \leq x \leq t_3 \\ & \vdots \\ S_{n-1}(x) & t_{n-1} \leq x \leq t_n \end{cases} \qquad (6.37)$$

where, $S_i(x)$ denotes the cubic polynomial that will be used in the subinterval $[t_i, t_{i+1}]$. It is evident from the above that a piecewise polynomial of degree 3 with two continuous derivatives gives a spline function that is not just a single polynomial throughout the interval (like the cubic polynomial formulation explained earlier). There are standard algorithms defined and available in packages to derive the cubic spline. It was seen that the cubic spline provided extremely good and accurate interpolation.

At each step of the integration of the equations (6.26) and (6.27), the spline function is called. The argument to the spline function is the time instant. Corresponding to this particular instant in time, the spline function returns with the value of E_q' and E_d'. These values are then used in the integration. This procedure is continued till the integration process is complete and the potential energy evaluated. As a result, this procedure provides a more accurate stability assessment.

6.2.1 Sample results with the spline fit

The concept of the spline fit was tested on the 50 generator IEEE test system (with exciters). This system has 44 machines modeled classically and 6 machines modeled in detail. The values of E_q' and E_d' along the parallel trajectory and the corresponding time instant are stored in separate arrays. The spline function is then called. Table 6.1 gives the value of the normalised energy margin at the exit point and minimum gradient point for five diifferent faults (with and without the spline fit). It can be seen from this table that there could be quite a difference in stability asessment (eg., a difference of 0.16 pu for case #5). The reason for the fact that the normalised energy margin is not

provided at the minimum gradient point for all the cases is that these have a negative $\Delta V_{napprox1}$ (at the exit point). As a result, these cases go directly to the third level of inertial filters. The results for case 2 are explained in more detail in tables 6.2, 6.3, 6.4 and 6.5. Tables 6.2 and 6.4 show the accuracy of the spline fit for machines 1 and 2 (with respect to E_q' and E_d') at different instants of time. The values obtained from the parallel trajectory are compared with those obtained from the spline fit.

Also, when the potential energy is being evaluated, it was mentioned that the integration is done from 0 to 1.0 sec. (time scaling). The potential energy is evaluated by the integration of equations 6.26 and 6.27. At each step of this integration, the values of E_q' and E_d' are derived from the spline function. Tables 6.3 and 6.5 give the time intervals of integration and the corresponding values of E_q' and E_d' .as obtained from the spline function.

Table 6.1. Comparison of the approximate energy margins at the exit point and minimum gradient point

Case#	Flt Bus	Line Cleared	No Spline		With Spline	
			$\Delta V_{napprox1}$	$\Delta V_{napprox2}$	$\Delta V_{napprox1}$	$\Delta V_{napprox2}$
1	106	74-106 1	-0.50454		-0.48734	
2	7	6-7 1	-0.56558		-0.50863	
3	112	69-112 1	0.61405	0.59646	0.59874	0.58012
4	105	73-105 1	-0.44201		-0.40616	
		73-105 2				
5	33	33-39 1	2.244	2.24918	2.08594	2.09963

Table 6.2. Illustration of the accuracy of the spline fit with respect to $E_q^{'}$ for case 2

Time (s)	$E_q^{'}$ *for mc #1 (Parallel Traj)*	$E_q^{'}$ *for mc #1 (Spline Fit)*	$E_q^{'}$ *for mc #2 (Parallel Traj)*	$E_q^{'}$ *for mc #2 (Spline Fit)*
0.13983758	1.20253849	1.20253849	0.92609107	0.92609107
0.15116185	1.21083593	1.21083593	0.93294257	0.93294257
0.16248614	1.21635807	1.21635807	0.93963271	0.93963271
0.18115154	1.21549237	1.21549237	0.95036829	0.95036829
0.19981696	1.21059108	1.21059108	0.96060717	0.96060717
0.20448330	1.20934927	1.20934927	0.96303928	0.96303928
0.20914966	1.20813668	1.20813668	0.96543795	0.96543795
0.21381602	1.20699215	1.20699215	0.96780306	0.96780306
0.21848236	1.20594728	1.20594728	0.97013456	0.97013456
0.22609569	1.20452356	1.20452356	0.97388256	0.97388256
0.23370904	1.20349073	1.20349073	0.97754169	0.97754169
0.24132237	1.20291364	1.20291364	0.98111314	0.98111314
0.24893570	1.20283592	1.20283592	0.98459899	0.98459899
0.26516792	1.20459163	1.20459163	0.99184865	0.99184865

Table 6.3. Illustration of the use of spline fit to calculate $E_q^{'}$ in the potential energy evaluation for case 2

Time (s)	$E_q^{'}$ *for mc #1*	$E_q^{'}$ *for mc #2*
0.00000000	1.20253849	0.92609107
0.03148362	1.20556404	0.92848934
0.06296725	1.20847818	0.93087855
0.19833961	1.21683956	0.94092154
0.33371198	1.21537346	0.95065645
0.46908435	1.21091270	0.95997899
0.78106345	1.20312930	0.97943814
1.00000000	1.20459163	0.99184865

Table 6.4. Illustration of the accuracy of the spline fit with respect to $E_d^{'}$ for case 2

Time (s)	$E_d^{'}$ *for mc #1 (Parallel Traj)*	$E_d^{'}$ *for mc #1 (Spline Fit)*	$E_d^{'}$ *for mc #2 (Parallel Traj)*	$E_d^{'}$ *for mc #2 (Spline Fit)*
0.13983758	-0.28372905	-0.28372905	-0.46485773	-0.46485773
0.15116185	-0.28374466	-0.28374466	-0.46920580	-0.46920580
0.16248614	-0.28364396	-0.28364396	-0.47347820	-0.47347820
0.18115154	-0.28326803	-0.28326803	-0.48025769	-0.48025769
0.19981696	-0.28251103	-0.28251103	-0.48638228	-0.48638228
0.20448330	-0.28222221	-0.28222221	-0.48765898	-0.48765898
0.20914966	-0.28190860	-0.28190860	-0.48885125	-0.48885125
0.21381602	-0.28157023	-0.28157023	-0.48995143	-0.48995143
0.21848236	-0.28120720	-0.28120720	-0.49095160	-0.49095160
0.22609569	-0.28057557	-0.28057557	-0.49240583	-0.49240583
0.23370904	-0.27987978	-0.27987978	-0.49354353	-0.49354354
0.24132237	-0.27912137	-0.27912137	-0.49432784	-0.49432784
0.24893570	-0.27830240	-0.27830240	-0.49472132	-0.49472132
0.26516792	-0.27644038	-0.27644038	-0.49467209	-0.49467209

Table 6.5. Illustration of the use of spline fit to calculate $E_d^{'}$ in the potential energy evaluation for case 2

Time (s)	$E_d^{'}$ *for mc #1*	$E_d^{'}$ *for mc #2*
0.00000000	-0.28372905	-0.46485773
0.03148362	-0.28374239	-0.46637698
0.06296725	-0.28374918	-0.46789274
0.19833961	-0.28361264	-0.47429858
0.33371198	-0.28325376	-0.48043816
0.46908435	-0.28257799	-0.48603806
0.78106345	-0.27948717	-0.49400486
1.00000000	-0.27644038	-0.49467209

6.3 Alternate Method of Determining the MOD

It is quite possible that there might be systems which under certain conditions have a controlling UEP where no angle is advanced beyond 90 degrees. In this circumstance, it is essential to be able to identify the MOD of the controlling UEP. This is required for the calculation of the normalized energy margin. Also, the MOD identified be accurate. This procedure should take into account the severity of the disturbance. There are two different checks made which try to account for this severity. The first check involves the conditions at clearing [20, chapter 6].

Check 1

- Obtain the kinetic energy of each of the machines using the conditions at clearing. This is calculated as $\frac{1}{2} M_i \, (\tilde{\omega}_i^{cl})^2$ where $\tilde{\omega}_i^{cl}$ is the speed at clearing with respect to the COI and M_i is the inertia constant.
- Obtain the acceleration of each of the machines using the conditions at the end of the disturbance. This is given by $f_i(\theta^{cl})/M_i$ where $f_i(\theta^{cl})$ represent the accelerating power with respect to the COI.
- Each of the two lists obtained above are sorted in the descending order. The machines which are in the top 2% of each of the lists are chosen.
- The machines which are in the top 2% of both the lists are identified and the rest eliminated.

Check 2

- Calculate the absolute difference from $(\theta^{cl}$ to $\theta^{u})$ and $(\theta^{u}$ to $90)$.
- All machines where the difference from $(\theta^{cl}$ to $\theta^{u})$ is greater than the difference from $(\theta^{u}$ to $90)$ are flagged.

The last step is to identify the machines which are common in both check 1 and check 2. These machines then constitute the MOD of the controlling UEP and are used in the calculation of the corrected kinetic energy. An example of such a scenario is given below. Table 6.6 provides the results obtained from check 1 on the PSE&G system. The four machines identified are those which are in the top 2% of both the kinetic energy and acceleration lists. The next step is to perform check 2 and identify the machines which satisfy it. Table 6.7 lists the machines which satisfy check 2. Results obtained from the two checks are correlated and the final list of machines obtained. In this particular case, the machines which are used to calculate the corrected kinetic energy (and which meet both check 1 and check 2) are 113, 114 and 115 respectively. These machines constitute the MOD of the controlling UEP.

Table 6.6. Results from check 1 performed on the PSE&G system

Machine	Acceleration (pu)	Kinetic Energy (pu)
171	0.004744	21.6472
115	0.162896	234.209
114	0.159192	238.307
113	0.171095	257.922

Table 6.7. Results from check 2 performed on the PSE&G system

Machine	$(\theta^{cl}$ to $\theta^{u})$	$(\theta^{u}$ to $90)$
113	84.223	9.607
114	81.521	16.389
115	81.114	16.937

6.4 Scaffolding

The TEF method as it existed was capable of only assessing the system stability for a single contingency. If the transient stability needed to be assessed for a second contingency, the program would have to be rerun. In the real environment, there are hundreds of cases which need to be assessed in 15 to 30 minute periods. Hence in the proposed framework, it is essential that the TEF be capable of cycling through all the contingencies in one run. This would reduce the total computational time required to screen and determine the critical contingencies. Chapter 3 detailed the filtering scheme. It is evident in the scheme that any contingency could be eliminated in either *PITF 1*, *PITF 2* or *PITF 3*. Also, there is the possibility that a contingency could go directly to *ITF 3* from *ITF 1*. The obvious option is to discard the case which gets eliminated (in any of the three levels of filters) and start the process of screening the next contingency. The layout of the TEF method is given in figure 6.14. The boxes in this layout correspond to the main routines called in the TEF program. A brief description of these routines follows.

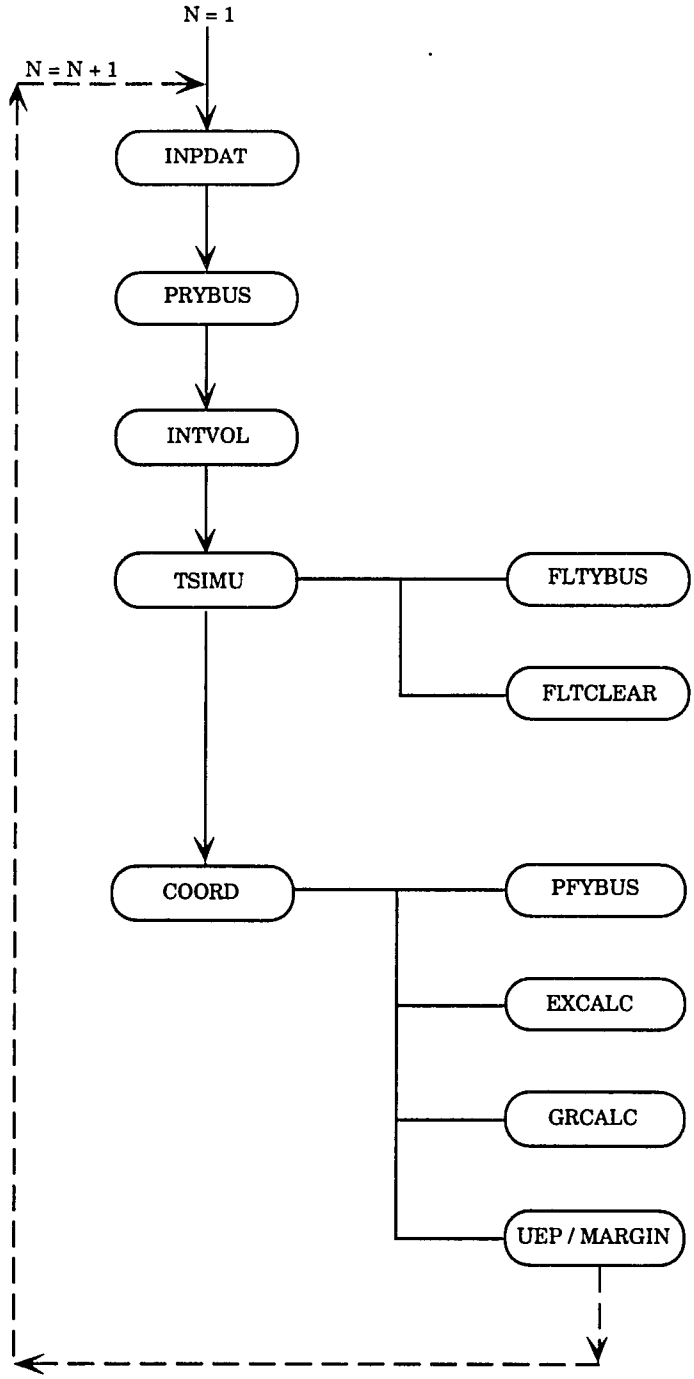

Fig. 6.14. Layout of the TEF method

- *INPDAT* reads in the input data. This data includes the loadflow, dynamic and control data files. The control data contains information regarding the contingency.
- *PRYBUS* forms the pre-fault *Y-bus*.. This information is obtained from the loadflow file.
- *INTVOL* calculates the internal voltage and angle at the generator buses.
- *TSIMU* - This routine calls *FLTYBUS* and *FLTCLEAR*.
    - *FLTYBUS* forms the faulted *Y-bus*.
    - *FLTCLEAR* integrates the system equations till end of the disturbance. This gives us the conditions at clearing.
- *COORD* - This routine calls *PFYBUS*, *EXCALC*, *GRCALC*, *UEP* and *MARGIN*.
    - *PFYBUS* forms the post-fault *Y-bus*.
    - *EXCALC* determines the exit point. Once the exit point is found, the routines *ITF 1* and *PITF 1* are called. In these routines, the filter calculations are made as explained in chapter 3.
    - GRCALC determines the minimum gradient point. Once the minimum gradient point is found, the routines *ITF 2* and *PITF 2* are called. These correpond to the second level of filters.
    - *UEP* is the routine that solves for the exact controlling unstable equilibrium point. The routine *MARGIN*

calculates the energy margin. *ITF 3* and *PITF 3*, are the routines which perform the requisite calculations in the third and final level of filters.

- *RANK* is the routine which ranks the contingencies based on their severity in *ITF 3* and *PITF 3* respectively.

If the TEF method is being rerun for every contingency, it can be seen that the routine *INPDAT* is called each time. The loadflow and dynamic data remain the same for each of the contingencies. It is not required to have to read and process them for each case. This was changed in the following fashion. All the cases which need to be screened are listed one below the other in the control data file. The routine *INPDAT* is called only once. The information regarding all the contingencies is stored in the form of arrays.

Also, the pre-fault*Y-bus* is the same for each of the contingencies. It is only the faulted and post-fault*Y-bus* parameters that are different for different cases. Hence, the pre-fault*Y-bus* needs to be calculated only once.

The routine *INTVOL* as explained earlier, calculates the internal voltage and angles at the generator buses in the pre-fault stage. However, this is based on the information provided in the loadflow. These initial internal voltage magnitudes and angles remain unchanged for each contingency.

Figure 6.15 describes the changes that were made to the structure of the TEF program. When a case gets eliminated in *PITF 1* or *PITF 2*, the analysis of the next contingency is started immediately. Similar is the case in *PITF 3*.

For each of the contingencies, a small summary file is created. This file keeps track of the contingency as it progresses through the different filters. This assists the operator in keeping track of all the contingencies. Fig. 6.16

For each of the contingencies, a small summary file is created. This file keeps track of the contingency as it progresses through the different filters. This assists the operator in keeping track of all the contingencies. Fig. 6.16 through 6.18 describe the summary files for three different contingencies. The first contingency, depicted in figure 6.16, is a critical contingency with respect to the inertial transient period. The second contingency, shown in figure 6.17, gets eliminated in the *PITF 1* itself. This is because it does not violate any checks. The third contingency, shown in figure 6.18, is severe with respect to the post inertial transient period.

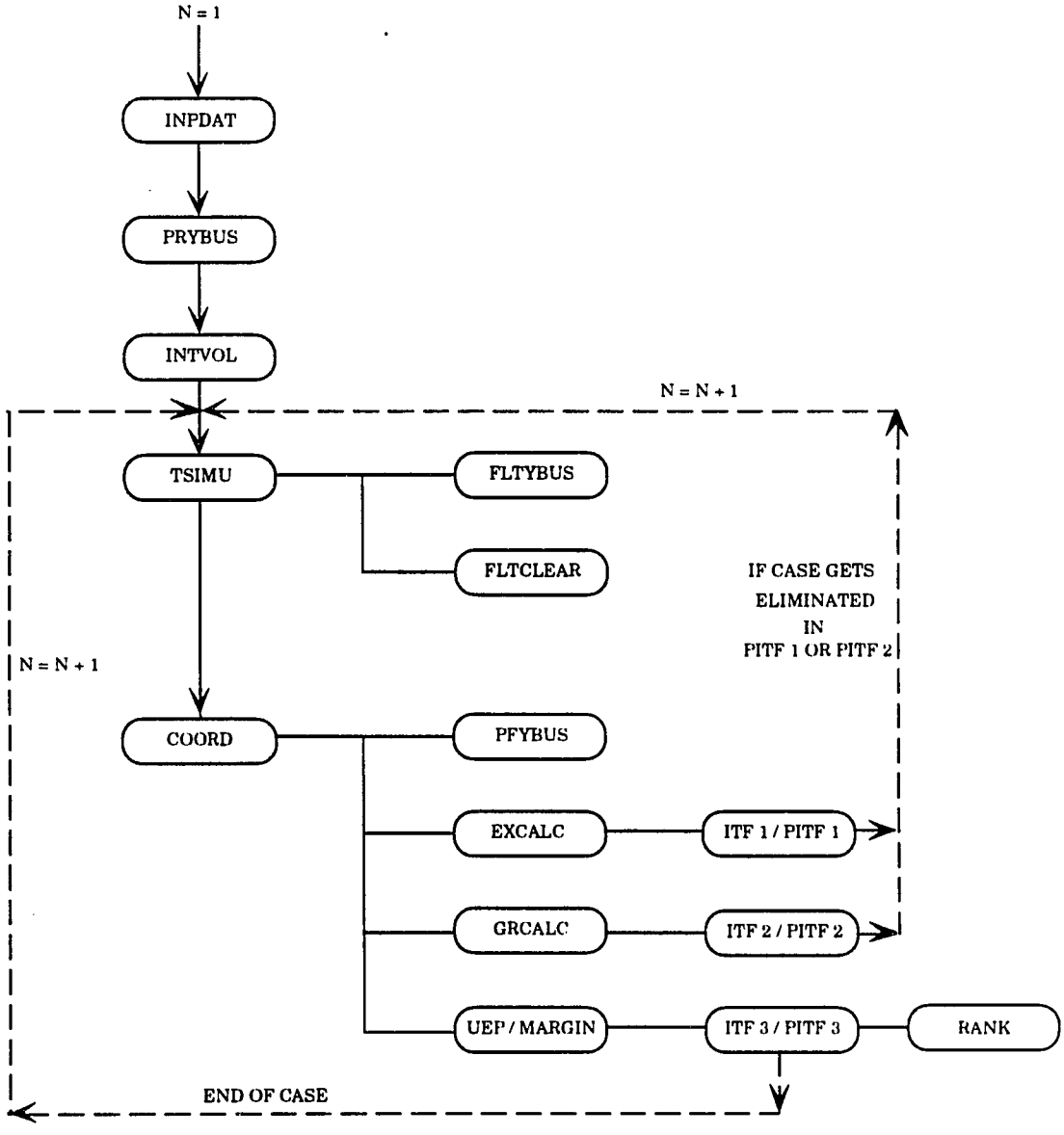

Fig. 6.15. Changes made to the existing TEF method

THE FAULT IS AT BUS# 1662

LINE CLEARED 1662 1709 1
THE CLEARING TIME IS 0.10000000

****
RESULTS OF case1 IN ITF1
****

THE THRESHOLD FOR Vnapprox1 IN ITF1 IS = 1.50000
Vnapprox1 IN ITF1 FOR case1 IS = 0.717450

Vnapprox1 IS LESS THAN THE THRESHOLD

THIS CASE NEEDS FURTHER EXAMINATION

THIS CASE IS SENT TO ITF2
****

****
RESULTS OF case1 IN ITF2
****

THE THRESHOLD FOR Vnapprox1 IN ITF2 IS = 0.450000
Vnapprox1 IN ITF2 FOR case1 IS = -0.504830

Vnapprox1 IS LESS THAN THE THRESHOLD

THIS CASE NEEDS FURTHER EXAMINATION

THIS CASE IS SENT TO ITF3
****

Figure 6.16. Summary file of a contingency which is severe with respect to the inertial transient period

THE FAULT IS AT BUS# 1656

LINE CLEARED 1506 1656 1
THE CLEARING TIME IS 0.16600000

****
RESULTS OF case2 IN ITF1
****

THE THRESHOLD FOR Vnapprox1 IN ITF1 IS = 1.50000
Vnapprox1 IN ITF1 FOR case2 IS = 2.48830

Vnapprox1 IS GREATER THAN THE THRESHOLD

THIS CASE NEEDS FURTHER EXAMINATION

THIS CASE IS SENT TO PITF1
****

****
RESULTS OF case2 IN PITF1
****

THE THRESHOLD FOR Vnapprox1 IN PITF1= 1.60000
Vnapprox1 IN PITF1 FOR case2 IS = 2.48830
Vnapprox1 IS GREATER THAN THE THRESHOLD

THE THRESHOLD FOR TOTAL KE IN PITF1= 6.25000
TOTAL KE IN PITF1 FOR case2 IS = 3.39018
TOTAL KE IS LESS THAN THE THRESHOLD

THE CONDITIONS (Vnapprox1 > SPECIFIED THRESHOLD)
AND (TOTAL KE < SPECIFIED THRESHOLD) ARE MET

NOW CHECKING FOR SYN. POW. AND TERM. VOLT:

THE THRESHOLD FOR SYN. POW. IN PITF1= 2.00000
THE THRESHOLD FOR TERM. VOL. IN PITF1= 0.750000

THE CONDITIONS (Si > SPECIFIED THRESHOLD)
AND (|Vi| > SPECIFIED THRESHOLD) ARE MET

THIS CASE GETS ELIMINATED IN PITF1
****

Figure 6.17. Summary file of a contingency which gets eliminated in *PITF 1*

THE FAULT IS AT BUS# 506

LINE CLEARED 506 605 1
THE CLEARING TIME IS 0.10000000

****
RESULTS OF case3 IN ITF1
****

THE THRESHOLD FOR Vnapprox1 IN ITF1 IS = 1.50000
Vnapprox1 IN ITF1 FOR case3 IS = 4.66308

Vnapprox1 IS GREATER THAN THE THRESHOLD

THIS CASE NEEDS FURTHER EXAMINATION

THIS CASE IS SENT TO PITF1
****

****
RESULTS OF case3 IN PITF1
****

THE THRESHOLD FOR Vnapprox1 IN PITF1= 1.60000
Vnapprox1 IN PITF1 FOR case3 IS = 4.66308
Vnapprox1 IS GREATER THAN THE THRESHOLD

THE THRESHOLD FOR TOTAL KE IN PITF1= 6.25000
TOTAL KE IN PITF1 FOR case3 IS = 1.10114
TOTAL KE IS LESS THAN THE THRESHOLD

THE CONDITIONS (Vnapprox1 > SPECIFIED THRESHOLD) AND (TOTAL KE < SPECIFIED THRESHOLD) ARE MET

NOW CHECKING FOR SYN. POW. AND TERM. VOLT:

THE THRESHOLD FOR SYN. POW. IN PITF1= 2.00000
THE THRESHOLD FOR TERM. VOL. IN PITF1= 0.750000

FOR MACHINE : 12
SYNCHRONIZING POWER COEFF. IS 0.173032
TERMINAL VOLTAGE IS 0.212849

THE CONDITIONS (Si > SPECIFIED THRESHOLD) AND (|Vi| > SPECIFIED THRESHOLD) ARE NOT MET

THIS CASE NEEDS FURTHER EXAMINATION

THIS CASE IS SENT TO ITF2
****

Figure 6.18. Summary file of a contingency which is severe with respect to the post inertial transient period

****
RESULTS OF case3 IN ITF2
****

THE THRESHOLD FOR Vnapprox1 IN ITF2 IS = 0.450000
Vnapprox1 IN ITF2 FOR case3 IS = 3.44342

Vnapprox1 IS GREATER THAN THE THRESHOLD

THIS CASE NEEDS FURTHER EXAMINATION

THIS CASE IS SENT TO PITF2
****

****
RESULTS OF case3 IN PITF2
****

THE THRESHOLD FOR Vnapprox2 IN PITF2 IS = 0.500000
Vnapprox2 IN PITF2 FOR case3 IS = 3.44342
Vnapprox2 IS GREATER THAN THE THRESHOLD

THE THRESHOLD FOR TOTAL KE IN PITF2 IS = 6.00000
TOTAL KE IN PITF2 FOR case3 IS = 1.10114
TOTAL KE IS LESS THAN THE THRESHOLD

THE CONDITIONS (Vnapprox1 > SPECIFIED THRESHOLD)
AND (TOTAL KE < SPECIFIED THRESHOLD) ARE MET

NOW CHECKING FOR SYN. POW. AND TERM. VOLT:
THE THRESHOLD FOR SYN. POW. IN PITF2= 2.00000
THE THRESHOLD FOR TERM. VOL. IN PITF2= 0.750000

FOR MACHINE : 13
SYNCHRONIZING POWER COEFF. IS -0.321803
TERMINAL VOLTAGE IS 0.177946

THE CONDITIONS (Si > SPECIFIED THRESHOLD)
AND (|Vi| > SPECIFIED THRESHOLD) ARE NOT MET

THIS CASE NEEDS FURTHER EXAMINATION

THIS CASE IS SENT TO ITF3
****

Figure 6.18.(contd.) Summary file of a contingency which is severe with respect to the post inertial transient period

7 RESULTS

This chapter pertains to results that were obtained from the contingency filtering scheme. The system used in this research for purposes of testing the filtering scheme is the 161-generator Northern States Power (NSP) system [44]. This system consists of 161 generators, 901 buses and 1500 lines. Also, the tool used for demonstrating the feasibilty of the filtering scheme is the reduced formulation of the TEF method. A list of 80 contingencies were provided by the system operators. Table 7.1 lists $\Delta V_{napprox1}$, ΔV_n, V_{ke}, the rank of a contingency based on $\Delta V_{napprox1}$ and the rank based onΔV_n. It can be seen from table 7.1 that the proposed scheme is conservative ($\Delta V_{napprox1}$ is less than the exact index ΔV_n).

7.1 Results in ITF 1 and PITF 1

In *ITF 1*, the threshold chosen for $\Delta V_{napprox1}$ is 1.5 pu. Cases which are below this threshold are passed on to *ITF 2*. Using this threshold, 22 cases are classified as being severe with respect to the inertial period. The 80 cases that enter *ITF 1* can be divided as

- 2 steady state unstable cases (post-disturbance equilibrium point is the same as the unstable equilibrium point).
- 4 unstable cases (negative $\Delta V_{napprox1}$).
- 16 potentially severe cases (with respect to the inertial period).
- 58 non severe cases (with respect to the inertial period).

The 2 steady state unstable cases along with the 4 unstable cases are sent directly to *ITF 3*. The 16 potentially severe cases are sent to *ITF 2*. These 22 cases are listed in table 7.2 along with the value of $\Delta V_{napprox1}$.

All the other cases (which have $\Delta V_{napprox1} > 1.5$) are sent to *PITF 1* for further analysis. In *PITF 1*, thresholds are set for V_{KE} and $\Delta V_{napprox1}$ of the form

- $\Delta V_{napprox1} > 1.75$ pu and $V_{KE} < 6.0$ pu.

This results in 45 cases (case 36 through case 80) meeting the threshold check. These cases were then analyzed for P_{sij} and large angles in θ^{s2}. The thresholds chosen here are of the form

- If the smallest value of $P_{sij} < -0.05$ or
- Any angle in $\theta^{s2} > 90$ deg.

If either of these conditions is violated, the case is deemed as being potentially severe with respect to the post inertial period and sent to the next level of inertial transient filters. In *PITF 1*, none of the 45 cases violated the check based on P_{sij} and large angles in θ^{s2}. As a result, all the 45 cases are eliminated.

It should be mentioned at this point that the synchronizing power coefficients when applied with the reduced formulation (as explained in chapter 3) did not provide a good measure of relative stress between different cases. For all cases, the values ranged from -0.002 to 5 pu. The base conditions of the 161 generator NSP system are already stressed. Also, the reduced formulation destroys the identity of the network. This implies that for most disturbances, the values of P_{sij} reflect the stressed condition (through the admittance matrix). When the stress in the system was further increased, the

smallest values of P_{sij} dropped to -0.06 pu. As a result, the threshold for P_{sij} was chosen to be -0.05 pu in this research. This threshold, as mentioned earlier, is system dependent. For the 161 generator NSP system, values of P_{sij} below -0.05 pu reflect a higher level of stress (compared to the base case). This problem is avoided in the sparse formulation. In the sparse formulation, the entire structure of the network is retained. Also, the synchronizing power coefficient captures the effect of the interaction between the synchronous machines and the network more accurately. Another advantage is the availability of the terminal voltages of the machines. Here, the synchronizing power coefficients provide an excellent measure of relative stress between different cases. Chapter 5 details the concept of P_{sij} with respect to the sparse network.

The cases remaining in *PITF 1* are now analyzed using analytical sensitivities. $\Delta V_{napprox1}$ for a specified change in generation is evaluated. The change in generation pattern adopted is an increase in generation of 100 MW each at machines 38 and 41. This change represents an increase in generation at two of the most economic units. The results indicate that among the remaining 13 cases in *PITF 1*, cases 23, 24, 25 and 26 are the most susceptible to generation change. Similar to generation changes, analytical sensitivities to post-disturbance network changes is also calculated. None of the cases were vulnerable to an additional post-disturbance network change. The change introduced in the network is different for different cases. The choice of which line gets tripped additionally depends on the probability of its occurrence. This data is provided by the operator as an input. Table 7.3 lists

the cases that are sent to the next level of inertial filters. This is divided into three categories

- based on susceptibility to generation change
- based on susceptibility to network topology changes
- based on P_{sij} or large angles in θ^{s2}

The thresholds corresponding to each of the above signatures are given in table 7.3.

7.2 Results in ITF 2 and PITF 2

ITF 2 now analyzes the 16 cases that come from *ITF 1*. In addition 4 cases come from *PITF 1*. The TEF calculations are performed using the minimum gradient point as an approximation to the UEP. A threshold of 0.30 is used for $\Delta V_{napprox2}$. Cases which fall below this threshold are sent to *ITF 3*. These are case 7 - case 13 and case 15 - case 18. Table 7.4 lists the cases which are potentially severe with respect to the inertial transient period along with the values of $\Delta V_{napprox2}$. In addition, the remaining nine cases are analyzed by *PITF 2*. The 20 cases entering *ITF 2* can be divided as

- 11 potentially severe cases (with respect to the inertial period).
- 9 non severe cases (with respect to the inertial period).

The 9 non severe cases are sent to *PITF 2*. Similar to *PITF 1*, thresholds are set for $\Delta V_{napprox2}$ and V_{KE} of the form

- $\Delta V_{napprox2} > 0.75$ and $V_{KE} < 6.0$

Of the 9 cases analyzed in *PITF 2*, 5 cases met the threshold check. These 5 cases did not violate the check corresponding to P_{sij} and large angles in θ^{s2} either. As a result, these are eliminated. The remaining 4 cases (cases 14, 20,

21 and 22) are now analyzed using analytical sensitivities. None of these were susceptible to changes in generation. However, case 21 was susceptible to network topology change. As a result, case 21 is sent to *ITF 3*. Table 7.5 lists the cases that are sent to the next level of inertial filters from *PITF 2*.

7.3 Results in ITF 3 and PITF 3

ITF 3 analyzes

- 6 cases (from *ITF 1*)
- 11 cases (from *ITF 2*)
- 1 case (from *PITF 2*)

The 6 cases from ITF 1 are those which come down directly to ITF 3 as a result of being steady state unstable or having negative $\Delta V_{napprox1}$. These cases are not solved for the UEP. The reasoning behind this fact is that there is a considerable chance these cases are either unstable or have a low normalized energy margin ($\Delta V_n < 0$ or low value of ΔV_n) at the UEP. These cases are ranked above all the other cases based on the value of $\Delta V_{napprox1}$ ($\Delta V_{napprox1}$ is treated as ΔV_n for these cases). The threshold chosen for ΔV_n in *ITF 3* is 0.85 pu. With this threshold, the critical contingencies are chosen as cases 1, 2, 3, 4, 5, 6, 9, 10, 11. These critical cases are listed in table 7.6 along with the values of ΔV_n. This implies that the cases in *ITF 3* can be analyzed as

- 9 severe cases (with respect to the inertial period)
- 9 non severe cases (with respect to the inertial period)

The 9 non severe cases are sent to *PITF 3*. Similar to *PITF 1*, thresholds are set for ΔV_n and V_{KE} of the form

- $\Delta V_n > 1.5$ and $\Delta V_{KEcorr} < 4.0$

Of the 9 cases analyzed in *PITF 3*, 4 cases met the threshold check. These 4 cases did not violate the check corresponding to P_{sij} and large angles in θ^{s2} either. These 4 cases are eliminated. The remaining 5 cases (cases 7, 8, 12, 13, 21) are now analyzed using analytical sensitivities. Cases 7, 12 and 13 are susceptible to generation change. Case 21 is susceptible to network topology change. Table 7.7 lists the cases that are retained in *PITF 3*.

The cases retained in *ITF 3* and *PITF 3* are now ranked. This is discussed in the next section.

7.4 Final Ranking

The results shown in Table 7.8 and 7.9 now provide an overall ranking of the cases retained in *ITF 3* . Table 7.8 provides the ranking based on ΔV_n. Table 7.9 provides the ranking of the cases in *ITF 3* based on sensitivity to generation changes. The term NA in this table refers to the fact that sensitivity analysis is not done on cases with negative ΔV_n. Actually, these are the cases which come directly from *ITF 1*. These cases are ranked at the top of the lists provided in table 7.8 and 7.9. This is beacuse of the fact that these are classified as being very severe with respect to the inertial transient. Table 7.10 provides the ranking of the cases in *PITF 3* based on ΔV_n. For the cases in *PITF 3*, the sensitivity analysis is done for both plant generation and network topology changes. The ranking in table 7.11 and 7.12 is based on susceptibility to generation changes network topology changes respectively. The motivation for this is to provide the operator with a comprehensive set of critical cases based on both current operating and diverse conditions.

Table 7.1. Results to illustrate conservativeness of filters

Cases Ranked by $\Delta V_{napprox1}$	V_{ke}	$\Delta V_{napprox1}$	ΔV_n	*Rank Based on* ΔV_n
1		Steady State Unst.		1
2		Steady State Unst.		2
3	18.382	-0.340	-0.640	3
4	15.149	-0.307	-0.471	4
5	13.352	-0.143	-0.279	5
6	15.291	-0.029	-0.114	6
7	9.166	0.605	0.873	10
8	6.954	0.721	1.139	12
9	9.166	0.775	0.825	8
10	9.166	0.783	0.813	7
11	9.166	0.791	0.827	9
12	9.166	0.867	1.417	15
13	7.523	0.919	0.924	11
14	5.873	0.973	1.423	16
15	7.523	1.0004	1.590	18
16	7.523	1.0005	1.614	20
17	7.523	1.015	1.607	19
18	6.954	1.098	1.558	17
19	5.876	1.167	1.325	14
20	7.523	1.207	1.699	22

Table 7.1. Continued

Cases Ranked by $\Delta V_{napprox1}$	V_{ke}	$\Delta V_{napprox1}$	ΔV_n	*Rank Based on* ΔV_n
21	5.652	1.237	1.266	13
22	5.259	1.450	1.644	21
23	5.876	1.516	2.911	35
24	5.650	1.580	2.166	24
25	5.876	1.615	2.900	33
26	5.876	1.623	2.344	29
27	5.872	1.652	2.311	28
28	5.872	1.655	2.283	25
29	6.052	1.665	2.291	26
30	6.052	1.666	2.292	27
31	6.052	1.683	3.752	44
32	5.872	1.690	2.468	32
33	5.872	1.696	2.467	31
34	6.052	1.711	2.379	30
35	5.650	1.739	2.158	23
36	1.982	1.817	4.241	45
37	5.652	1.850	3.495	41
38	5.652	1.863	3.609	42
39	5.267	1.921	3.670	43
40	5.267	1.974	2.905	34

Table 7.1. Continued

Cases Ranked by $\Delta V_{napprox1}$	V_{ke}	$\Delta V_{napprox1}$	ΔV_n	*Rank Based on* ΔV_n
41	5.258	2.018	3.135	36
42	5.258	2.035	3.254	39
43	5.258	2.037	3.256	40
44	4.917	2.267	3.174	37
45	4.917	2.271	3.183	38
46	2.375	2.349	4.689	47
47	3.395	2.589	4.297	46
48	1.811	2.882	9.295	57
49	1.811	3.030	9.430	58
50	3.313	3.195	5.636	51
51	1.242	3.260	13.282	66
52	3.313	3.490	5.342	49
53	2.703	3.656	5.992	53
54	2.703	3.719	6.164	54
55	0.491	3.739	24.028	75
56	2.501	4.616	4.916	48
57	2.321	4.690	6.904	56
58	2.501	4.719	6.623	55
59	1.093	4.741	14.075	68
60	1.369	5.042	10.656	61

Table 7.1. Continued

Cases Ranked by $\Delta V_{napprox1}$	V_{ke}	$\Delta V_{napprox1}$	ΔV_n	*Rank Based on* ΔV_n
61	1.943	5.185	5.436	50
62	1.797	5.581	9.512	59
63	1.797	5.693	10.106	60
64	1.286	5.790	5.827	52
65	1.301	6.119	11.029	63
66	1.708	6.155	14.382	69
67	1.320	7.912	10.822	62
68	1.182	8.126	15.507	70
69	1.182	8.137	15.515	71
70	1.087	8.683	12.937	65
71	1.320	9.214	13.507	67
72	0.668	9.853	20.206	73
73	0.405	10.670	27.987	78
74	1.087	10.678	12.539	64
75	0.750	13.204	19.826	72
76	0.846	14.584	25.984	77
77	0.711	14.705	25.599	76
78	0.782	15.052	21.691	74
79	0.675	19.106	31.128	79
80	0.465	26.417	32.473	80

Table 7.2. Cases retained in *ITF 1*

Case Number	$\Delta V_{napprox1}$
1	Steady State Unstable
2	Steady State Unstable
3	-0.340
4	-0.307
5	-0.143
6	-0.029
7	0.605
8	0.721
9	0.775
10	0.783
11	0.791
12	0.867
13	0.919
14	0.973
15	1.0004
16	1.0005
17	1.015
18	1.098
19	1.167
20	1.207
21	1.237
22	1.450
(Using a threshold of 1.5 pu)	

Table 7.3. Cases retained in *ITF 2*

Case Number	$\Delta V_{napprox2}$
7	-0.089
8	-0.156
9	-0.059
10	-0.065
11	-0.060
12	-0.222
13	0.257
15	0.267
16	0.259
17	0.275
18	0.035
(Using a threshold of 0.30 pu)	

Table 7.4. Cases retained in *ITF 3*

Case Number	ΔV_n
9	0.825
10	0.813
11	0.827
(Using a threshold of 0.85 pu)	

Table 7.5. Cases retained in *PITF 1*

Cases retained by means of violating threshold set on *New* $\Delta V_{napprox1}$ (from sensitivity with respect to generation change)		
Case Number	*Base* $\Delta V_{napprox1}$	*New* $\Delta V_{napprox1}$ *(Sen.)*
23	1.516	1.137
24	1.580	1.202
25	1.615	1.229
26	1.623	1.234
(Using a threshold of 1.25 pu on *New* $\Delta V_{napprox1}$)		
Cases retained by means of violating threshold set on *New* $\Delta V_{napprox1}$ (from sensitivity with respect to network topology changes)		
Case Number	*Base* $\Delta V_{napprox1}$	*New* $\Delta V_{napprox1}$ *(Sen.)*
No Cases violate threshold on *New* $\Delta V_{napprox1}$ (Using a threshold of 1.25 pu on *New* $\Delta V_{napprox1}$)		
Cases retained by means of violating threshold set on P_{sij} and θ^{s2}		
Case Number	*Syn. Power Coeff.* (P_{sij})	*Large angles in* θ^{s2}
No Cases violate thresholds based on P_{sij} and Large angles in θ^{s2} (Using a threshold of P_{sij} < -0.05 pu and any angle in θ^{s2} > 90 deg)		

Table 7.6. Cases retained in *PITF 2*

Cases retained by means of violating threshold set on *New* $\Delta V_{napprox2}$ (from sensitivity with respect to generation change)		
Case Number	*Base* $\Delta V_{napprox2}$	*New* $\Delta V_{napprox2}$ *(Sen.)*
No Cases violate threshold on *New* $\Delta V_{napprox2}$ (Using a threshold of 0.30 pu on *New* $\Delta V_{napprox2}$)		
Cases retained by means of violating threshold set on *New* $\Delta V_{napprox2}$ (from sensitivity with respect to network topology changes)		
Case Number	*Base* $\Delta V_{napprox2}$	*New* $\Delta V_{napprox2}$ *(Sen.)*
21	0.736	0.534
(Using a threshold of 0.6 pu on *New* $\Delta V_{napprox2}$)		
Cases retained by means of violating threshold set on P_{sij} and θ^{s2}		
Case Number	*Syn. Power Coeff.* (P_{sij})	*Large angles in* θ^{s2}
No Cases violate thresholds based on P_{sij} and Large angles in θ^{s2} (Using a threshold of $P_{sij} < -0.05$ pu and any angle in $\theta^{s2} > 90$ deg)		

Table 7.7. Cases retained in *PITF 3*

Cases retained by means of violating threshold set on *New* ΔV_n (from sensitivity with respect to generation change)		
Case Number	*Base* ΔV_n	*New* ΔV_n *(Sen.)*
7	0.873	0.387
12	1.417	0.935
13	0.924	0.699
(Using a threshold of 1.00 pu on *New* ΔV_n)		
Cases retained by means of violating threshold set on *New* ΔV_n (from sensitivity with respect to network topology changes)		
Case Number	*Base* ΔV_n	*New* ΔV_n *(Sen.)*
21	1.266	0.985
(Using a threshold of 1.00 pu on *New* ΔV_n)		
Cases retained by means of violating threshold set on P_{sij} and θ^{s2}		
Case Number	*Syn. Power Coeff.* (P_{sij})	*Large angles in* θ^{s2}
No Cases violate thresholds based on P_{sij} and Large angles in θ^{s2} (Using a threshold of $P_{sij} < -0.05$ pu and any angle in $\theta^{s2} > 90$ deg)		

Table 7.8. Ranking based on ΔV_n in *ITF 3*

Case Number	ΔV_n	*Rank*
1	Steady State Unst	1
2	Steady State Unst	2
3	-0.340	3
4	-0.307	4
5	-0.143	5
6	-0.029	6
10	0.813	7
9	0.825	8
11	0.827	9

Table 7.9. Ranking based on sensitivity of ΔV_n to generation change in *ITF 3*

Case Number	*Base* ΔV_n	*New* ΔV_n	*Rank*
1	Steady State Unst.	NA	1
2	Steady State Unst.	NA	2
3	-0.340	NA	3
4	-0.307	NA	4
5	-0.143	NA	5
6	-0.029	NA	6
9	0.825	0.372	7
10	0.813	0.375	8
11	0.827	0.376	9

Table 7.10. Ranking based on ΔV_n in *PITF 3*

Case Number	ΔV_n	*Rank*
7	0.873	1
13	0.924	2
21	1.266	3
12	1.417	4

Table 7.11. Ranking based on sensitivity of ΔV_n to plant generation change in *PITF 3*

Case Number	*Base* ΔV_n	*New* ΔV_n	*Rank*
7	0.873	0.387	1
13	0.924	0.699	2
12	1.417	0.935	3
21	1.266	0.991	4

Table 7.12. Ranking based on sensitivity of ΔV_n to network topology change in *PITF 3*

Case Number	*Base* ΔV_n	*New* ΔV_n	*Rank*
7	0.873	0.640	1
13	0.924	0.866	2
21	1.266	0.985	3
12	1.417	1.326	4

The comparison presented in table 7.1 between $\Delta V_{napprox1}$ and ΔV_n is shown in figure 7.1. The values of $\Delta V_{napprox1}$ and ΔV_n are plotted for each case ranked according to $\Delta V_{napprox1}$. This figure illustrates the conservativeness of the filtering scheme. In figure 7.2, the plot of exact index ranking is plotted against the approximate index ranking. It can be seen that there is a very good correlation between the two different rankings. Figures 7.3, 7.4 and 7.5 are plots of the relative rotor angle of one of the most disturbed machines for cases 1, 2, 3, 4, 5, 6, 9, 10, and 11. This plot is from the time domain simulation program ETMSP (version 3.0). These figures indicate that the ranking provided by the *ITF 3* agrees exactly with the severity predicted by the rotor angle positions. Figure 7.6 provides a sample of several other cases. These cases were chosen at random and provide a good illustration of the accuracy of the filtering scheme. Figure 7.7 provides a summary of the 80 different contingencies that were used to validate the contingency filtering scheme.

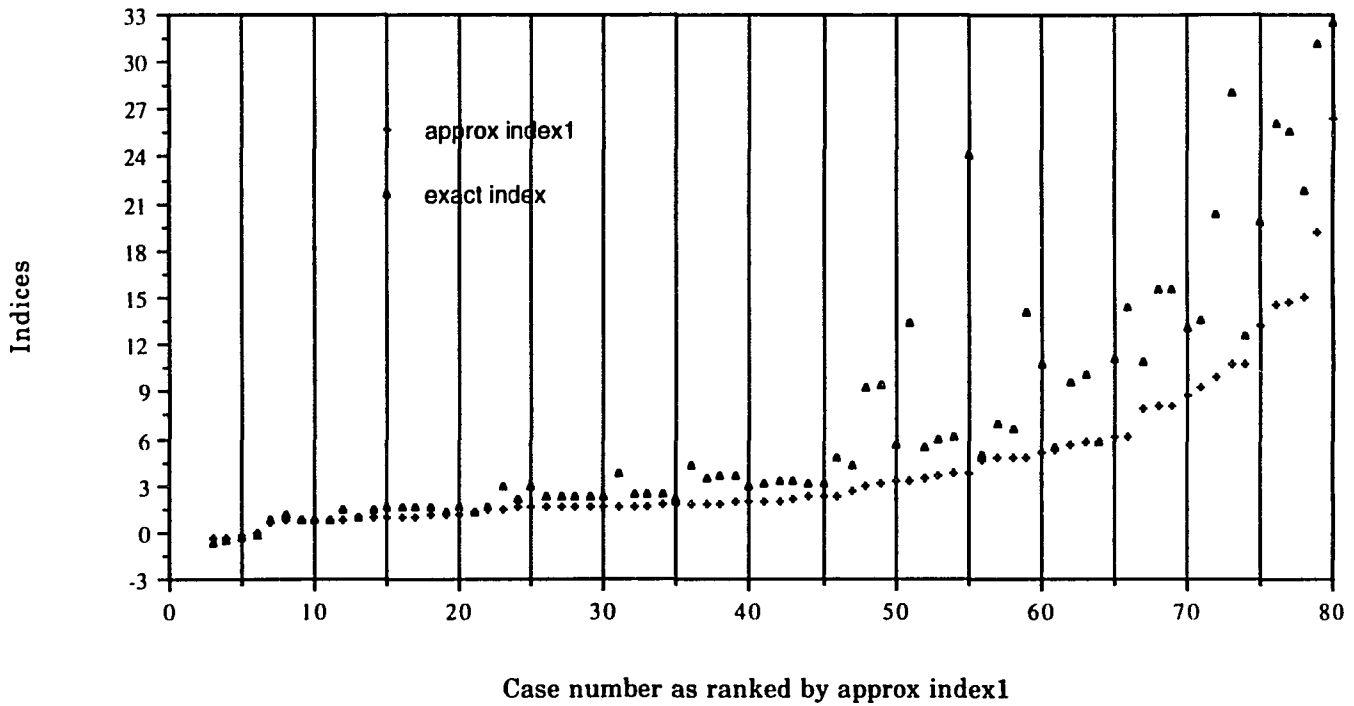

Fig. 7.1. Approximate ($\Delta V_{napprox1}$) and Exact indices (ΔV_n) Vs. Case Number

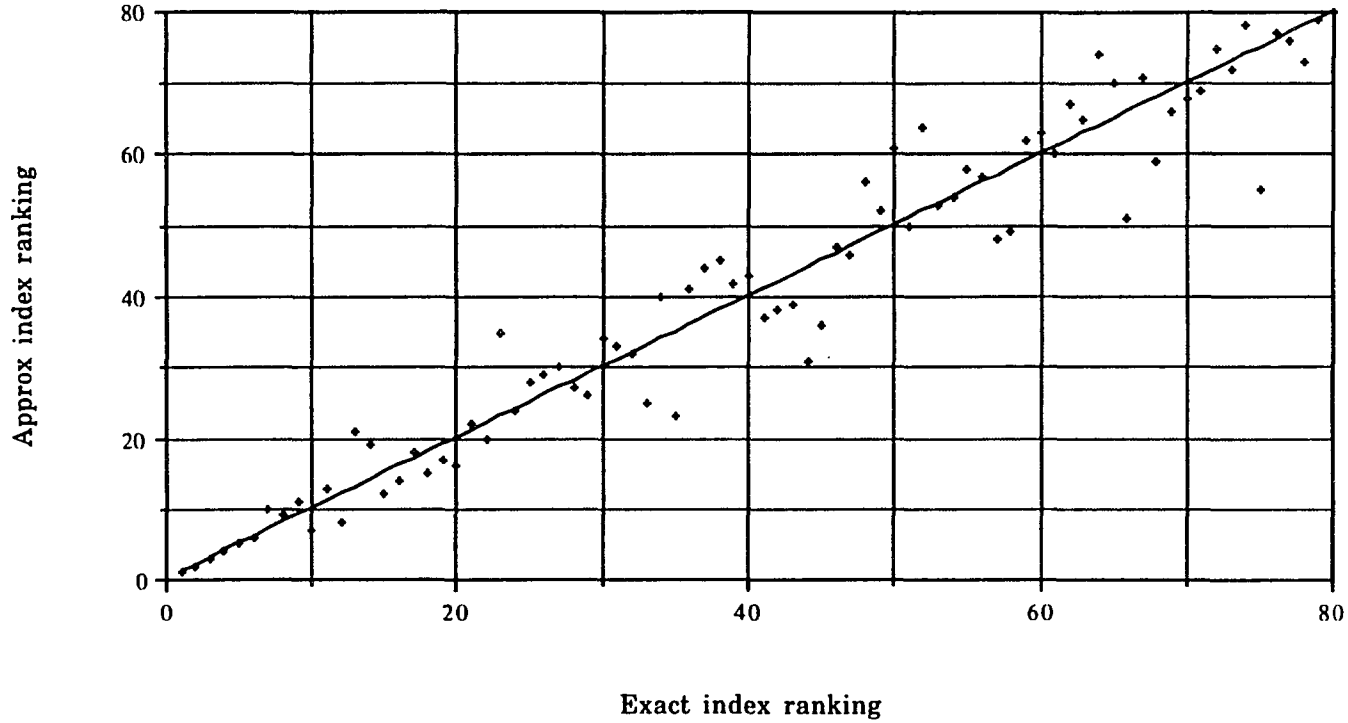

Fig. 7.2. Plot of Exact Index (ΔV_n) Ranking Vs Approx Index ($\Delta V_{napprox1}$) Ranking

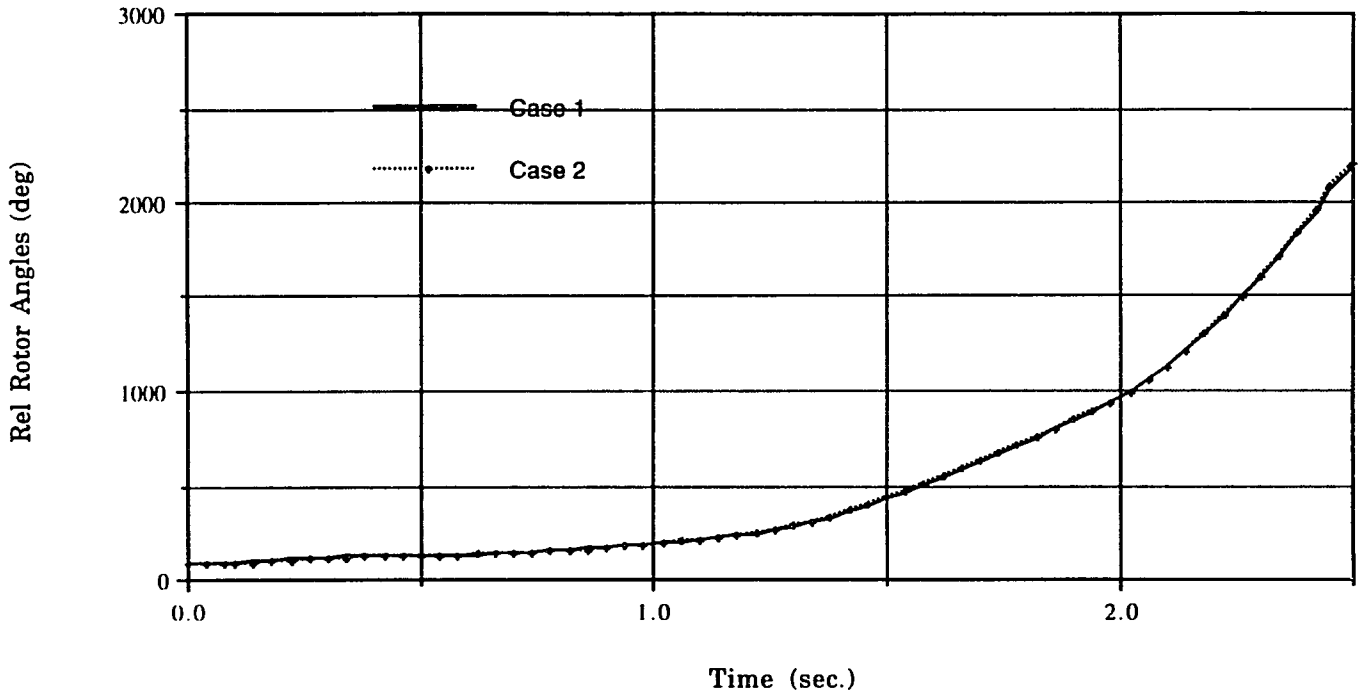

Fig. 7.3. Relative rotor angle plot of machine #77 for cases 1 and 2

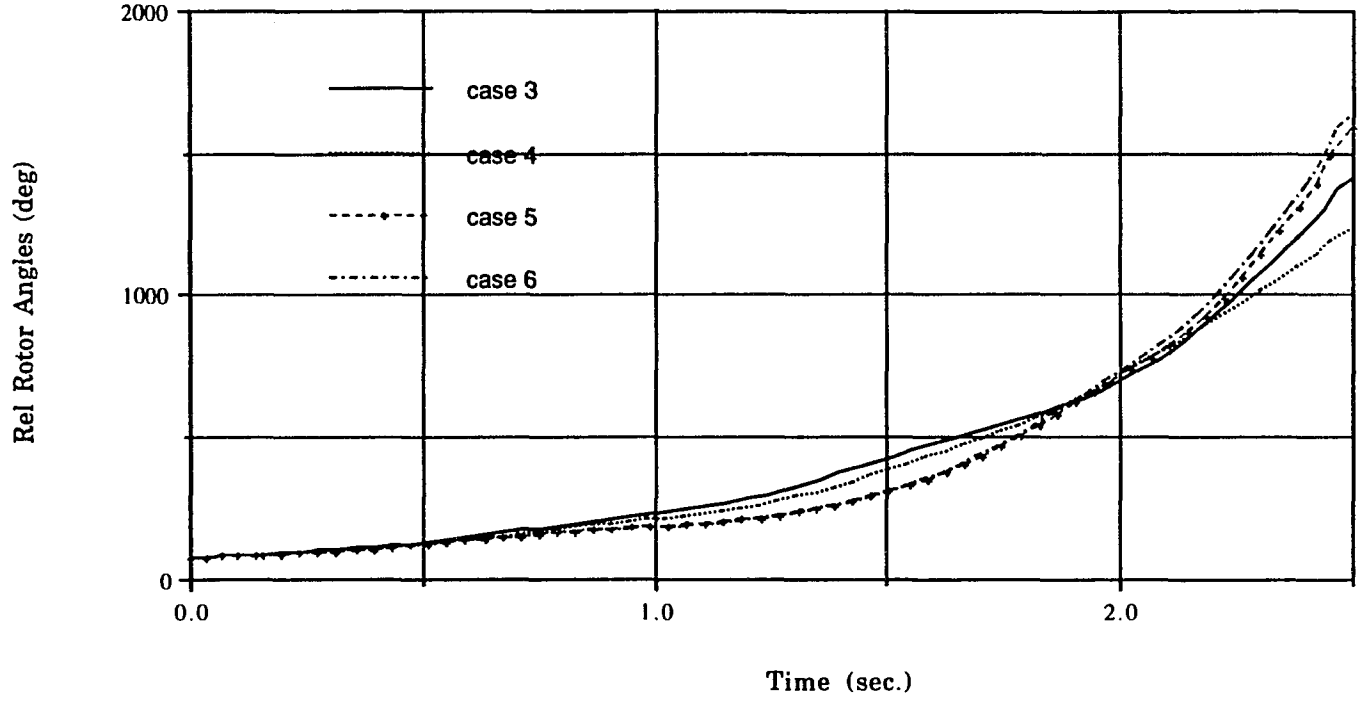

Fig. 7.4. Relative rotor angle plot of machine #77 for cases 3, 4, 5 and 6

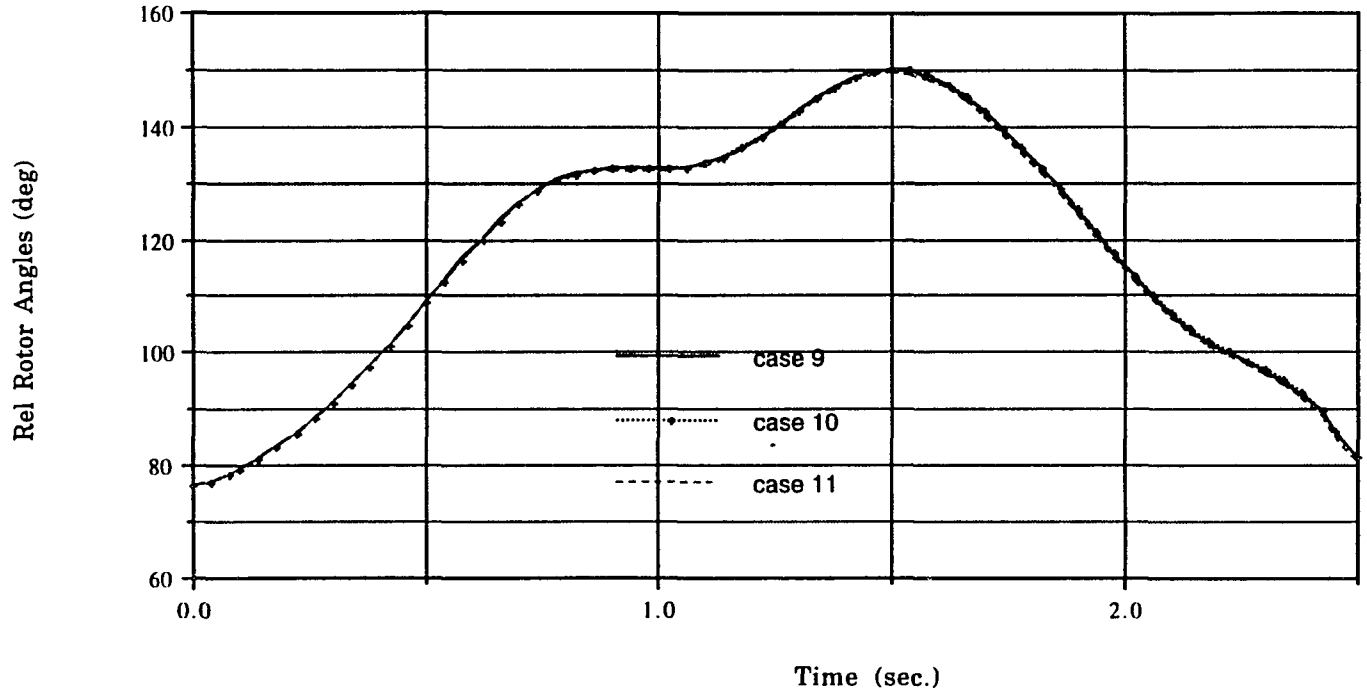

Fig. 7.5. Relative rotor angle plot of machine #77 for cases 9, 10 and 11

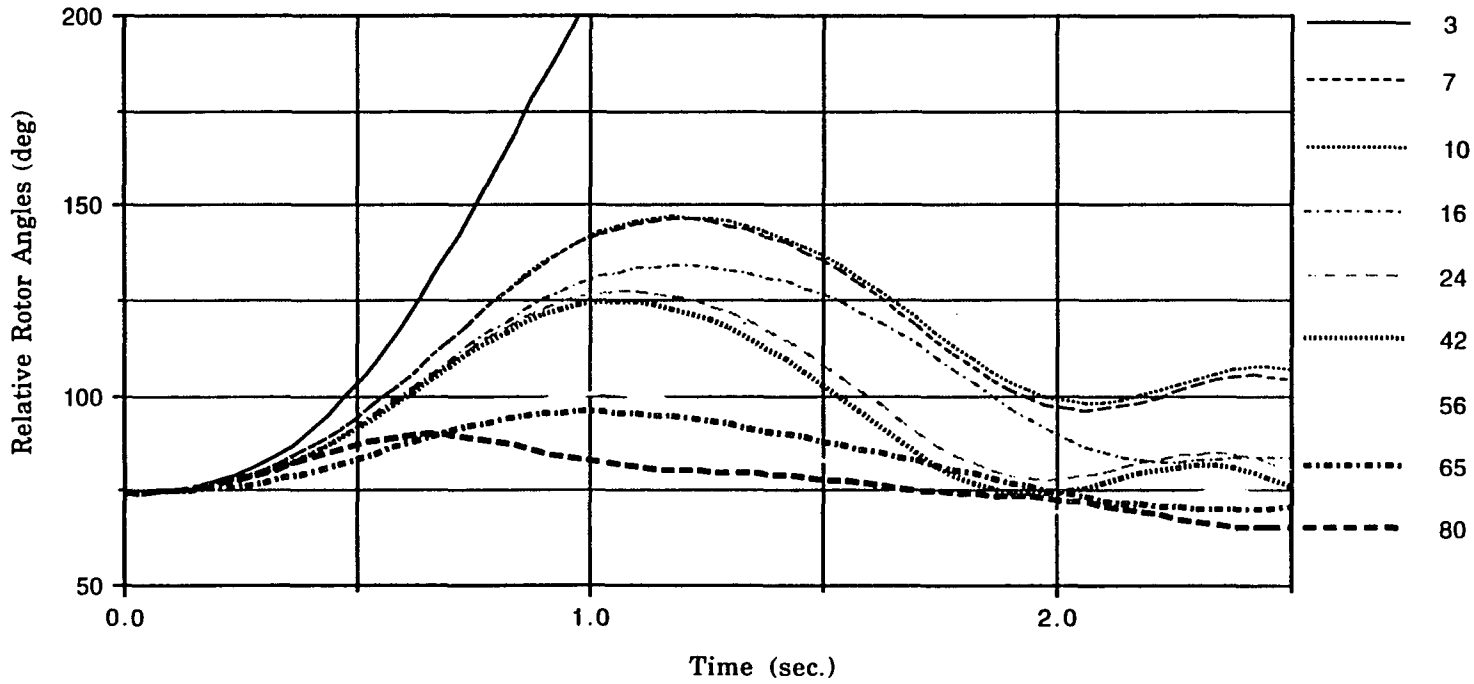

Fig. 7.6. Relative rotor angle plot of machine #35

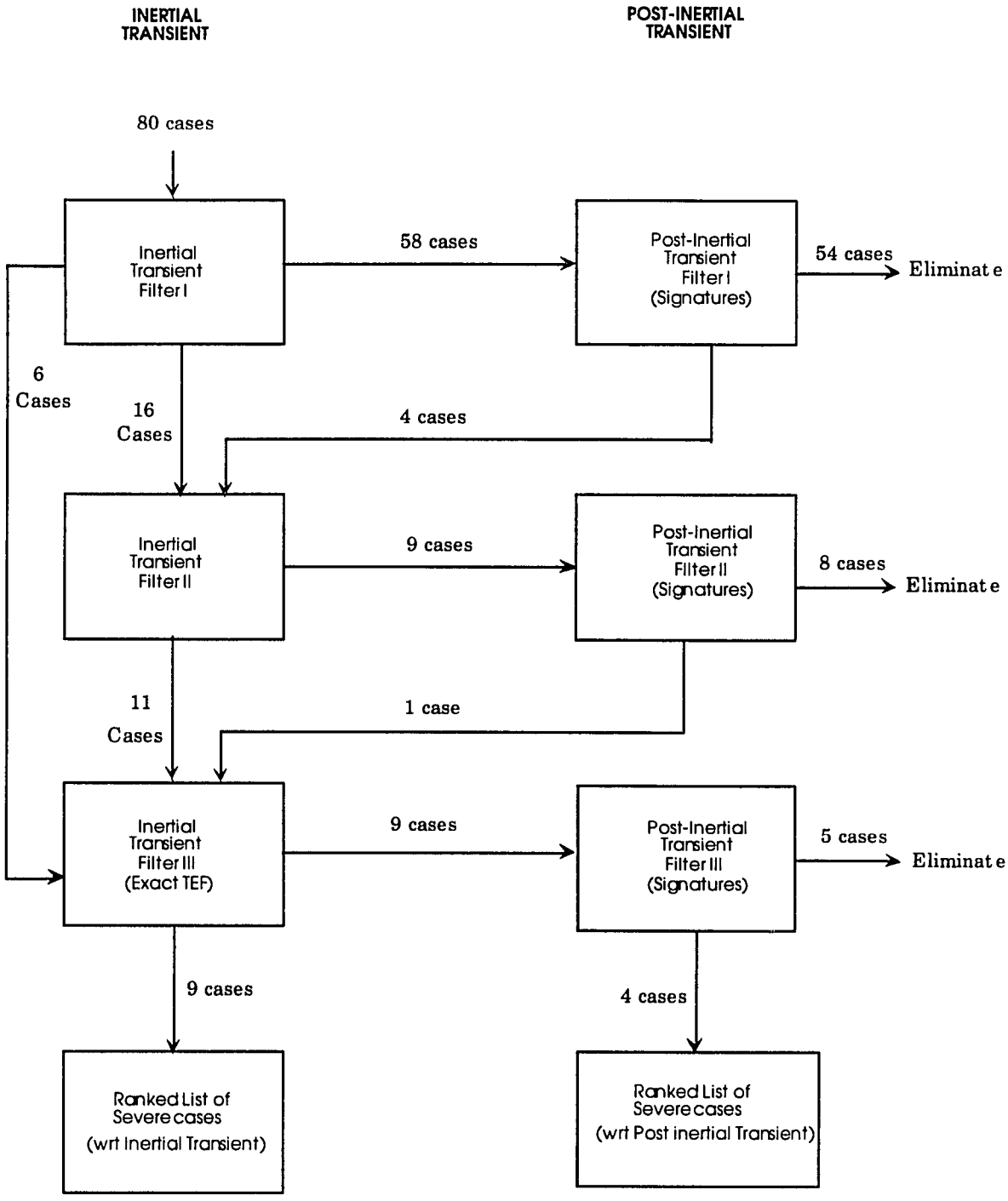

Fig. 7.7. Contingency filtering scheme for the 80 cases

8 CONCLUSIONS

The research work reported in this dissertation investigated the concept of the contingency filtering scheme as a means for on-line dynamic security assessment.

The feasibility of using the contingency filtering scheme for on-line dynamic security assessment was successfully tested. The efficacy of the filtering scheme is demonstrated by comparing the results against those obtained using a conventional time domain simulation program (EPRI-ETMSP). Signatures to appropriately identify system behavior in the inertial and post-inertial transient filters were developed.

A new technique to determine the sensitivities to network topology changes was developed. This is important in terms of assessing the stability of the system for additional changes in the post disturbance network. Relaxing the assumption that the MOD does not change, adds validity to the analytic sensitivity technique.

The sparse TEF is instrumental in enabling the power system operator to screen hundreds of contingencies in near real time. Enhancements made to the sparse TEF method include the use of exciters, spline function and a modified technique to determine the controlling UEP (when no angle is advanced beyond 90 degrees in the UEP). The spline function provides for extremely accurate assessment when exciters are modeled. Further work is essential in the area of analytical sensitivity formulation for the sparse TEF

method. Scaffolding of the existing TEF method was necessary to eliminate unnecessary calculations and to provide faster filtering.

Filters 1 and 2 are very effective as they are both fast and conservative at the same time. The post-inertial filters are critical in that they capture cases which are potentially severe with respect to the post-inertial transient. Synchronizing power coefficients when applied with the sparse formulation provide a very good indication of the stress in the post disturbance network. This adds a new dimension to the TEF method as potential multi-swing unstable cases can be identified much earlier.

The need for a dynamic security assessment technique which can be used for on-line purposes has been repeatedly stressed by the industry. The filtering scheme with the sparse formulation of the TEF method is in full implementation in the Energy Management System (EMS) of the NSP company.

BIBLIOGRAPHY

[1] Design of Electric Power Systems for Maximum Service Reliability" by Concordia. C., *Cigre, Report No. 32-08*, 1968.

[2] *Annual Data Summary Report for the Regional Councils of NERC.* Princeton, NJ: North American Electric Reliability Council, 1985.

[3] Fouad, A. A., Kruempel, K. C., Mamandur, K. R. C., Stanton, S. E., Pai, M. A., and Vittal, V. "Transient Stability Margin as a Tool for Dynamic Security Assessment." *EPRI Report EL-1755*, March 1981.

[4] *Proposed Terms and Definitions for Power System Stability*, by the Task Force on Terms and Definitions, System Dynamic Performance Subcommittee, PES, *IEEE Transactions on PAS-101*, (1982): 1894-1898.

[5] Kimbark, E. W. *Power System Stability. Vol. I.* New York: John Wiley & Sons, Inc., 1948.

[6] *Criteria of Stability of Electric Power Systems.* A report published by the all Union Institute of Scientific and Technological Information and the Academy of Sciences of the USSR Electric Technology and Electric Power Series, Moscow, USSR, 1971.

[7] Magnusson, P. C. "Transient Energy Method of Calculating Stability." *AIEE Transactions, vol 66* (1947): 747-755.

[8] Aylett, P. D. "The Energy Integral Criterion of Transient Stability Limits of Power Systems." *Proceedings of the IEE 105(C)* (1958): 527-536.

[9] Gless, G. E. "Direct Method of Lyapunov Applied to Transient Power System Stability." *IEEE Transactions on PAS - 85* , February 1966: 159-168.

[10] El-Abiad, A. H. and Nagappan, K. "Transient Stability Regions of Multimachine Power Systems." *IEEE Transactions on PAS - 85*, February 1966: 169-179.

[11] Uemura, K., Matsuki, J., Yamada, I., and Tsuji. T. "Approximation of an Energy Function in Transient Stability Analysis of Power Systems," *Electrical Engineering in Japan, Vol. 92*, No. 6: 96-100.

[12] Tavora, C. J. and Smith, O. J. M. "Characterization of Equilibrium and Stability in Power Systems." *IEEE Transactions on PAS - 91*, May 1972: 1127-1130.

[13] Athay, T., Sherket, V., Podmore, R., Virmani, S., and Puech, C. "Transient Energy Stability Analysis." Proc. Conference on Systems Engineering for Power: Emergency Operating State Control, Davos, Switzerland, 1979. *U.S. Dept. of Energy Publication No. CONF-790904-PL, Section IV.*

[14] Kakimoto, N., Ohsawa, Y., and Hayashi, M. "Transient Stability Analysis of Electric Power Systems via Lur'e Type Lyapunov Function." *Proceedings of IEE Japan 98* , May 1978: 63-78.

[15] Bergen, A. R., and Hill, D. J. "A Structure Preserving Model for Power System Stability Analysis." *IEEE Transactions on PAS - 100* , March 1981: 25-35.

[16] Fouad, A. A. and Stanton, S. E. "Transient Stability Analysis of a Multimachine Power System. Part I: Investigation of System Trajectory; and Part II: Critical Transient Energy." *IEEE Transactions on PAS - 100* August 1981: 3408-3424.

[17] Fouad, A. A., Kruempel, K. C., Mamandur, K. R. C., Stanton, S. E. "Contingency Analysis Using the Transient Energy Margin Technique". *Paper 815M397-9 IEEE PES summer meeting,* Portland, OR, 1981.

[18] Fouad, A. A., V. Vittal, and T. Oh. "Critical Energy for Transient Stability Assessment of a Multimachine Power System." *IEEE Transactions on PAS - 103* (1984): 2199-2206.

[19] Chiang, H. D. "A Theory-Based Controlling UEP Method for Direct Analysis of Power System Transient Stability." *Proceedings of the 1989 International Symposium on Circuits and Systems, Vol. 3*: 1980-1983.

[20] Fouad, A. A., and Vittal, V. *Power System Transient Stability Analysis Using the Transient Energy Function Method.* Prentice Hall, 1992.

[21] Fouad, A. A., Ghafurian, A., Nodehi, K., and Mansour, Y. "Calculation of Generation-Shedding Requirements of B.C. Hydro System Using Transient Energy Function." *IEEE Transactions on PWRS - 1, No. 2* (1986): 17-24.

[22] El-Kady, M. A., Tang, C. K., Carvalho, V. F., Fouad, A. A., and Vittal, V. "Dynamic Security Assessment Utilizing the Transient Energy Function Method." *Proceedings of 1985 PICA conference,* San Francisco, CA, May 1985: 132-139.

[23] Rajagopal, S. *"Application of the TEF Method to Stressed Large-Scale Power Systems."* Ph.D. Dissertation, Iowa State University, Ames, IA, 1987.

[24] Oh, T. K. *"Correlation of the Transient Energy Margin to Out-of-Step Relay Operation."* Ph.D. Dissertation, Iowa State University, Ames, IA, 1986.

[25] Nodehi, K. *"Incorporating the Effect of Exciter in the TEF Method."* Ph.D. Dissertation, Iowa State University, Ames, IA, 1987.

[26] Ni, Y. X., and Fouad, A. A. "Simplified Two-Terminal HVDC Model and Its use in Direct Transient Stability Assessment." *IEEE/PES 1987* Winter Meeting, New Orleans, LA, February 1987.

[27] Neelu Bhatia. *"Incorporating Non-linear load models in the TEF Method."* Ph.D. Dissertation, Iowa State University, Ames, IA, 1989.

[28] Hwang, C. *"Sensitivity Analysis of the Transient Energy Function Method."* Ph.D. Dissertation, Iowa State University, Ames, IA, 1989.

[29] Romeo D'Souza. "*Sensitivity Analysis of the Transient Energy Function Method using a Second Order Analytic Technique.*" M. S. Thesis, Iowa State University, Ames, IA, 1989.

[30] Anderson, P. M., and Fouad, A. A. *Power System Control and Stability. Vol. 1.* Ames, Iowa: The Iowa State University Press, 1977.

[31] Gupta, C. L., and A. H. El-Abiad. "Determination of the Closest Unstable Equilibrium State for Lyapunov's Method in Transient Stability Studies." *IEEE Transactions on PAS-95* , October 1976.

[32] Ribbens-Pavella, M. P. G. Murthy, and J. L. Howard. "The Acceleration Approach to Practical Stability Domain Estimation in Power Systems." In *Proceedings of 20th IEEE Conference on Decision and Control*, 1981.

[33] Athay, T., Podmore, R., and Virmani, S. "A Practical Method for Direct Analysis of Transient Stability." *IEEE Transactions on PAS - 98* (1979): 573-584.

[34] Chiang, H. D., Wu, F. F., and Varaiya, P. P. "Foundations of the Potential Energy Boundary Surface Method for Power System Transient Stability Analysis." *IEEE Transactions on Circuits and Systems, CAS - 35*, June 1988: 712-728.

[35] Sauer, P. W., Demaree, K. D., and Pai, M. A. "Stability Limited Load Supply and Interchange Capability." *IEEE Transactions on PAS - 102* August 1986: 284-291.

[36] Pai, M. A., Sauer, P. W., and Demaree, K. A. "Direct Methods of Stability Analysis in Dynamic Security Assessment." *Proc. 9th IFAC World Congress,* Budapest, July 1984.

[37] Vittal, V., Fouad, A. A., and Kundur, P. "Determination of Transient Stability Constrained Plant Generation Limits." *Proceedings of IFAC symposium on Automation and Instrumentation of Power Plants*, Bangalore, India, December 1986: A-8-1-A-8-5.

[38] Moore, J. L. "Power System Stability Behavior for Multiple Generation Shifts." *Proceedings of the Twentieth North American Power Symposium,* West Lafayette, IN, September 1988: 292-296.

[39] Vittal, V., Zhou, E. Z., Hwang, C., Fouad, A. A. "Derivation of Stability Limits using Analytic Sensitivity of the Transient Energy Margin." *IEEE-PES paper WM 207-2.PWRS*, Winter Meeting Power Engg. Society, New York, NY, February 1989.

[40] Vittal, V., D'souza, R., and Fouad, A. A. "Analytical Sensitivity of Transient Energy Margin Including Second Order." *Proceedings of the 10th PSCC Conference,* Graz, Austria, August 1990.

[41] Debs, A. S., and Dominguez, F., "Sensitivity Analysis of Voltage Dip Computation Using the TEF Method," 29th *IEEE Conference on Decision and Control*, Honolulu, Hawaii, December 1990.

[42] Tong, J., Chiang, H. D., and Conneen, T. P., "A Sensitivity Based BCU Method for Fast Derivation of Stability Limits in Electric Power Systems," *IEEE Transactions on Power Systems.*

[43] IEEE Stability Test Systems Task Force, " Transient Stability Test Systems for Direct Stability Methods", System Dynamic Performance Subcommittee PES, *IEEE Trans. PAS,* Vol. 7, No. 1, February 1992: 37-40.

[44] Treinen, R., Vittal, V., Fouad, A. A., "Application of a Modal Based Transient Energy Function to a Large-Scale Stressed Power System: Assessment of Transient Stability and Transient Voltage Dip." *International Journal of Electric Power and Energy Systems*, Vol. 15, No.2, October 1993: 117-125.

[45] Abu-Elnaga, M. M., M. A. El Kady, and R. D. Findlay. "Sparse Formulation of the Transient Energy Function Method for Applications to Large-Scale Power Systems." *IEEE Transactions on PAS, Vol. 3, No. 4*, November 1988.

[46] Ejebe, G. C., Irisarri, G. D., Tinney, W. F., Vittal, V., and Fouad, A. A. "A Sparse Formulation and Implementation of the Transient Energy Function Method for Dynamic Security Analysis." *Proceedings of the 1993 PICA Conference.*

[47] Hindmarsh, A. C. "*ODEPACK, A Systemized Collection of ODE solvers*", Scientific Computing, R. S. Steplemen, et. al. (Eds.) North Holland Publishing Co., Amsterdam, 1983.

[48] Dommel, H. W., and Sato, N. "Fast Transient Stability Solutions." *IEEE Transactions on PAS -91*, July/August 1972.

[49] Vittal, V., and Fouad, A. A. "A Noise Equivalent Bandwidth Approach To Obtain Reduced Order Models For Power System Excitation Control." *Electrical Machines and Power Systems, Vol. 17, No. 1*, 1989.

[50] Sauer, P. W., Behera, A. K., Pai, M. A., Winkleman, J. R., Chow, J. H., "Trajectory Approximations for Direct Energy Methods that use Sustained Faults with Detailed Power System Models." *IEEE Transactions on PAS*, May 1989: 499-506.

[51] Ni, Y.-X., C. G. Shin, and A. A. Fouad, "TEF Method Solution With Exciter: Numerical Technique Used." *Proceedings of the 1987 North American Power Symposium*. Edmonton, Alberta, October 1987.

[52] Fouad, A. A., Y.-X. Ni, V. Vittal, et al, "Incorporating Excitation Control in the Transient Energy Function Method: Selection of Generators with Exciters." *Proceedings of the 12th IMACS World Congress 3*, July 1988: 114-116.

[53] Fouad, A. A., et al., "Direct Transient Stability Assessment with Excitation Control." *IEEE Transactions on Power Systems 4*, February 1989: 75-82.

APPENDIX A

This appendix explains how the sensitivity variables $\frac{\partial E_i}{\partial P_{mk}}$ and $\frac{\partial P_{mi}}{\partial P_{mk}}$ are determined.

- Determining $\frac{\partial E_i}{\partial P_{mk}}$

The procedure followed to determine $\frac{\partial E_i}{\partial P_{mk}}$ is the same as in [28]. To obtain the exact value of $\frac{\partial E_i}{\partial P_{mk}}$, two power flow solutions are needed for each generation change. The first power flow corresponds to the base case and the other with the generation change included. To avoid this process a simplified method is developed.

As the internal voltage of the generator whose generation is changing varies much more than the other generators, $\frac{\partial E_i}{\partial P_{mk}}$ $(i \neq k)$ is assumed to be zero. Only $\frac{\partial E_k}{\partial P_{mk}}$ is approximated using Kirchhoff's law.

When there is generation change, it is assumed that only real power is changing. In actual power flow, the reactive power also changes at generators where real power changes.

Figure A1 shows the generator terminal branch which participates in generation change for the base power flow case. If there is a complex power change $(\Delta P_{mk} + \Delta Q_k)$ at the machine terminal with the terminal voltage V_k

held constant, E_k will change to $E_k^{'}$. By applying Kirchhoff's law at this branch, we have,

$$E_k^{'} = \frac{P_{mk} + \Delta P_{mk} - j(Q_k + \Delta Q_k)}{V_k^*}(jX_d^{'}) + V_k \qquad \text{(a1)}$$

Then $\frac{\partial E_k}{\partial P_{mk}}$ can be approximated as

$$\frac{\partial E_k}{\partial P_{mk}} \approx \frac{|E_k^{'}| - |E_k|}{\Delta P_{mk}} \qquad \text{(a2)}$$

The value used for ΔQ_k is $\Delta Q = \frac{Q_k}{P_k}\Delta P_{mk}$.

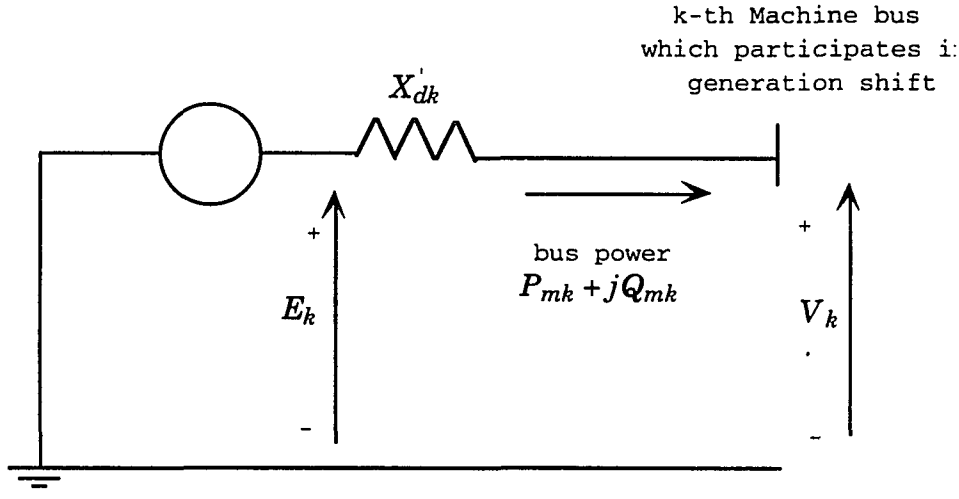

Figure A1. Equivalent circuit of Classical Machine Model

- Determining $\frac{\partial P_{mi}}{\partial P_{mk}}$

The value of $\frac{\partial P_{mi}}{\partial P_{mk}}$ for $(i \neq k)$ is assumed to be zero. When i = k, the value of $\frac{\partial P_{mi}}{\partial P_{mk}}$ is taken as 1. The sensitivity variable $\frac{\partial P_{mi}}{\partial P_{mk}}$ can be represented as

$$\frac{\partial P_{mi}}{\partial P_{mk}} = \delta_{ik} \tag{a3}$$

where

δ_{ik} is the kronecker delta. This is given by

$$\delta_{ik} = 1 \qquad for\ i = k$$

$$\delta_{ik} = 0 \qquad for\ i \neq k$$

ACKNOWLEDGEMENTS

I am deeply indebted to my major professor Dr. Vijay Vittal for providing me with guidance and direction during the period of my research work and times of doubt. His constant encouragement and attention were of great help in this research work. I would like to sincerely thank Dr. A. A. Fouad for his invaluable advice and words of wisdom throughout my course of study here. Special thanks are extended to Dr. John Lamont, Dr. Wolfgang Kliemann and Dr. Mustafa Khammash for taking time out of their busy schedule and agreeing to be a part of my graduate committee.

I would also like to extend my gratitude to the graduate college for providing me with financial assistance during my graduate program and the members of the power faculty under whom I undertook graduate courses.

To all the graduate students in the power group, who were really a great circle of friends to study with, thanks!

I would also like to thank the secretaries of the Electrical Engineering and Computer Engineering Department.

Finally, I would like to thank my family members without whose help and encouragement my enrollment in graduate school would not have been possible.